Spring 5-8-2017

EFFECTS OF PROCESSING PARAMETERS ON PROPERTIES OF NOVEL SILICA-FILLED POLYSILOXANE MATERIALS

Kyle W. Schwenker
Pittsburg State University, kyleschwenker@gus.pittstate.edu

EFFECTS OF PROCESSING PARAMETERS ON PROPERTIES OF NOVEL SILICA-FILLED POLYSILOXANE MATERIALS

A Thesis Submitted to the Graduate School
in Partial Fulfillment of the Requirements
for the Degree of Master of Science

Kyle Schwenker

Pittsburg State University

Pittsburg, Kansas

April, 2017

EFFECTS OF PROCESSING PARAMETERS ON PROPERTIES OF NOVEL SILICA-FILLED POLYSILOXANE MATERIALS

Kyle Schwenker

APPROVED:

Thesis Advisor _____
Dr. Jeanne H. Norton, The Department of Plastics Engineering Technology

Committee Member _____
Dr. Petar R. Dvornic, The Department of Chemistry

Committee Member _____
Dr. Charles Neef, The Department of Chemistry

Committee Member _____
Mr. Paul Herring, The Department of Plastics Engineering Technology

Committee Member _____
Dr. Jamie M. Messman, Honeywell FM&T

ACKNOWLEDGEMENTS

I would like to thank and express my great appreciation to my mentor and advisor, Dr. Jeanne H. Norton. Dr. Norton has been my professor, supervisor, mentor, advisor, and a friend to me throughout my college education. As my advisor, Dr. Norton has taught me so much about science and engineering, academics, research, and life. Dr. Norton's dedication and excitement for chemistry and engineering inspired me to pursue my graduate degree, and she has provided me confidence to look forward to the next step in my career.

I would also like to acknowledge and thank my committee members: Dr. Petar R. Dvornic, Dr. Charles Neef, Mr. Paul Herring, and Dr. Jamie M. Messman for their advice and encouragement towards my research. I would like to thank the Department of Chemistry and the Polymer Chemistry Initiative at Pittsburg State University for funding my position as a graduate research assistant. I am grateful for the faculty and staff, laboratory space, and equipment in the Department of Chemistry; the Kansas Polymer Research Center; and the Department of Plastics Engineering Technology at PSU. Everyone was always eager to give me advice and assistance.

Finally, I wish to thank my family and friends for their constant support and advice when my days in class or in the lab did not go as planned. Above all else, I would like to thank my parents, Bonnie and Jon Schwenker. They have supported me through everything that I have done, whether it was financially, physically, or emotionally. They suggested that I pursue an engineering degree as an undergraduate, and they were very supportive of me pursuing a chemistry degree as a graduate student. I would like to dedicate this thesis to everyone mentioned above, because without these people, this thesis would not have been possible. Thank you!

EFFECTS OF PROCESSING PARAMETERS ON PROPERTIES OF NOVEL SILICA-FILLED POLYSILOXANE MATERIALS

An Abstract of the Thesis by
Kyle Schwenker

Polysiloxanes are a class of materials that possess high temperature stability and the ability to remain flexible at extremely low temperatures. Their elastomers generally exhibit low strength and have poor mechanical properties unless reinforced with fillers. Reinforcement can be accomplished by compounding reinforcing silica fillers with polysiloxanes by twin-screw extrusion compounding that vigorously mixes the fillers into a polymer matrix. In this thesis, a lab-scale twin-screw extruder was utilized to compound thermoplastic materials to determine the effects of processing on the thermoplastics material properties, as well as to determine the extruder's compounding effectiveness. Processing via lab-scale twin-screw extrusion did not negatively affect the thermoplastic material properties. A thermoplastic and titanium dioxide formulation was effectively compounded, as well. Lab-scale twin-screw extrusion was also utilized to compound two model polysiloxanes (a vinyl-terminated polydimethylsiloxane (Gelest DMS-V31), and a vinyl-terminated diphenyl-dimethyl siloxane copolymer (Gelest PDV-0331)) and four experimentally-synthesized polysiloxanes with three silica fillers (Hi-Sil™ 135, Hi-Sil™ 233D, and Cab-O-Sil® M-7D) to produce well-dispersed compounded materials.

The filled polysiloxanes were characterized by thermogravimetric analysis to evaluate the distribution of filler. Oscillatory rheometry and flow rheology were used to evaluate the yield stress and thixotropic behavior, respectively. Processing parameters,

filler type, and amount of filler were evaluated in the polysiloxane formulations and compared to a commercial reference silicone rein to evaluate the formulations for their viability in applications that currently use the reference silicone.

Thermogravimetric analysis confirmed that the compounded materials possessed an even distribution of filler in most formulations. Thermal stability, yield stress, and thixotropic behavior of the filled materials were most dependent on the type and amount of filler used in each formulation, rather than chemical characteristics of the polysiloxanes studied, including molecular weight and copolymer composition. Cab-O-Sil-filled materials resulted in the most thermally stable materials with the highest yield stress and the greatest degree of thixotropy. However, despite these properties, the Cab-O-Sil-filled materials were too stiff to replace the reference silicone. The Hi-Sil-233D-filled materials attained similar rheological properties to the reference silicone, and may be a more viable alternative in applications where the reference silicone is currently utilized.

TABLE OF CONTENTS

CHAPTER PAGE

LIST OF TABLES

TABLE PAGE

LIST OF FIGURES

FIGURE PAGE

LIST OF SCHEMES

SCHEME PAGE

LIST OF ABBREVIATIONS

μm – Micrometer

Å – Angstrom

ABS – Acrylonitrile butadiene styrene

D_3 – Hexamethylcyclotrisiloxane

D_4 – Octamethylcyclotetrasiloxane

DiEt – Diethyl

DiMe – Dimethyl

DiPh – Diphenyl

DSC – Differential scanning calorimetry

g/hr – Grams per hour

in/sec – Inches per second

J/g – Joules per gram

kcal/mol – Kilocalories per mole

kg/hr – Kilograms per hour

L:D ratio– Length to diameter ratio

m^2/g – Meters squared per gram

mL/min – Milliliters per minute

mm – Millimeter

mm/min – Millimeters per minute

M_n – Number-average molecular weight

mol% – Mole percent

M_p – Peak molecular weight

MPa – Megapascal

M_w – Weight-average molecular weight

N – Newtons

N m – Newton meter

Pa – Pascal

Pa·s – Pascal-second

PDI – Polydispersity Index

PDMS – Polydimethylsiloxane

ROP – Ring-opening polymerization

rpm – Revolutions per minute

sec – second

SEM – Scanning electron microscopy

T_c – Crystallization temperature

T_g – Glass transition temperature

TGA – Thermogravimetric analysis

TiO_2 – Titanium dioxide

T_m – Melting temperature

wt% – Weight percent

CHAPTER I

1. INTRODUCTION

1.1 Polysiloxanes

Polysiloxane elastomers are unique among elastomeric materials. Polysiloxanes are stable at high temperatures and can maintain their flexibility at extremely low temperatures. For example, natural rubber has an upper use temperature of 80°C and has a glass transition temperature (T_g) at -72°C, while polydimethylsiloxane (PDMS) has an upper use temperature of 400°C and has a T_g at -123°C.[1,2] These versatile properties allow polysiloxane materials to be used in a wide variety of applications such as O-rings, gaskets, sealants, coatings, and adhesives in extreme environments where other elastomers would be unsuitable.[1]

Siloxane polymers (polysiloxanes) are the most prominent organosilicon polymers that are currently used in polymer chemistry.[3] These polymers comprise of long chains of alternating silicon and oxygen atoms with every silicon atom carrying two organic functional groups. The basic structure of polysiloxanes is the siloxane bond that is shown in Figure 1.[1] Silicon is found in the Group IVA of the periodic table and is the most abundant element of Group IVA. Silicon makes up about 27% of the earth's crust by mass second only to oxygen, which makes up about 50% of the earth's crust by mass. These values indicate that roughly 77% of the earth's crust is comprised of silicon and

oxygen. In nature, silicon is rarely found in elemental form and is usually bonded to oxygen as silicon dioxide (SiO_2 or SiO_4).[3,4] Figure 1 shows the general structure of a siloxane bond, silicon dioxide, and silicate.

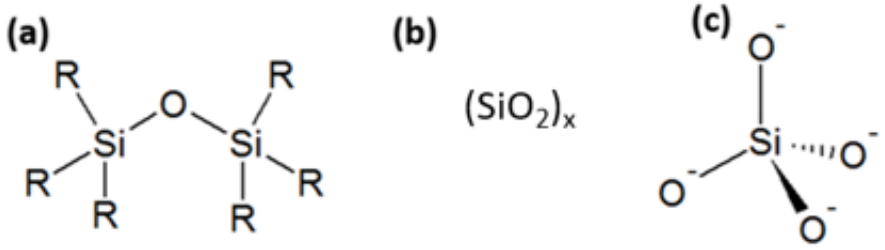

Figure 1. General structure of (a) siloxane bond, (b) silicon dioxide, (c) silicate.

Synthetic polysiloxanes possess exceptional properties including: high temperature stability, flexibility at extremely low temperatures, gas permeability, and low surface energy. The first two properties are the result of the unique features of the siloxane bond.[1] The siloxane bond possesses partial ionic and partial double bond characteristics. The partial ionic characteristic, which is estimated to be 37% to 51% ionic, is attributed to the large difference in electronegativity of silicon (1.8) and oxygen (3.5) that were described by Pauling and others.[1,5,6] The partial double bond characteristic of the siloxane bond is a result of vacant low-energy silicon *d* orbitals that partially overlap with the *p* orbitals of the oxygen atom. The relative difference in sizes of the large silicon atom and the smaller oxygen atom contribute to the overlapping of these orbitals and enables the oxygen atom to back-donate its lone electron pairs to create a d_π-p_π bond (partial double bond) instead of a normal sigma (σ), or single bond. The partial ionic and partial double bond characteristics of the siloxane bond provides the high temperature properties found in polysiloxanes.[1]

The bond between silicon and oxygen possesses a high degree of strength and is much stronger when compared to the bond between carbon and oxygen. The dissociation energy that is required to break a siloxane bond is about 106 kcal/mol compared to 85.5 kcal/mol to break a carbon-oxygen bond. Dvornic and coworkers stated that higher bond strengths are associated with an increasing amount of ionic character in chemical bonds.[1] In addition to the partial ionic character of the siloxane bond attributing to the high dissociation energies required to break the bond, the formation of the d_{π}-p_{π} partial double bond between silicon and oxygen is also associated with the high strength of the siloxane bond. Generally, it is more difficult to break double bonds compared to single bonds.[1]

The perception of the d_{π}-p_{π} as a partial double bond is further supported by the length of the siloxane bond. The average siloxane bond length measures between 1.63 Å to 1.66 Å, which is shorter than a calculated σ bond between silicon and oxygen that is estimated to be 1.83 Å long. This indicates that the siloxane bond is shorter and is not a normal σ bond. The attractive forces between the silicon and oxygen allow the bond to be stronger than expected with a partial double bond characteristic.[1] Furthermore, when comparing the lengths of a siloxane bond and a normal σ bond between silicon and carbon, the siloxane bond is also shorter than the estimated silicon-carbon bond at 1.85 Å long. Figure 2 displays the comparison bond lengths of a siloxane bond and a silicon-carbon bond.[7]

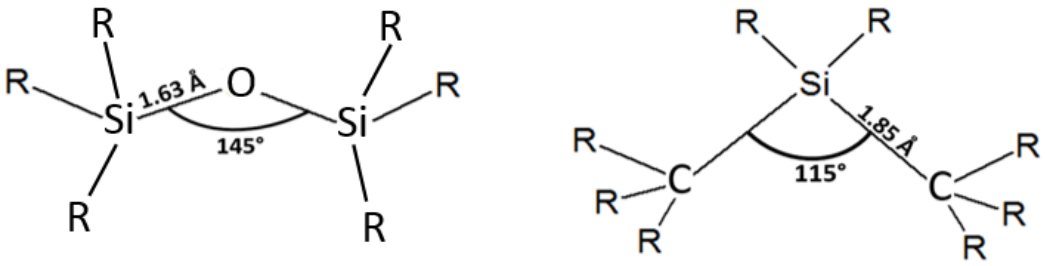

Figure 2. Comparison structures of (a) siloxane bond and (b) silicon-carbon bond with their respectable bond lengths and bond angles.[7]

In addition to the high temperature properties attributed by the siloxane bond, the bond also provides the ability for these materials to remain flexible at extremely low temperatures. The bond angles between O-Si-O normally measures between 106° to 120°, compared to C-Si-C (silicon-carbon bond), which normally measures between 106° to 118°, which are expected for normal single bond angles. Additionally, the siloxane bond (Si-O-Si) angles vary between 104° to 180°, with 144° to 150° being the most widely reported. These measured results indicate a wide range of stable bond angles associated with the siloxane bond and demonstrates that the angle between silicon and oxygen can increase to allow two silicon atoms to rotate relatively freely about their common oxygen atom. These measurements indicate that the siloxane bond is highly deformable, and therefore, highly flexible. Figure 2 compares the bond angles of a siloxane bond and a silicon-carbon bond.[7] The flexibility properties at extremely low temperatures are additionally attributed to their low T_g, which is the lowest T_g in polymer science.[1] Table 1 displays the glass transition temperatures of common polysiloxanes.[1]

Table 1. Glass transition temperatures of common polysiloxanes.[1]

Polymer	T_g (°C)
Natural Rubber	-72
Polymethylphenylsiloxane	-28
Poly(diphenyl-co-dimethyl) (30:70 mol%)	-64
Polydimethylsiloxane	-123
Polymethylethylsiloxane	-135
Polydiethylsiloxane	-139

The unique high thermal stability and low-temperature flexibility properties contribute to polysiloxanes as the high-performance materials of choice in a variety of applications that require the polymers to perform in extreme conditions. These applications include artificial organs, contact lenses, high-performance elastomers, electrical insulators, mold release agents, adhesives, and protective coatings.[1,3,6]

1.2 Polymerization of polysiloxanes

Polysiloxanes can be produced by various reactions, but the two main reactions include ring-opening polymerization (ROP) and equilibration of siloxanes. ROP of cyclic siloxanes produce high molecular weight polysiloxanes using either an acid or base initiator by either anionic or cationic reactions. The resulting linear polymers contain a residue of the initiator as the end group. These ROP reactions are displayed in Scheme 1.[1]

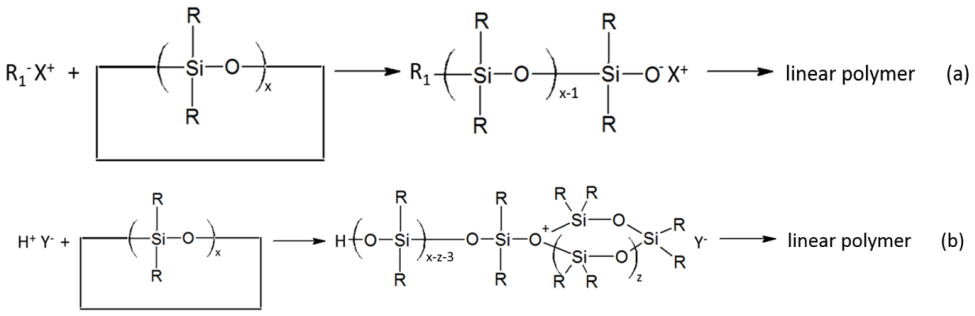

Scheme 1. (a) Anionic ring-opening polymerization of cyclic siloxanes and (b) cationic ring-opening polymerization of cyclic siloxanes.[1]

Scheme 1 represents the chain-growth polymerization reactions that produce linear polymers from cyclic monomers. These reactions are kinetically-governed addition reactions in which the cyclic monomer species and the propagating active centers react with each other to incorporate the monomer unit into the growing polymer chain, and additionally regenerate an identical active center at the newly formed chain end.[1]

The principal method to produce high molecular weight polysiloxanes is anionic polymerization.[1,8] Scheme 2 shows the anionic ring-opening polymerization mechanism for polysiloxanes. Initiation occurs by a nucleophilic attack of an organic base on the cyclic siloxane monomer to open the siloxy bond. The silanolate anion is the active center for propagation, and additionally contains a counter ion. The active center continues to open the monomer's siloxy bonds, thereby adding the monomer to the growing chain. Termination can occur with undesirable impurities that can be present in the system or with terminating reagents that are purposely added to the system, such as dimethylvinyl terminated oligomeric dimethylsiloxane.[1]

Initiation:

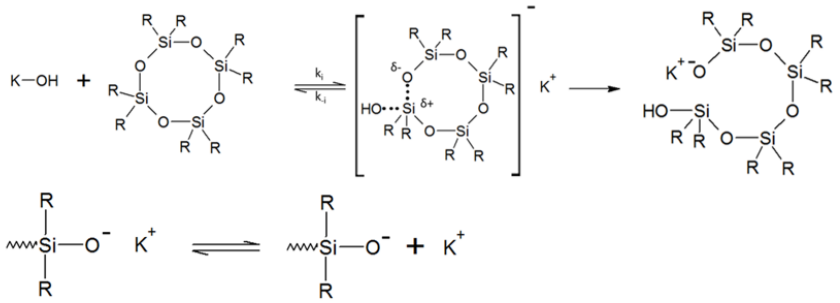

Propagation:

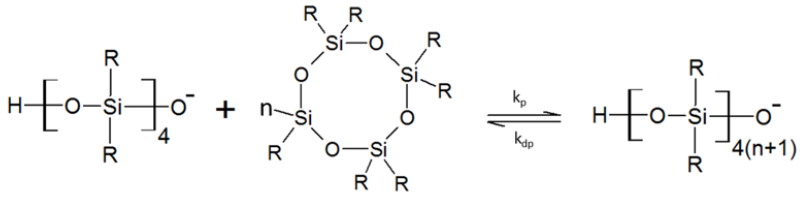

Termination:

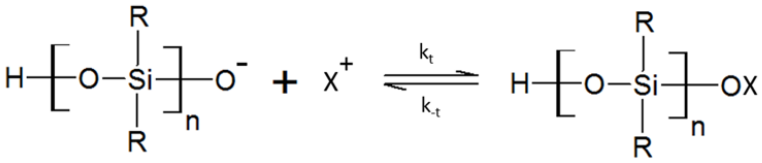

Scheme 2. Polysiloxane anionic ring-opening polymerization mechanism.[1]

Anionic polymerization is relatively fast and the mobility of the atoms within the polymer chains are dependent on the ring size and ring strain of the monomers. A trimer cyclic siloxane, such as hexamethylcyclotrisiloxane (D_3), will undergo anionic polymerization much faster than a tetramer cyclic siloxane, such as octamethylcyclotetrasiloxane (D_4). The siloxane bond angles are much larger than carbon-carbon bonds which make the eight-membered siloxane ring of D_4 more stable than the six-membered ring of D_3. Additionally, if the methyl groups attached to the silicon atoms are replaced with bulkier side groups, the polymerization reaction proceeds at a much slower rate. The mobility of the atoms within the siloxane backbone is reduced due to the steric demands of the larger side groups.[9]

For many siloxane polymerization systems, the chain-growth reactions are either competing with or followed by equilibration reactions that are thermodynamically controlled.[1,10] The siloxane equilibration reactions consist of breaking and reforming siloxane linkages to form a mixture of cyclic and linear siloxane species until a thermodynamic equilibrium between the two species is achieved. Possible equilibration reactions of the siloxane bond are displayed in Scheme 3. The siloxane bond is prone to attack by ionic reagents and these equilibration reactions begin with certain acids and bases referred to as equilibration catalysts. These reactions are the main reason for the production of a mixture of cyclic and linear siloxane species. Common equilibration catalysts are strong mineral acids, alkali metal hydroxides, alkali metal silanolates, and tetraalkylammonium hydroxides.[1]

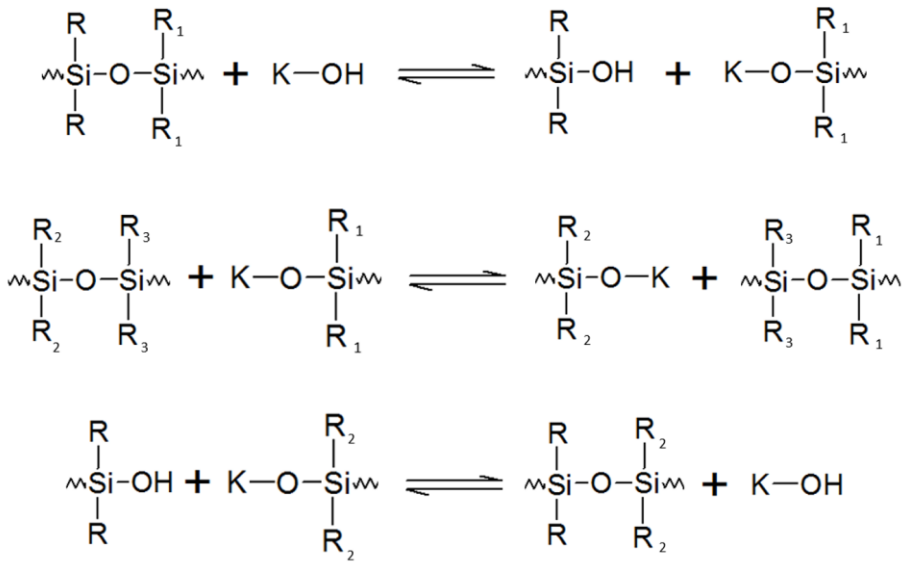

Scheme 3. Siloxane equilibration reactions with anionic catalysts.[1]

Additionally, the polymerization reactions of polysiloxanes can be controlled to regulate the molecular weights of the polymers. Monofunctional silanols (R_3Si-OH) can be added in small amounts to the reaction mixture to prevent an extensive amount of

condensation and control the molecular weight to stabilize the properties of the polymer product. This molecular weight controlling process is called end-capping.[1] Controlling the molecular weight of the polymer product is important for almost all polysiloxane applications that require certain viscosity characteristics, thermal properties, or other physical properties. However, to achieve these polymer properties, the equilibration catalyst must be removed from the polymer product by washing, neutralization, deactivation, and filtration. Because the catalyst removal process is difficult, "transient" catalysts were developed to overcome this difficulty. Polymerization reactions with transient catalysts proceed at lower temperatures, but when heated to higher temperatures such as 130°C to 150°C, the catalyst fully decomposes.[1,4]

Another set of reactions that follows anionic and cationic polymerization reactions are inter- and intramolecular secondary reactions of the cyclic siloxanes. Scheme 4 shows the different types of secondary reactions that can occur. During propagation, the active centers on the siloxane bonds can attack the linear polymer molecules due the partial ionic character of the siloxane bonds. Intramolecular, or "back-biting" reactions lead to the formation of cyclic siloxane oligomers. Each cyclic oligomer formed by back-biting can be used again in the polymerization reaction until equilibration has been achieved for every cyclic siloxane.[1]

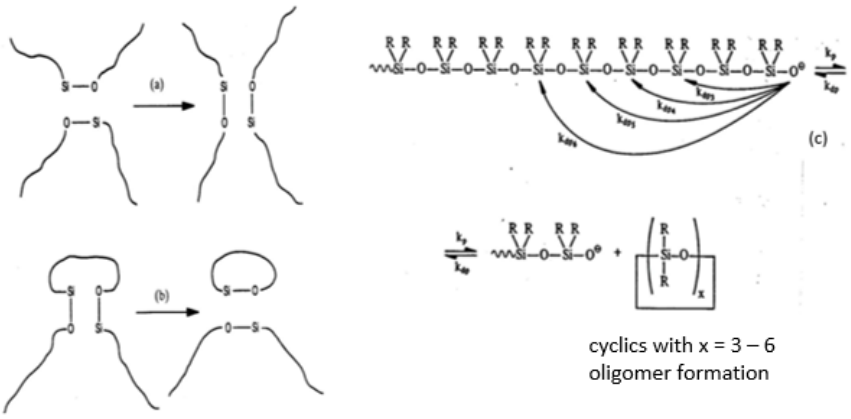

Scheme 4. Secondary reactions: a) intermolecular, b) intramolecular, and c) back-biting.[1]

The four vinyl-terminated polysiloxanes used in this thesis were synthesized using a mixture of cyclic siloxanes by anionic ROP in combination with equilibration, followed by thermal decomposition of the transient catalyst/initiator. The reaction was thermodynamically controlled to generate linear, high molecular weight polymers. The catalyst was believed to initiate both the ROP and the competing equilibration reactions. The synthesized polysiloxanes were expected to be linear, high molecular weight materials with little to no branching. The synthesized polysiloxanes retained their low-temperature flexibility properties by eliminating low-temperature crystallization and maintained their desired surface and high temperature properties. The four synthesized polysiloxanes were vinyl-terminated and were produced with varied amounts of dimethyl-, diphenyl-, and diethyl-containing siloxane units.

Branching was reduced and/or eliminated by the incorporation of diethyl units in the copolymers. Branching was hypothesized to occur at the diphenyl units in the presence of a strong ionic species like a silanolate anion as a result of the tendency to desilylate at the Si-Ph bond. Thus, replacing the diphenyl units with diethyl units reduced

and/or eliminated branching.[11] Diphenyl and diethyl units were incorporated into the polymers to eliminate low-temperature crystallinity. The bulkier units reduce the mobility in the siloxane backbone to prevent crystallization which preserves the low-temperature flexibility properties.[12,13] The copolymers were vinyl-terminated to eventually aid in vulcanization of the polysiloxane elastomeric materials. A crosslinking agent, such as an organic peroxide can react with the vinyl groups to create covalently-bonded crosslinks between another vinyl-terminated polymer chain.[14]

1.3 Fillers in polysiloxane elastomers

Polysiloxane elastomers alone, generally exhibit low strength and possess poor mechanical properties unless combined with other additives. Additives, such as stabilizers and fillers are incorporated in the elastomeric materials to enhance the material properties for the practical applications mentioned earlier. Without fillers, polysiloxane elastomers would be very weak and would have no practical use for their desired applications. For example, unfilled polysiloxane elastomers exhibit a tensile strength of only 0.34 MPa, whereas silica-filled polysiloxane elastomers exhibit an enhanced tensile strength that can range from 10 MPa to 14MPa. Typical polysiloxane elastomers can contain 17 wt% to 41 wt% or higher of filler.[1] These additives are vigorously mixed with polysiloxanes under high shear conditions through the process of compounding.

Fillers are divided up into two categories: extending fillers and reinforcing fillers. Extending fillers are known as either semi-reinforcing or non-reinforcing fillers. These fillers usually “extend” the formulation by reducing the cost of the filled polymeric resin.[15] Materials that are filled with reinforcing fillers can achieve improved mechanical properties compared to unfilled materials.[16,17] Reinforcing fillers can be further divided

into two main groups: inactive and active fillers. Inactive fillers, such as natural silicates, chalks, clays, and calcium carbonates, are usually incorporated into the elastomers for economic purposes and will only weakly reinforce the elastomers. Active fillers are chemically-treated silica fillers that strongly reinforce and significantly improve the physical properties of polysiloxane elastomers. These properties include: tensile strength, abrasion resistance, and heat aging characteristics.

Reinforcing fillers consist of precipitated and fumed silica fillers. Precipitated silica is produced from the reaction of a mineral acid, such as sulfuric acid, with an alkaline silicate solution, such as a sodium silicate. The acid and silicate solution are added together with water and are agitated until precipitation occurs. The particle size and porosity are dependent on the speed of agitation, the duration of the reaction, the amount of reactants, as well as the temperature, concentration, and pH of the reaction. The particles are filtered and washed to remove the salt byproduct, which is usually sodium sulfate. The particles are then dried to remove moisture.[18] However, precipitated silica can contain up to 7% of various impurities and moisture as a result of the difficulty to remove the sodium salt byproduct.[19]

Fumed silica is the purest form of synthetic silica that is commercially-available at 99.8% pure silica.[19] The filler is manufactured by hydrolysis of a chlorosilane, such as silicon tetrachloride that is burned in an oxygen and hydrogen flame through a pyrogenic process. This produces molten spheres of silicon dioxide and hydrogen chloride, which is later removed. During the production of fumed silica, hydroxyl groups become attached to the surface of the particles, generating a hydrophilic surface that can participate in hydrogen bonding. Generally, fumed silica particles are smaller than precipitated silica

particles, and possess higher surface areas.[20] For a given volume, smaller particles can pack closer to each other and obtain higher total surface areas than larger particles.[21-23]

Silica fillers contain active hydroxyl groups (-OH), which when attached to silicon atoms (Si) are known as silanol groups (≡Si-OH). These groups are polar and are present on both the surface of the filler and inside the silica skeleton. The silanol groups are displayed in Figure 3 and can be divided into three groups: (a) isolated single silanols, (b) geminal silanediols, and (c) vicinal-bridged silanols through hydrogen bonding. In addition to silanol groups on the surface of the silica, there are also surface siloxane groups and adsorbed water present.[24,25]

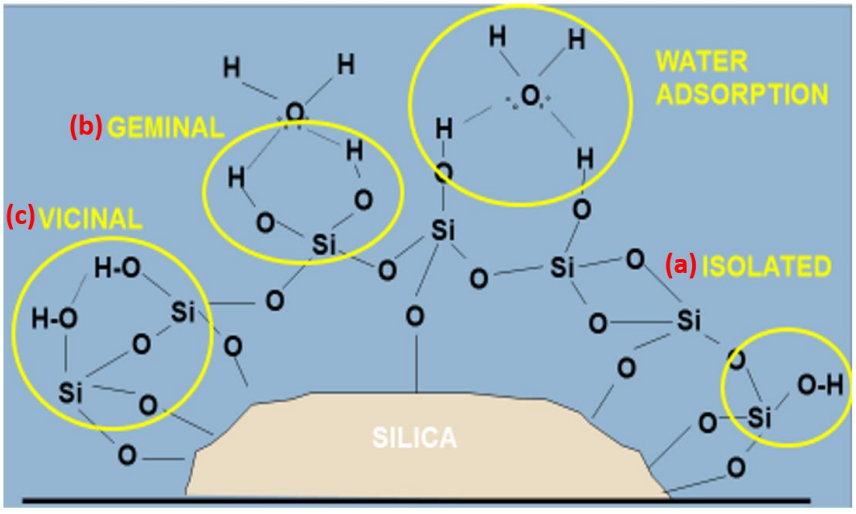

Figure 3. Silanol groups on the surface of silica: (a) isolated silanols, (b) geminal silanols, and (c) vicinal-bridged silanols. Also shown: adsorbed water.[25]

The silanol groups on the surface of the silica fillers are important for a variety of reasons, but one particular reason is because they can interact with the polysiloxane polymer backbone through hydrogen bonding. The polymer chains become adsorbed on the surface of the silica due to the wetting of the filler by the polymer.[21,26,27] These interactions hinder the mobility of the polymer chains, thus reinforcing the filled material

and improving the thermal, mechanical, and rheological properties.[17,28] The interaction between a surface functional group of a silica particle and the polymer backbone is shown in Figure 4.

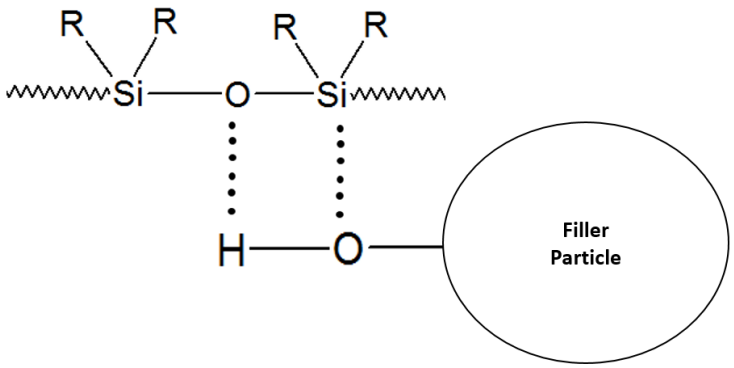

Figure 4. Interaction of a surface silanol group of a silica particle and the polymer backbone.

Not only can the surface silanol groups interact with the polysiloxane polymer backbone, they can also interact with each other, through a process called aggregation. Aggregation can occur during the production of the silica fillers, as well as through compounding, as the particles are being distributed throughout the polymer matrix. Aggregation occurs as a result of the high surface area of silica fillers. Silica fillers with large surface areas contain an abundance of silanol groups that can interact with each other through hydrogen bonding to create an aggregated network structure.[21,27,29-31] An aggregated network structure of silica particles with their surface silanol groups is displayed in Figure 5.[32] Smaller particles can aggregate more rapidly than larger particles due to the ability of the smaller particles to pack closer together.

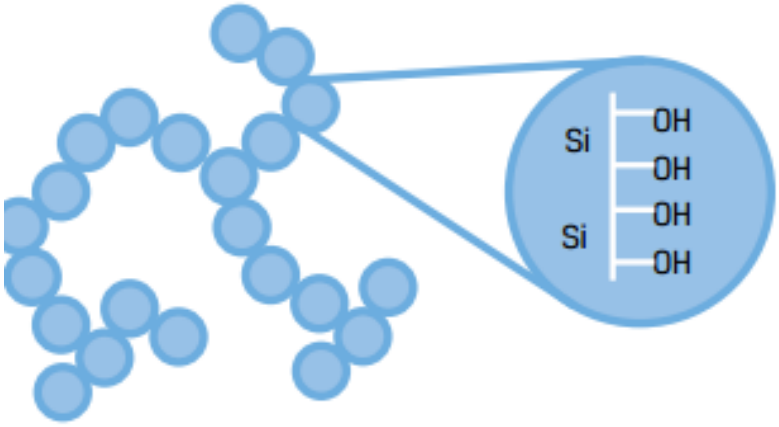

Figure 5. Aggregated network structure of silica particles with surface silanol groups.[32]

As fillers begin to aggregate, the aggregates also can interact with the polymer backbone. Fillers with smaller diameters and larger surface areas usually provide greater interaction and reinforcement for polysiloxane elastomers compared to fillers with smaller surface areas as a result of the additional functional groups that may potentially interact with the polymer backbone.[21-23] The interaction between aggregates and the polymer backbone increases the thermal, mechanical, and rheological properties. The network structure generates a protective barrier that disrupts the release of the cyclic volatiles during thermal decomposition, thus enhancing thermal stability. The substantial number of interacting bonds strengthens the filled material, enhancing the mechanical properties. Finally, the aggregated network structure hinders the mobility of the polymer chains to enhance the rheological properties.[21,27,31,33-43]

Although silica aggregation can enhance the aforementioned polymer properties, it can also disrupt these properties at higher aggregation levels. Silica prefers to interact with other silica particles, thus aggregated network structures can further interact with other separate aggregates to create sizable agglomerates. An agglomerate is considered a collection of silica aggregates. Figure 6 shows a filler network structure comprised of

aggregates and agglomerates.[44] Agglomeration can occur as a result of the filler not being evenly distributed throughout the polymer matrix and they interact more with each other and assemble together to form larger particles, instead of interacting with the polymer backbone and reinforcing the elastomer.[1,45,46] Massive agglomerates can reduce the polymer properties of the filled materials by disrupting the ability of the silanol groups on the filler particles that make up the agglomerate to interact with the polymer backbone. In turn, they act as mechanical faults and reduce mechanical and rheological properties, as they assume a substantial amount space in the polymer matrix.[21,29,31,37,47-50]

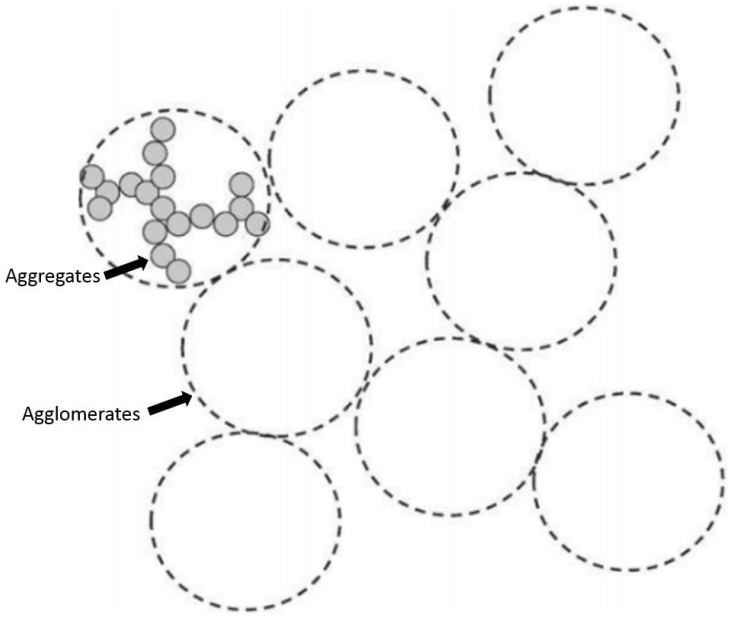

Figure 6. Filler network structure comprised of aggregates and aggloermates.[44]

In filled polysiloxane systems, the polymer properties can be additionally reduced due to polysiloxanes being traditionally hydrophobic. The hydrophobic nature of polysiloxanes in these particular systems result in poor wetting of the silica surface and the polysiloxane matrix. This phenomenon was reported by DeGroot and coworkers comparing rheological properties of silica-filled PDMS to silica-filled polyisoprene. The

results indicated that the rheological properties of silica-filled PDMS were four orders of magnitude lower than the rheological properties of silica-filled polyisoprene, indicating poor wetting and poor reinforcement with the silica-filled PDMS.[21]

In addition to the incorporation of fillers, elastomers possess enhanced mechanical properties due to the process of vulcanization, or crosslinking of rubber. The vulcanization process consists of chemical reactions that create permanent covalent bonds known as crosslinks between adjacent molecules, which results in a complex interconnected network structure.[1,51] The crosslinks contribute to the elastomeric properties by preventing the individual polymer chains from slipping past each other, even when heated.[51] However, because the crosslinks are permanent bonds, if excessive heat and extreme stresses are applied to the crosslinked elastomers, the crosslinks will break and are unable to be reformed, which results in material degradation.[52] The activated cure method is one typical approach for vulcanizing polysiloxane elastomers. This method uses a crosslinking agent, generally an organic peroxide, together with heat and pressure to accomplish vulcanization. The conditions under which vulcanization is performed, the degree of crosslinking, and the chemical nature of the crosslinks determine the mechanical properties of elastomers.[1] After the elastomers are filled and crosslinked, the tensile strengths of the elastomers can increase up to 40 times more than if the elastomers were unfilled.

Filled polysiloxane elastomers can be used in various applications in extreme temperatures for long periods of times. The most common applications for polysiloxane elastomers are O-rings, gaskets, and sealants that are used in the aircraft/aerospace, military, and automotive industries. These elastomeric products include but are not

limited to door seals for aircraft and oven doors, belts for conveyor lines, engine and transmission seals, and protective coatings for jets, submarines, and rockets.[1,53]

1.4 Twin-screw extrusion compounding

Fillers are incorporated into polysiloxanes to produce novel polysiloxane elastomers through a process called compounding. If each new application required a novel polysiloxane polymer to be synthesized, the use of polysiloxanes would become cost-prohibitive. However, existing polysiloxane materials can be tailored to a variety of applications at a more reasonable cost through the process of compounding. There are various methods of compounding that utilize various equipment, such as internal mixers, two-roll mills, torque rheometers, or twin-screw extruders.[10,54-58] Twin-screw extrusion compounding is arguably the best process for producing polysiloxane elastomers because it is a versatile, efficient, and continuous process.[10,58]

The process of twin-screw extrusion blends various stabilizers, additives, and fillers with various polymers or base resins to prepare specialized plastic formulations.[10,58] Not only is twin-screw extrusion versatile and efficient, it also prevents agglomeration of filler particles, which is difficult to accomplish by the other compounding methods mentioned. The mechanical shearing of the screws and barrel pulverizes the agglomerates into single particles and disperses the particles evenly throughout the polymer matrix to give the compounded material enhanced properties that it did not have prior to compounding.[21,23,27,29,38,58,59] Figure 7 shows the breakdown of the filler agglomerates into single particles by twin-screw extrusion.[58]

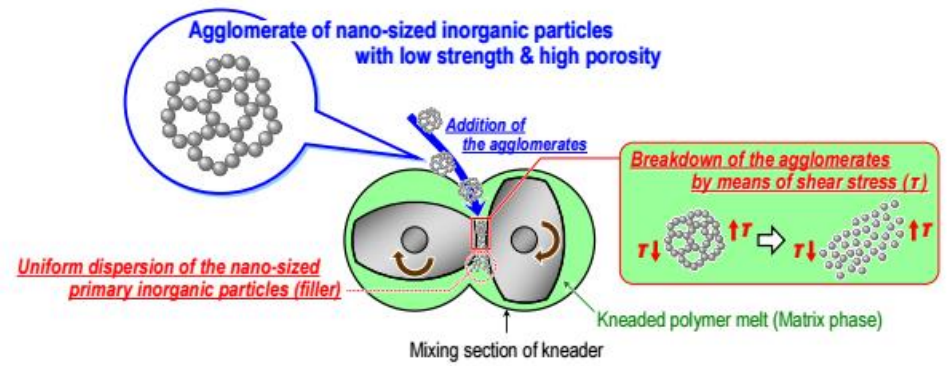

Figure 7. Breakdown of the filler agglomerates into single particles by twin-screw extrusion.[58]

Twin-screw extrusion may employ one of two types of screw rotation: counter-rotating or co-rotating screws. The direction of rotation for counter-rotating and co-rotating screws are shown in Figure 8.[60] Counter-rotating extruders obtain high-pressure buildup during processing as a result of the screws rotating in opposite directions. Co-rotating extruders achieves higher degrees of mixing during processing as a result of the screws rotating in the same direction.[61,62] Extrusion screws are evaluated by their length to diameter, or L:D ratio. The L:D ratio is the ratio of the length of the screw to the outside diameter of the screw. A common L:D ratio is 20:1, but longer extruders of 30:1 or 40:1 L:D ratios have been manufactured. Higher degrees of mixing can be achieved with larger L:D ratios that results in a more homogeneous mixture.[63]

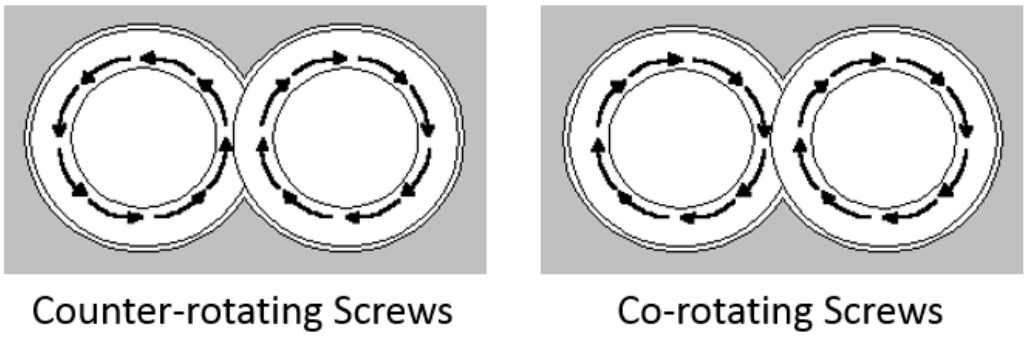

Figure 8. The direction of rotation for counter-rotating and co-rotating screws.[60]

The two screws of a twin-screw extruder contain various screw elements than can be configured to further improve the mixing capability of the extruder and achieve different material properties in the compounded extrudate.[10] The various screw elements and screw configurations make the twin-screw extrusion compounding process very advantageous for producing polysiloxane elastomers. Figure 9 displays the extrusion screws that contain various screw elements used for twin-screw extrusion compounding.[64]

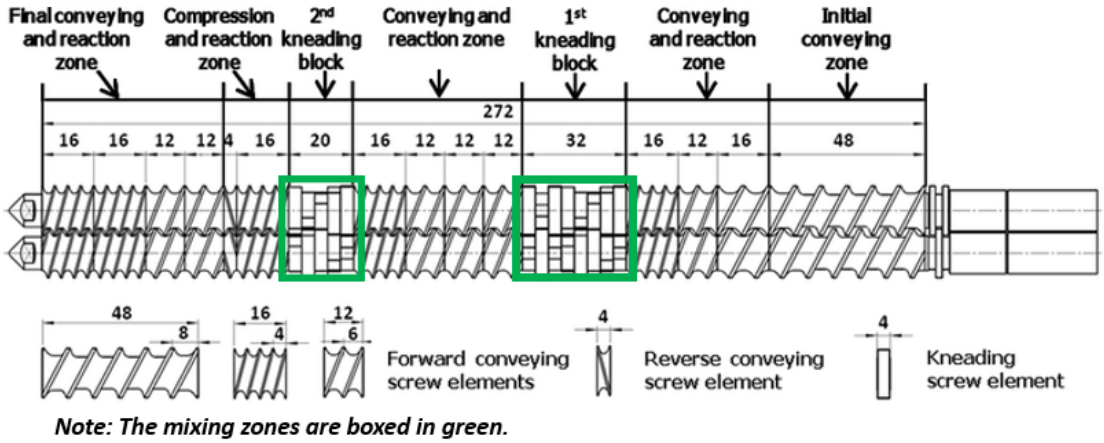

Figure 9. Extrusion screws containing various screw elements used for twin-screw extrusion compounding.[64]

Numerous screw elements consist of conveying and kneading elements that can be incorporated into the screws to provide appropriate pressure build up, elongation flow, shearing, and mixing to properly blend the plastic formulation. The two screws can be divided up into seven sections: the initial conveying zone, the conveying and reaction zone, the first kneading block (mixing zone), another conveying and reaction zone, the second kneading block (mixing zone), the compression and reaction zone, and the final conveying and reaction zone.[64]

The initial conveying zone consists of forward conveying elements to transport the material from the hopper forward. The materials that are to be compounded are gravity fed from the hopper and conveyed forward by the rotation of the screws in the initial conveying zone. The flights of the screws in this zone are generally the largest for proper conveying of the materials and the channel depth of the screws are typically the same throughout the zone.[64] The material is transported from the initial conveying zone to the conveying and reaction zone where the barrel's channel depth and the flights of the screws get progressively smaller. The mixing zones consist of kneading elements or kneading disks that are typically staggered at 30°, 45°, 60°, and 90° angles to produce high shearing stresses on the materials to provide intensive mixing. The kneading elements also contain very small clearances between the disks and between the barrel surfaces to further enhance mixing.

The material moves through additional conveying and reaction zones as well as additional mixing zones depending on the screw design and the screw configuration. Towards the end of the compounding process, the material proceeds to the compression and reaction zone that consists of backward-conveying or reverse screw elements. These elements hold the material in this specific area of the screw for a longer amount of time with severe compression to provide one last opportunity for thorough mixing. The final conveying and reaction zone conveys the material to the end of the extruder and the material is guided through a die and exits the extruder.[64,65]

1.5 Rheology and rheometry

Rheology is the science of studying the deformation and flow of matter. It is commonly reported that the incorporation of additives, such as fillers, can enhance the

rheological properties in the filled materials.[29-77] The filler can interact with the polymer backbone and restrict the mobility of the polymer chains. Regarding the polymer-filler interaction, a filler particle can be imagined as a hard core surrounded by a polymer shell that exhibits little mobility. Generally, filled materials only exhibit reinforcement characteristics as long as a parameter known as the *percolation threshold* is reached.[39,66] The percolation threshold is defined as the minimum critical amount of filler required for the material to convert from a liquid-like to solid-like material by promoting interactions between the filler and polymer matrix.[21,27,29,67,68] When the percolation threshold of the filled materials is reached, the material exhibits viscoelastic behavior.[66,69]

In addition to the interactions between the filler and the polymer matrix, aggregation of filler particles is another reinforcing mechanism in filled materials.[21,27,31,39-43] Aggregation is the supreme reinforcing mechanism in filled materials as aggregates are dispersed throughout the matrix and interact with the polymer chains. Polymer adsorption on the aggregated filler particles restricts the mobility of the chains.[27,29,31,39,70] The creation of an aggregated network structure interacts with the polymer matrix to exhibit viscoelastic behavior in the materials.[21,39]

Rheometry investigates materials in simple flows, such as oscillatory-shear flow.[71] Oscillatory rheometry is a dynamic rheological technique that consists of applying a low-amplitude oscillatory shear stress that increases in a sinusoidal fashion to a material as the analysis progresses. The procedure measures the elastic and viscous behavior of the filled materials simultaneously by determining the storage modulus (G') and loss modulus (G").[39,72,73] The storage modulus expresses the elastic component of the testing material and represents the energy stored and recovered in the system. When the storage

modulus is greater than the loss modulus, it indicates that the material is highly elastic. The loss modulus expresses the viscous component of the material and represents the energy lost in the system. When the loss modulus is greater than the storage modulus, it indicates that the material is more viscous than elastic.[40,73,74]

Oscillatory rheometry can also measure the yield stress of filled materials. The yield stress is the force at which the internal network structure of a filled material is adequately destroyed to initiate flow.[21,30,41,72,74,75] The yield stress is dependent on the network structure of the material and is the stress at which the material converts from solid-like to liquid-like.[66,75] During oscillatory analysis of a typical viscoelastic material, the viscosity, storage modulus, and loss modulus for a "typical" viscoelastic material begins to increase. This is the result of low shearing on the material that further distributes the silica particles throughout the matrix and further constructs an aggregated network structure.[43,76] As the analysis progresses, the yield stress is reached and the viscosity, storage modulus, and loss modulus begin to decrease and the material begins to flow. One approach of determining the yield stress of silica-filled materials is the point at which the storage modulus (G') and the loss modulus (G") curves intersect. This is demonstrated in Figure 10. The aggregates are destroyed as the analysis continues by elevated shearing until the yield stress is obtained and the aggregated network structure is dismantled.[41,43,70,72,77,78] Given enough time after the conclusion of the analysis, the network structure will eventually recover and return to its original state, in a phenomenon known as thixotropy.[29,39,42, 66,73,75]

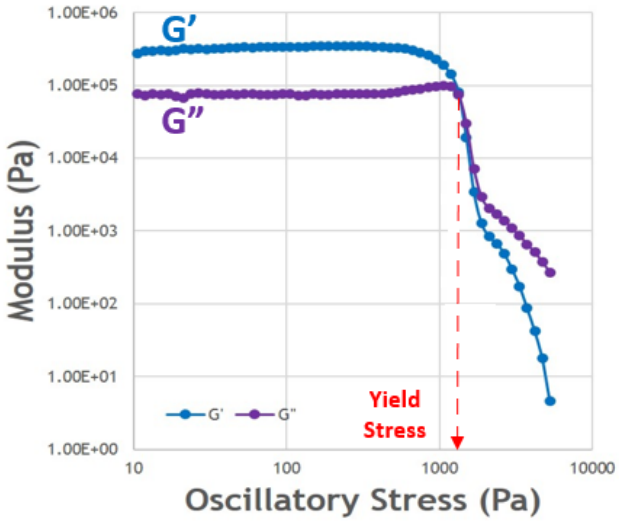

Figure 10. Storage and loss modulus versus oscillatory stress for a typical filled material. Yield stress is determined by the point where the G' (•) and G" (•) curves intersect.

Thixotropy is a material property demonstrated by a time-dependent decrease in viscosity under a constant shear stress or shear rate that is followed by a gradual recovery in viscosity when the shear stress is removed. The flow properties and the thixotropic behavior of filled materials are generally dependent on the size of the filler, the filler loading amount, the interactions between the filler and the polymer matrix, and the interactions between the filler particles.[78] Flow rheology is a dynamic rheological technique that evaluates the thixotropic behavior of a filled material by controlling the shear rate in two stages to generate a thixotropic or hysteresis loop. Figure 11 displays a typical thixotropic loop.[79] The first stage of analysis consists of increasing the shear rate over time until a maximum shear rate is obtained, generating an "up" curve. The second stage consists of decreasing the shear rate to zero, generating a "down" curve. The area between the up and down curves make up the thixotropic loop. A large thixotropic area between the up and down curves demonstrates that the filled system requires a longer time for the network structure to be reconstructed.[80]

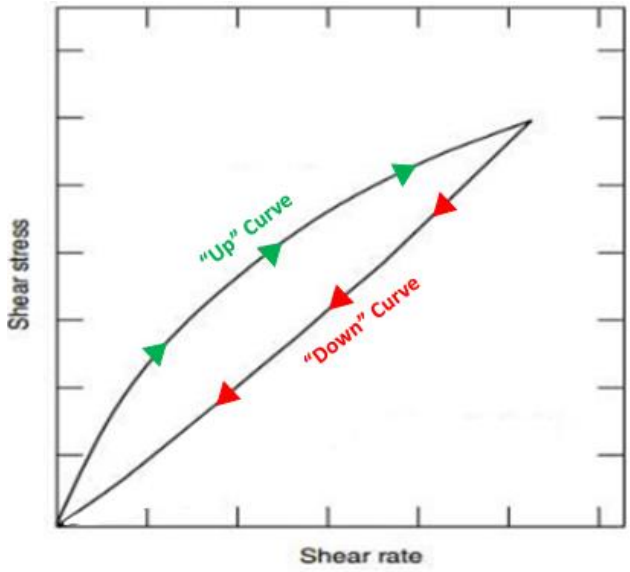

Figure 11. A typical thixotropic loop.[79]

During the first stage of the flow rheology procedure, the viscosity of the filled materials decreases as the shear rate increases. This is attributed to the destruction of the filler network structure by the increased shear rates that break the hydrogen bonds between the filler and polymer matrix, as well as the bonds between the filler particles. During the second stage of the flow rheology procedure, the viscosity of the filled materials increases as the shear rate decreases. This is attributed to the reconstruction of the filler network structure over time. The hydrogen bonds between the filler and polymer, as well as the bonds between the filler particles, begin to reform until the original network structure is obtained.[21,80] The particle interactions in thixotropic materials are displayed in Figure 12.[81]

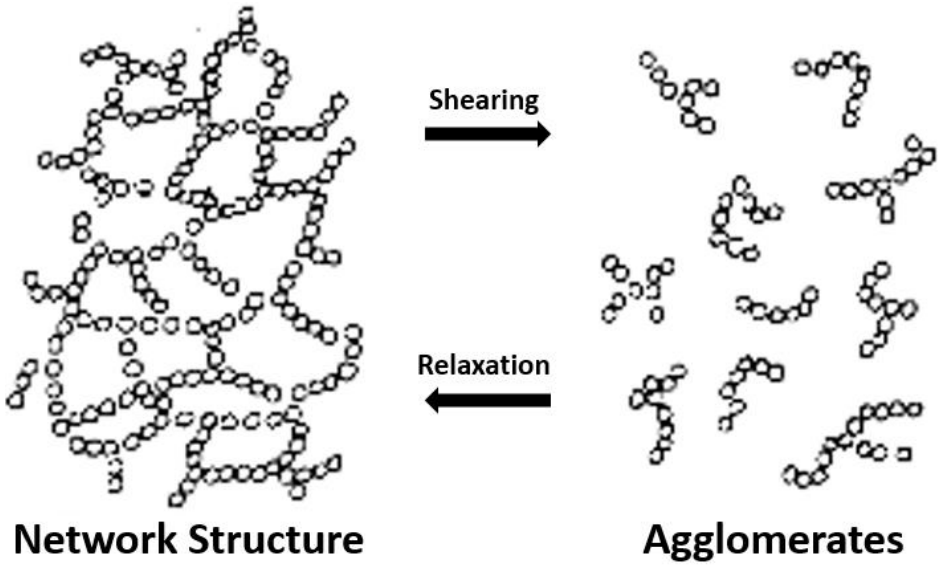

Figure 12. Particle interactions in thixotropic materials.[81]

This thesis evaluates the interactions between polysiloxanes and reinforcing fillers compounded using twin-screw extrusion. Model polysiloxanes and experimentally-synthesized polysiloxanes were filled and characterized. The materials processed by twin-screw extrusion were evaluated for their thermal stability, filler dispersion in the polysiloxane matrix, yield stress, and thixotropic behavior by thermogravimetric analysis and rheological characterization, respectively. In each case, the filled polysiloxane materials were compared to a commercially-available silicone resin to evaluate the formulations for their efficacy in applications in which the commercial resin is currently utilized.

CHAPTER II

2. OBJECTIVES

2.1 Evaluate effects of twin-screw extrusion on traditional thermoplastic materials

The effects of twin-screw extrusion on four traditional thermoplastic materials utilizing a lab-scale twin-screw extruder were investigated. The extruder, known as the Process 11, was applied to compound amorphous and semi-crystalline thermoplastic materials. The compounded materials were evaluated to ensure the formulations were appropriate for injection molding, the prime manufacturing process in the plastics industry. The process conditions to demonstrate the appropriate injection molding formulation included the following steps:

1) Extruding the plastic materials using the Process 11

2) Grinding up the compounded extrudate material

3) Injection molding the ground up material

The thermal and mechanical polymer properties of the materials were evaluated to determine the effects on the properties by different processing methods, such as extrusion processing, subsequent regrinding, and injection molding. The extrudate and injection molded test bar samples were characterized by thermogravimetric analysis (TGA), differential scanning calorimetry (DSC), capillary rheometry, and tensile testing.

2.2 Determine compounding effectiveness of twin-screw extrusion

Subsequent to the evaluation of the Process 11 on four thermoplastic materials, the compounding effectiveness was determined by twin-screw extrusion. The Process 11 was used to compound an amorphous Starex thermoplastic formulation with titanium dioxide (TiO_2). The dispersion of the TiO_2 filler in the Starex matrix was evaluated for the overall formulation. The process conditions to demonstrate the appropriate compounded formulation included the following steps:

1) Compounding the formulation using the Process 11

2) Grinding up the compounded formulation

3) Injection molding the ground up material

The effect of the TiO_2 filler had on the polymer properties was determined by characterizing the thermal and mechanical properties. The extrudate and injection molded test bar samples were characterized by TGA, DSC, tensile testing, and scanning electron microscopy (SEM).

2.3 Compound polysiloxanes by twin-screw extrusion

Various model and synthesized polysiloxanes were compounded with silica fillers by twin-screw extrusion and were evaluated. The Process 11 was used to compound two commercially-available model polysiloxanes with three synthetic, amorphous silica fillers to produce well-mixed silica-filled polysiloxane extrudate materials.

Prior to compounding, the silica fillers were premixed into the polysiloxanes in order to more conveniently feed the materials into the extruder. The premixed materials were then hand-fed into the Process 11 to be further mixed and processed into extrudate materials. The resulting compounded materials were expected to possess high thermal

stability and desirable rheological characteristics prior to vulcanization. The composition, uniformity, and physical properties of the filled polysiloxane materials were evaluated by TGA, oscillatory rheometry, and flow rheology.

The compounded materials were characterized by their filler dispersion, yield stress, and thixotropic behavior. Processing parameters, filler content, and filler type were evaluated to determine the processing conditions needed to obtain an appropriate yield stress and thixotropic behavior in the filled materials. All filled materials were compared to an existing commercial reference silicone material. The two model copolymers were vinyl-terminated and are listed as follows:

- Polydimethylsiloxane (PDMS) with a molecular weight of 28,000 g/mol
- Dimethyl- 3.0-3.5% diphenylsiloxane copolymer with a molecular weight of 27,000 g/mol

The three synthetic, amorphous silica fillers are listed as follows:

- Hi-Sil™ 135 (Hi-Sil-135): synthetic reinforcing precipitated silica filler
- Hi-Sil™ 233-D (Hi-Sil-233D): synthetic reinforcing precipitated silica filler
- Cab-O-Sil® M-7D (Cab-O-Sil): synthetic reinforcing fumed silica filler

2.4 Characterize model components and evaluate filled PDMS

The model polymers were characterized by gel permeation chromatography (GPC), DSC, and TGA to evaluate the molecular weight, low-temperature crystallization, and thermal stability of the polymers prior to compounding. The silica fillers were characterized by SEM and TGA to evaluate the filler particle size, purity, and water content of the fillers. PDMS was compounded with the three fillers at various processing

temperatures and filler loadings. The resulting filled materials were compared to a reference silicone and evaluated by TGA, oscillatory rheometry, and flow rheology.

2.5 Evaluate filled model copolymer

The model copolymer was compounded with the three fillers at different processing temperatures and filler loadings. The resulting compounded materials were compared to a reference silicone and evaluated by TGA, oscillatory rheometry, and flow rheology. The appropriate processing parameters, filler content, and filler type were determined for use in compounding the experimentally-synthesized polysiloxanes using the results of the model copolymer.

2.6 Evaluate filled synthesized polysiloxanes

The synthesized polysiloxanes were linear, high molecular weight materials that possessed little to no branching, good low-temperature properties, no crystallinity, and maintained their desirable surface- and high-temperature properties. The four synthesized polysiloxanes contained various dimethyl-, diphenyl-, and diethyl-containing siloxane units, were vinyl-terminated, had an average molecular weight of 60,000 g/mol, and are listed as follows:

- Dimethyl- 5.3 mol% diphenylsiloxane copolymer with a degree of polymerization of 740 (DiMeDiPh$_{5.3}$-740)
- Dimethyl- 5 mol% diethylsiloxane copolymer with a degree of polymerization of 780 (DiMeDiEt$_5$-780)
- Dimethyl- 8 mol% diethylsiloxane copolymer with a degree of polymerization of 780 (DiMeDiEt$_8$-780)

- Dimethyl- 5.3 mol% diphenyl- 5 mol% diethylsiloxane copolymer with a degree of polymerization of 720 ($DiMeDiPh_{5.3}DiEt_5$-720)

The four synthesized polysiloxanes were characterized by GPC, DSC, and TGA to evaluate the molecular weight, low-temperature crystallization, and thermal stability of the polymers. The copolymers were compounded with 20 wt% Cab-O-Sil filler at 40°C. The resulting compounded materials were compared to a reference silicone and evaluated by TGA, oscillatory rheometry, and flow rheology.

CHAPTER III

3. EXPERIMENTAL

3.1 Materials

3.1.1 Thermoplastic materials

Two general purpose thermoplastic materials and two engineering thermoplastic materials were evaluated to determine the effects of processing by the Process 11 on the materials. The amorphous general purpose thermoplastic material was high heat crystal (clear) polystyrene from AmStyrenics (The Woodlands, Texas, United States).[82] The semi-crystalline general purpose thermoplastic material was homopolymer polypropylene, similar to Polystone® P polypropylene from Professional Plastics (Fullerton, California, United States).[83] The amorphous engineering thermoplastic material was Lexan® 143R polycarbonate from SABIC Innovative Plastics (Pittsfield, Massachusetts, United States).[84] The semi-crystalline engineering thermoplastic material was Capron® 8200 NL Nylon 6 from Honeywell (Morris Plains, New Jersey, United States).[85]

Starex acrylonitrile butadiene styrene (ABS) MP-0160R from Lotte Advanced Materials (Uiwang-si, Gyeonggi-do, South Korea)[86] and HITOX® STD titanium dioxide

(TiO_2) from TOR Specialty Minerals (Corpus Christi, Texas, United States)[87] were used to determine the compounding effectiveness of the Process 11.

3.1.2 Commercial polysiloxanes

Two commercially-available model polysiloxanes were evaluated utilizing the Process 11 to determine the appropriate processing parameters for polysiloxane materials. The first commercially-available product was a vinyl-terminated polydimethylsiloxane polymer (PDMS) DMS-V31 with a molecular weight of 28,000 g/mol. The second commercially-available product was a vinyl-terminated (3.0-3.5% diphenylsiloxane)-dimethyl siloxane copolymer (model copolymer) PDV-0331 with a molecular weight of 27,000 g/mol. Both commercially-available model polysiloxanes were purchased from Gelest (Morrisville, Pennsylvania, United States).[90]

3.1.3 Commercial fillers

Three commercial synthetic amorphous silica fillers were utilized for filling model and synthesized polysiloxanes. Hi-Sil™ 135 (Hi-Sil-135) synthetic precipitated silica filler was purchased from PPG (College Station, Texas, United States)[88] with particles ranging from 44 to 54 µm in size and a surface area of 150 m^2/g. Hi-Sil™ 233-D (Hi-Sil-233D) synthetic precipitated silica filler was also purchased from PPG (College Station, Texas, United States)[88] with particle sizes ranging from 64 to 77 µm and a surface area of 151 m^2/g. Cab-O-Sil® M-7D (Cab-O-Sil) synthetic fumed silica filler was purchased from Cabot Corporation (Alpharetta, Georgia, United States)[89] with particles of 38 µm in size and a surface area of 200 m^2/g.

3.1.4 Synthesized polysiloxanes

Four vinyl-terminated polysiloxanes were synthesized by anionic ring-opening polymerization of a mixture of cyclic siloxanes with equilibration followed by thermal decomposition of the transient initiator/catalyst. The synthesis was performed by Alisa Zlatanic and Dragana Radojcic at the Kansas Polymer Research Center (Pittsburg State University, Pittsburg, Kansas, United States). The anionic ring-opening polymerization reaction of the synthesized polysiloxanes are shown in scheme 5. The mixture of cyclic siloxanes contained octamethylcyclotetrasiloxane, octaphenylcyclotetrasiloxane, and hexaethylcyclotrisiloxane. The initiator/catalyst used for the reaction was tetramethylammonium silanolate. The molecular weight of the copolymers was controlled by a vinyl end blocker, dimethylvinyl terminated oligomeric dimethylsiloxane.

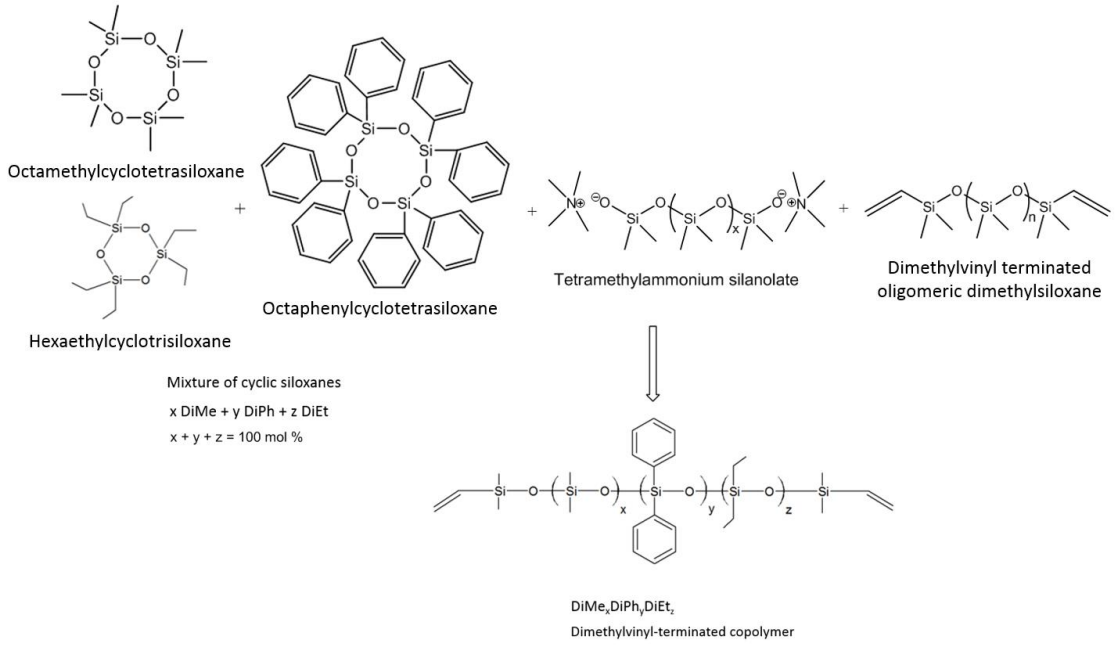

Scheme 5. Anionic ring-opening polymerization reaction of the synthesized polysiloxanes.

The four-synthesized vinyl-terminated polysiloxanes possessed an average molecular weight of 60,000 g/mol. The polysiloxanes contained dimethyl-, diphenyl-, and diethyl-containing siloxane units: a dimethyl, 5.3 mol% diphenyl copolymer ($DiMeDiPh_{5.3}$-740); a dimethyl, 5 mol% diethyl copolymer ($DiMeDiEt_5$-780); a dimethyl, 8 mol% diethyl copolymer ($DiMeDiEt_8$-780); and a dimethyl, 5.3 mol% diphenyl, and 5 mol% diethyl copolymer ($DiMeDiPh_{5.3}$-$DiEt_5$-720). The characterization of the vinyl-terminated polysiloxanes was performed by Mei Wan, Alisa Zlatanic, and Dragana Radojcic at the Kansas Polymer Research Center (Pittsburg State University, Pittsburg, Kansas, United States). The properties of the four synthesized polysiloxanes are given in Table 2.

Table 2. Properties of the four synthesized polysiloxanes.

Polysiloxane	**Degree of Polymerization**	**Viscosity (Pa·s)**	**Number-Average Molecular Weight (M_n) (g/mol)**	**Weight-Average Molecular Weight (M_w) (g/mol)**	**Polydispersity Index (PDI) (M_w/M_n)**
$DiMeDiPh_{5.3}$-740	740	24.03	41,190	65,540	1.59
$DiMeDiEt_5$-780	780	16.24	36,390	51,040	1.42
$DiMeDiEt_8$-780	780	19.49	35,890	59,470	1.66
$DiMeDiPh_{5.3}DiEt_5$-720	720	24.15	43,930	60,650	1.38

3.2 Methods

3.2.1 Thermoplastic materials processing

The Thermo Fisher Scientific Process 11 Parallel Twin-screw Extruder, Model 11 (Karlsruhe, Germany)[91] is a bench-top, lab-scale twin-screw extruder. Figure 13 displays the Process 11 twin-screw extruder. The throughput rates can range from 20 g/hr to 2.5 kg/hr with realistic screw geometry and processing conditions that can be scalable for

industrial compounding. The Process 11 contains a 40:1 L:D ratio barrel with two 11 mm fully segmented, co-rotating screws. The Process 11 includes a volumetric single screw feeder that can feed powder or pellets into the main hopper of the extruder and contains a chiller unit that circulates water through the feed throat of the extruder to maintain a consistent feed throat temperature.[92]

Figure 13. Thermo Fisher Scientific Process 11 twin-screw extruder.[92]

3.2.1.1 Effects of processing on thermoplastic materials by the Process 11

This study utilized the Process 11 twin-screw extruder to compound thermoplastic materials to demonstrate that any plastic formulation compounded using the Process 11 was appropriate for injection molding. Extrusion was followed by subsequent regrinding, and finally, injection molding to determine the effect that processing would have on thermal and mechanical polymer properties. Additionally, the differences in thermal and mechanical properties were compared between amorphous and semi-crystalline polymers to determine if they were impacted differently by processing.

Figure 14 displays the process chart that was used to determine the effects of processing using the Process 11 twin-screw extruder. All thermoplastic materials were

dried by an AEC Whitlock Desiccant Bed Drying Hopper, Model DH-3 OMIC HE-Q (New Berlin, Wisconsin, United States).[93] Plastic materials can hold moisture on the pellets' surface, which requires proper drying for effective processing. Each material has a recommended drying temperature and drying time depending on the hygroscopicity of the material. Table 3 displays the drying parameters used for each thermoplastic material.

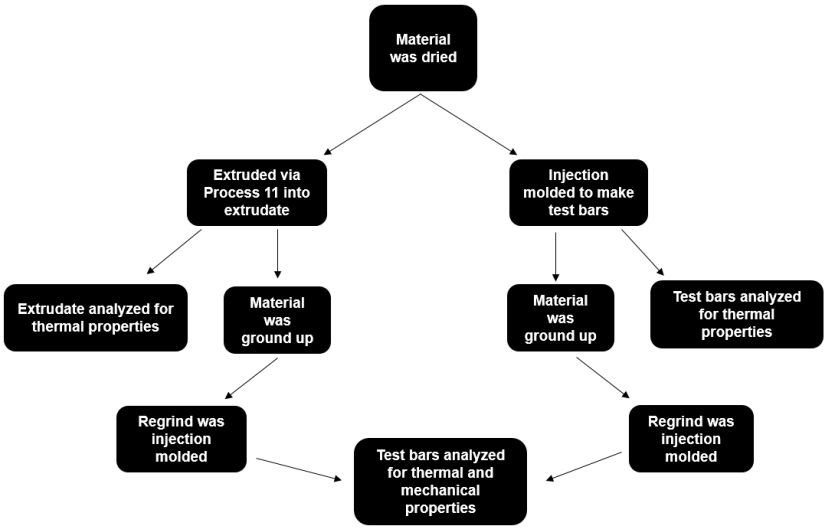

Figure 14. Process chart for determining the effects of processing using the Process 11 twin-screw extruder.

Table 3. Drying parameters used for each thermoplastic material.

Material	Drying Temperature (°C)	Drying Time (hours)
Polystyrene	70	2
Polypropylene	70	2
Polycarbonate	100	12
Nylon-6	90	24
Starex	80	12

Half of the dried virgin thermoplastic material was extruded using the Process 11. The extrudate was then ground using a Rotogran Plastic Granulator, Model PH-88

(Ontario, Canada).[94] The regrind material was then injection molded using Arburg Allrounder Injection Molding Machine, Model 320S 500-150 (Stammhaus Lossburg, Germany)[95] to produce test bars that were used for thermal and mechanical analysis. The other half of the dried virgin thermoplastic material was injection molded to produce test bars. The test bars were ground up using a Rotogran plastic granulator to be injection molded again to produce test bars for thermal and mechanical analysis. The extrudate and injection molded test bar samples were characterized by thermogravimetric analysis (TGA), differential scanning calorimetry (DSC), capillary rheometry, and tensile testing.

3.2.1.2 Compounding effectiveness of the Process 11

This study determined the compounding effectiveness of the Process 11 twin-screw extruder by compounding a Starex and TiO_2 formulation to evaluate the dispersion of the TiO_2 filler in the Starex matrix. Extrusion/compounding was followed by regrinding, and finally, injection molding to determine the effect of the TiO_2 filler would have on the thermal and mechanical polymer properties compared to the unfilled Starex materials.

The Starex material was dried by an AEC Whitlock desiccant bed drying hopper. Half of the dried Starex material was filled with TiO_2 filler and extruded/compounded using the Process 11 to produce extrudate. The extrudate was ground up using a Rotogran plastic granulator to be dried a second time. The dried regrind was then injection molded using an Arburg Allrounder injection molding machine to produce test bars for thermal and mechanical analysis. The other half of the dried virgin material was injection molded to produce test bars for thermal and mechanical analysis. Figure 15 displays the process chart that was used to determine the compounding effectiveness using the Process 11.

The extrudate and injection molded test bar samples were characterized by thermogravimetric analysis (TGA), differential scanning calorimetry (DSC), tensile testing, and scanning electron microscopy (SEM).

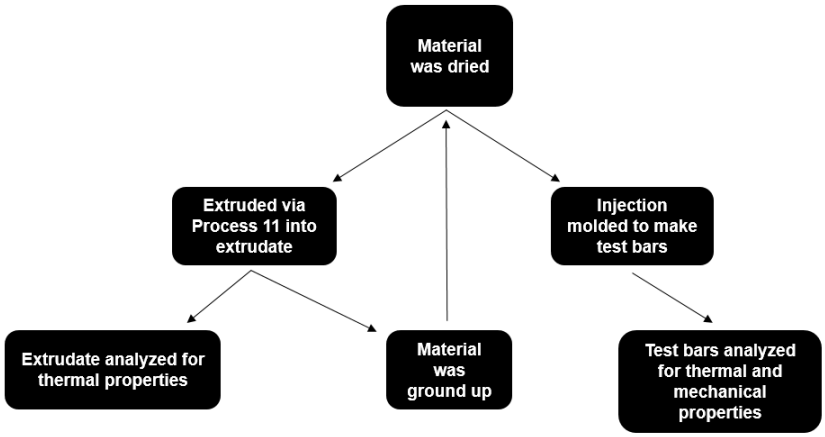

Figure 15. Process chart for determining the compounding effectiveness using the Process 11.

3.2.1.3 Compounding thermoplastic materials

Each thermoplastic material (500 g) was extruded/compounded using the Process 11 twin-screw extruder. Table 4 displays the extrusion/compounding parameters used for each thermoplastic material. Each thermoplastic material has a recommended extrusion melt temperature depending on the structure of the material. The chiller temperature was set relative to the temperature of the feed throat of the extruder. The screw speed was set relative to the speed that the material could be extruded/compounded at. The feed rate was set based on how effectively the material fed into the barrel and was expressed relative to the screw speed. The filled Starex/TiO_2 formulation consisted of Starex filled with seven weight percent (wt%) TiO_2 filler.

Table 4. Extrusion/compounding parameters used for each thermoplastic material.

Material	Extrusion Temperature (°C)	Chiller Temperature (°C)	Screw Speed (rpm)	Feed Rate (% of screw speed)
Polystyrene	210-230	20	65	10
Polypropylene	210-230	22	90	11
Polycarbonate	290-310	28	60	10
Nylon-6	250-270	28	80	8
Unfilled Starex	220-240	28	100	15
Filled Starex	225-245	28	60	-

3.2.1.4 Injection molding thermoplastic materials

Each thermoplastic material (500 g) was injection molded through an Arburg Allrounder injection molding machine. Table 5 displays the injection molding parameters used for each thermoplastic material. Each thermoplastic material has a recommended injection molding melt temperature depending on the structure of the material. Each thermoplastic material has a recommended mold temperature depending on the structure, crystallinity, and other properties of the material. The shot size, injection speeds, and holding times were set based on the shortest cycle time possible to produce reliable test bars.

Table 5. Injection molding parameters used for each thermoplastic material.

Material	Injection Temperature (°C)	Mold Temperature (°C)	Shot Size (mm)	Injection Speed (in/sec)	Holding Time (sec)
Polystyrene	188-221	32	50.8	3	1
Polypropylene	188-216	27	50.8	3	1
Polycarbonate	288-316	49	27.94	3	5
Nylon-6	238-282	49	27.94	1.5	8
Unfilled Starex	204-237	49	31.75	3	5
Filled Starex	204-237	49	31.75	3	5

3.2.2 Polysiloxane materials processing

This study utilizes the Process 11 twin-screw extruder to compound two commercially-available model polysiloxanes with three synthetic amorphous silica fillers to determine the appropriate processing parameters to develop a viable compounding process for the four synthesized polysiloxanes. Prior to compounding, the polysiloxanes and silica fillers were premixed for proper feeding into the extruder. The premixed material was then hand fed into the Process 11 twin-screw extruder to be further mixed and made into extrudate material. The resulting silica-filled polysiloxane materials were expected to possess high thermal stability and the desirable rheological characteristics prior to vulcanization for various applications. The polysiloxane compounded materials were characterized by thermogravimetric analysis (TGA), oscillatory rheometry, and flow rheology.

3.2.2.1 Premixing silica-filled polysiloxanes

Prior to compounding, the silica fillers were premixed with the polysiloxanes to prepare a paste-like material for proper feeding into the Process 11 twin-screw extruder. Table 6 shows the premixing parameters used for each silica-filled polysiloxane formulation. Premixing of polysiloxanes using the Hi-Sil-135 or Hi-Sil-233D silica fillers consisted of pouring the polysiloxanes into a 400mL beaker, adding the filler to the beaker at the desired loading level, and stirring the formulations by hand using a metal spatula until a visual homogenous mixture was obtained. Premixing of polysiloxanes with Cab-O-Sil silica filler consisted of pouring the polysiloxanes into a KitchenAid Classic 4.5 quart Mixer, Model K45SSWH (Benton Harbor, Michigan, United States),[96] adding

the filler to the mixer at the desired loading level, and stirring the formulations using the mixer until a visual homogenous mixture was obtained.

Table 6. Premixing parameters used for each silica-filled polysiloxane formulation.

Polysiloxane	Filler Type	Filler Loading Level (wt%)	Mixing Method
PDMS	Hi-Sil-135	20	Hand
Model Copolymer	Hi-Sil-135	20	Hand
PDMS	Hi-Sil-135	25	Hand
Model Copolymer	Hi-Sil-135	25	Hand
PDMS	Hi-Sil-135	30	Hand
Model Copolymer	Hi-Sil-135	30	Hand
PDMS	Hi-Sil-233D	20	Hand
Model Copolymer	Hi-Sil-233D	20	Hand
PDMS	Cab-O-Sil	20	Mixer
Model Copolymer	Cab-O-Sil	20	Mixer
$DiMeDiPh_{5.3}$-740	Cab-O-Sil	20	Mixer
$DiMeDiEt_5$-780	Cab-O-Sil	20	Mixer
$DiMeDiEt_8$-780	Cab-O-Sil	20	Mixer
$DiMeDiPh_{5.3}DiEt_5$-720	Cab-O-Sil	20	Mixer

3.2.2.2 Compounding silica-filled polysiloxanes

The premixed commercially-available polysiloxanes with the three silica fillers (100 g) were compounded through the Process 11 twin-screw extruder. The premixed synthesized polysiloxanes with the Cab-O-Sil filler (150 g) were compounded using the Process 11 twin-screw extruder. The compounding parameters used for each silica-filled polysiloxane formulation are shown in Table 7. The commercially-available polysiloxanes were filled with the three synthetic amorphous silica fillers. Each commercial polysiloxane filled formulation was processed at an extrusion temperature of 30°C, 40°C, or 50°C to determine an optimum process temperature for the polysiloxanes. The chiller temperature (25°C) was set relative to the temperature of the feed throat of the

extruder. The screw speed (75 rpm) was set relative to the mixing ability of the Process 11 twin-screw extruder.

Table 7. Compounding parameters used for each silica-filled polysiloxane formulation.

Polysiloxane	Filler Type	Filler Loading Level (wt%)	Extrusion Temperature (°C)
PDMS	Hi-Sil-135	20	30
Model Copolymer	Hi-Sil-135	20	30
PDMS	Hi-Sil-135	20	40
Model Copolymer	Hi-Sil-135	20	40
PDMS	Hi-Sil-135	20	50
Model Copolymer	Hi-Sil-135	20	50
PDMS	Hi-Sil-135	25	30
Model Copolymer	Hi-Sil-135	25	30
PDMS	Hi-Sil-135	30	30
Model Copolymer	Hi-Sil-135	30	30
PDMS	Hi-Sil-233D	20	30
Model Copolymer	Hi-Sil-233D	20	30
PDMS	Hi-Sil-233D	20	40
Model Copolymer	Hi-Sil-233D	20	40
PDMS	Hi-Sil-233D	20	50
Model Copolymer	Hi-Sil-233D	20	50
PDMS	Cab-O-Sil	20	30
Model Copolymer	Cab-O-Sil	20	30
Model Copolymer	Cab-O-Sil	20	40
Model Copolymer	Cab-O-Sil	20	50
$DiMeDiPh_{5.3}$-740	Cab-O-Sil	20	40
$DiMeDiEt_5$-780	Cab-O-Sil	20	40
$DiMeDiEt_8$-780	Cab-O-Sil	20	40
$DiMeDiPh_{5.3}DiEt_5$-720	Cab-O-Sil	20	40

3.3 Characterization methods

3.3.1 Thermal characterization

3.3.1.1 Thermogravimetric analysis

Thermogravimetric analysis (TGA) was used to determine the thermal stability of the thermoplastic materials by using a TA Instruments Thermogravimetric Analyzer,

Model Q50 (New Castle, DE United States).[97] All experiments were purged with nitrogen gas (60 mL/min purge flow rate), using standard aluminum pans at a heating rate of 10°C/min to 600°C. The onset of degradation temperatures for each material were recorded by TA Universal Analysis software.

TGA was used to evaluate the distribution of filler in the silica-filled polysiloxane materials by using a thermogravimetric analyzer, also. An even distribution of filler was determined by observing the percent residue of three specimens per compounded extrudate material. All experiments were purged with nitrogen gas (60 mL/min purge flow rate), at a heating rate of 10°C/min to 700°C. The three specimens tested per extrudate material were taken from the beginning of the compounding process, middle of the compounding process, and end of the compounding process. The temperature at 10% and 50% weight loss, as well as the residue percentage values of the compounded materials were recorded by TA Universal Analysis software.

3.3.1.2 Differential scanning calorimetry

Differential scanning calorimetry (DSC) was used to determine the glass transition temperature (T_g), melting temperature (T_m), and crystallization temperature (T_c) of the thermoplastic materials using a TA Instruments Differential Scanning Calorimeter, Model Q100 (New Castle, DE United States).[97] All experiments were purged with nitrogen gas (50 mL/min purge flow rate), using hermetic aluminum pans. The material was first equilibrated to -80°C. The first heating cycle was used to erase the previous thermal history of the materials at a heating rate of 10°C/min to 250°C or 280°C, depending on the material tested. The materials were then cooled at a cooling rate of 10°C/min to -80°C. The main heating cycle temperature for each material was set based

on the degradation temperatures displayed by the TGA thermograms at a heating rate of 10°C/min to 250°C or 280°C. The T_g, T_m, and T_c for each material were recorded by TA Universal Analysis software.

DSC was used to examine the melting behavior and the T_m of the commercially-available and the experimentally-synthesized polysiloxanes by using a differential scanning calorimeter, also. All experiments were purged with nitrogen gas (50 mL/min purge flow rate), using hermetic aluminum pans. The polymers were heated at a heating rate of 10°C/min to 50°C, then cooled at a cooling rate of 10°C/min to -80°C. The main heating cycle for the polymers were heated at a heating rate of 10°C/min to 50°C. The melting behaviors for each polymer were evaluated and the T_m was recorded for polysiloxanes by the TA Universal Analysis software.

3.3.2 Rheological characterization

3.3.2.1 Capillary rheometry

Capillary rheometry was performed on polypropylene by a Malvern Rosand Capillary Rheometer, RG2000 (Malvern, UK).[98] The tests were performed at 230°C and the instrument calculated the viscosity of the polypropylene material at shear rates of 50 sec^{-1}; 100 sec^{-1}; 200 sec^{-1}; 500 sec^{-1}; 1,000 sec^{-1}; 2,000 sec^{-1}; and 5,000 sec^{-1}. This shear rate range was chosen because shear rates from 100 sec^{-1} to 10,000 sec^{-1} are common during extrusion/compounding or injection molding.[99]

3.3.2.2 Oscillatory rheometry

Oscillatory rheometry was used to determine the rheological responses and yield stresses of the filled polysiloxane materials by using a TA Instruments Rotational

Rheometer, Ltd AR2000EX (New Castle, DE United States)[97] with a 40 mm diameter steel flat plate and a 1 mm gap at 25°C. The frequency was kept constant at 1 hertz and an oscillatory stress sweep from 3 Pa to 5,000 Pa was applied to the Hi-Sil-135-filled and the Hi-Sil-233D-filled formulations, and an oscillatory stress sweep from 3 Pa to 10,000 Pa was applied to the Cab-O-Sil-filled formulations and the reference silicone. The results were obtained by TA Data Analysis software.

3.3.2.3 Flow rheology

A rotational rheometer was used to perform flow rheology on the compounded materials, also. The rheometer used a 40 mm diameter steel flat plate and a 1 mm gap at 25°C. A linear shear rate from 0.01 sec^{-1} to 10 sec^{-1} was applied to the filled formulations, followed by a linear shear rate from 10 sec^{-1} to 0.01 sec^{-1}. The results were obtained by TA Data Analysis software.

3.3.3 Mechanical testing

Tensile testing was used to determine the mechanical properties for each thermoplastic material by using a MTS Corporation Qtest II Mechanical Tester (Eden Prairie, Minnesota, United States).[100] The mechanical properties for each thermoplastic material were determined according to the ASTM D638 procedure.[101] The distance between the grips were set to 24.5 mm and the maximum load cell was set to 1,250 N. Table 8 displays the crosshead speeds used for each thermoplastic material. Five small injection molded tensile test bars (63.5 mm long, 9.65 mm wide, 3.13 ±0.02 mm wide gauge, and 1.51 ±0.01 mm thick) from each thermoplastic material were analyzed at room temperature. Figure 16 displays the dimensions of a tensile test bar.[102] The yield

stress (MPa), break stress (MPa), and break elongation (%) were recorded by TestWorks QT software.

Table 8. Crosshead speeds used for each thermoplastic material.

Material	Crosshead Speed (mm/min)
Polystyrene	1
Polypropylene	50
Polycarbonate	10
Nylon-6	25
Starex	4

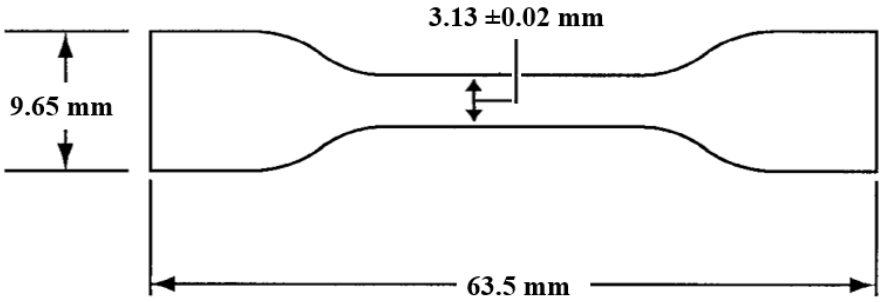

Figure 16. Dimensions of a tensile test bar.[28]

3.3.4 Scanning electron microscopy

The compounding effectiveness of the Starex and TiO_2 formulation was evaluated by scanning electron microscopy (SEM). SEM was performed by a Phenom Scanning Electron Microscope, Model 800-03103-05 (Dillenburgstraat, Eindhoven, Netherlands).[103] The samples tested were the break regions of various injection molded test bars or extrudate samples. Before analysis was performed, the samples were coated with gold in a Kurt J. Lesker Company 108 Sputter Coater (Pittsburgh, Pennsylvania, United States).[104]

The particle size of the silica fillers was also evaluated by SEM. Before analysis was performed, the fillers were coated with gold as described above.

3.3.5 Gel permeation chromatography

Gel permeation chromatography (GPC) was performed with a Wyatt Technology Gel Permeation Chromatograph (Santa Barbara, California, United States),[105] consisting of an Agilent HPLC pump (Santa Clara, California, United States),[106] an Agilent Auto Sampler, a set of four Phenomenex GPC/SEC 300 x 7.8 mm Phenogel 5µ columns (50 Å, 10^2 Å, 10^3 Å, and 10^4 Å) (Torrance, California, United States);[107] a Wyatt DAWN Hellos-II Multi-Angle Light Scattering Detector (MALS); a Wyatt Optilab T-rEX Differential Refractive Index (dRI) Detector; a Wyatt ViscoStar-II Differential Viscometer; and ASTRA 6.1 software. The flow rate of toluene eluent was 1 mL/min at 30°C. M_n, M_w, and polydispersity index (PDI) were calculated based on the peaks present in each chromatogram compared to polystyrene standard calibration.

CHAPTER IV

4. RESULTS AND DISCUSSION- THERMOPLASTIC MATERIALS

4.1 Compounding process

This chapter utilizes the Process 11, a lab-scale twin-screw extruder to compound thermoplastic materials to demonstrate that any plastic formulation that is compounded using the Process 11 is appropriate for injection molding. This study will include an understanding of how the different processing methods affect the thermal and mechanical polymer properties, as well as to understand if amorphous and semi-crystalline polymers are impacted differently by extrusion processing, subsequent regrinding, and injection molding. The compounded extrudate and injection molded test bars made from the amorphous and semi-crystalline materials were characterized by TGA, DSC, capillary rheometry, and tensile testing. The compounding effectiveness of the Process 11 was also studied by compounding a Starex and TiO_2 formulation. The dispersion of the TiO_2 filler in the Starex matrix was evaluated by TGA, DSC, tensile testing, and SEM.

4.2 Importance of injection molding

Injection molding is the most common and fastest growing process in the plastics industry. Injection molding utilizes high production rates and low cycle times to produce multiple complex parts of intricate shapes and sizes. Products made by injection molding

begin as plastic pellets. A schematic of an injection molding machine is shown in Figure 17.[108]

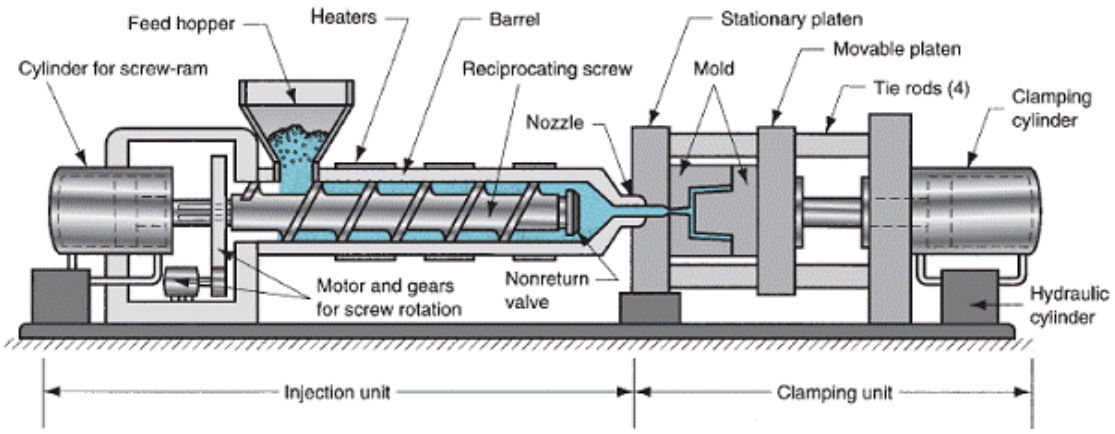

Figure 17. Schematic of an injection molding machine.[108]

Plastic pellets are conveyed from a feed hopper into the barrel by a rotating reciprocating single screw that melts and conveys the melted plastic through the barrel. As the plastic pellets are melted and conveyed, the reciprocating screw moves backwards to a predetermined volume measurement, called the shot size, or the amount of material that will be injected into the mold. Once the reciprocating screw reaches the predetermined shot size, the screw acts as a plunger and is rammed forward, injecting molten plastic that is in front of the screw through the nozzle into a closed mold. A schematic of a mold for injection molding is shown in Figure 18.[108]

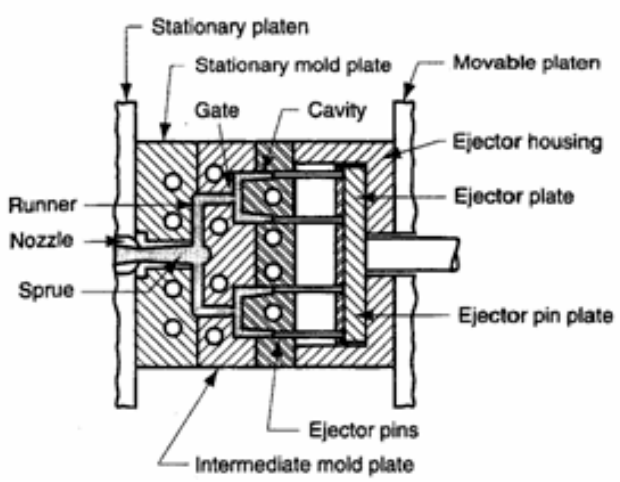

Figure 18. Schematic of a mold for injection molding.[108]

A sprue and runner system inside the mold directs the molten plastic to the mold cavity to form the desired part shape. The molten plastic is trapped inside of the mold for a predetermined amount of time called the cooling time. As the molten plastic is cooling, the reciprocating screw is rotating again to achieve the desired shot size. Once the cooling time is completed, the molten plastic has solidified to become a finished part. The mold will open; the part will be ejected from the mold cavity; the mold will close; and the process continuously repeats itself.[109]

Most injection molded parts are made from a blend of virgin and reground plastic material. Virgin plastic material is produced directly from petrochemicals and has never been processed prior to injection molding. Reground plastic material, which is commonly referred to as regrind, is recycled material that has been processed at least once before. Some common sources of regrind are sprues, runners, and bad parts that cannot be sold. These are known as "pre-consumer" waste. Post-consumer plastic waste such as bottles, storage containers, buckets, and crates are also sources of regrind.[110] These sources are

typically washed, ground up, and re-pelletized.[111] Generally injection molded parts consist of 20% to 25% regrind that has been blended with virgin plastic material.[112]

4.3 Recycling effects polymer properties

Adding regrind to virgin material saves money and resources. However, recycling regrind can affect the polymer properties which can result in a loss of performance in the finished plastic part. Plastic materials are comprised of a variety of fillers, additives, stabilizers, and very high molecular weight polymers. The high molecular weights of the thermoplastic polymers provide desired polymer properties, such as thermal stability, mechanical strength, and the desired viscosity of the polymeric material in the melt. When plastic materials are processed into regrind, the polymer molecular weight may decrease. The long polymer chains may break, resulting in lower molecular weight polymer chains and a wider molecular weight distribution. Lower molecular weight polymers and changes in the molecular weight distribution affect the formulation's processing characteristics, as well as the mechanical properties of the finished plastic part. After successive grinding occurrences on the plastic material, the base polymer's molecular weight may decrease so drastically that the plastic formulation will possess degraded physical, chemical, and rheological properties.[112]

In previous studies, the effects of regrind on the material properties in the final product were evaluated. Ronkay and coworkers compared various mixtures of virgin and regrind material to analyze the mechanical properties of polycarbonate injection molded parts. This study showed that the average molecular mass of the polycarbonate decreased by about 8% during the first injection molding cycle and with subsequent grinding cycles. A 25% increase in melt flow rate was also observed. The tensile strength did not decrease

significantly, but the elongation at break did show a dramatic decrease. Overall, they concluded that the mechanical properties of the material significantly deteriorated with more than 20% regrind added to the formulations.[113]

Aurrekoetxea and coworkers injected molded and reground polypropylene several times to mimic the effect of recycling. The main effect observed was that the melt viscosity decreased, which was attributed to a decrease in polymer molecular weight. The recycled polypropylene exhibited a greater crystallization rate and higher percentage crystallinity when compared to virgin polypropylene.[114] In another study, Duigou and coworkers repeatedly processed flax fiber reinforced poly(l-lactic acid) composites by injection molding, regrinding, and recycling. After three repeated injection molding cycles, the poly(l-lactic acid) composite with 100% regrind and no virgin material demonstrated a decrease in tensile properties. The glass transition temperature (T_g) decreased as well, while the degree of crystallinity increased. They concluded that degradation during processing induced higher chain molecular mobility due to the presence of shorter polymer chains with lower molecular weight compared to virgin poly(l-lactic acid).[115]

In this study, thermoplastic materials were compounded utilizing the Process 11 to demonstrate that any plastic formulation that was compounded by the Process 11 was appropriate for injection molding. The Process 11 was also used to compound a Starex and TiO_2 formulation to demonstrate compounding efficiency and distribution of filler in thermoplastic materials compounded with the Process 11. The thermal and mechanical polymer properties of the thermoplastic materials were characterized by TGA, DSC,

capillary rheometry, tensile testing, and SEM to evaluate the effects of regrinding on polymer properties.

4.4 Appearance of injection molded parts

The injection molded polystyrene, polypropylene, polycarbonate, and Nylon-6 test bar samples all experienced a color change after successive occurrences of processing. The engineering materials of polycarbonate and Nylon-6 had a more dramatic color change when compared to polystyrene and polypropylene. Figure 19 displays the color changes observed in the injection molded samples.

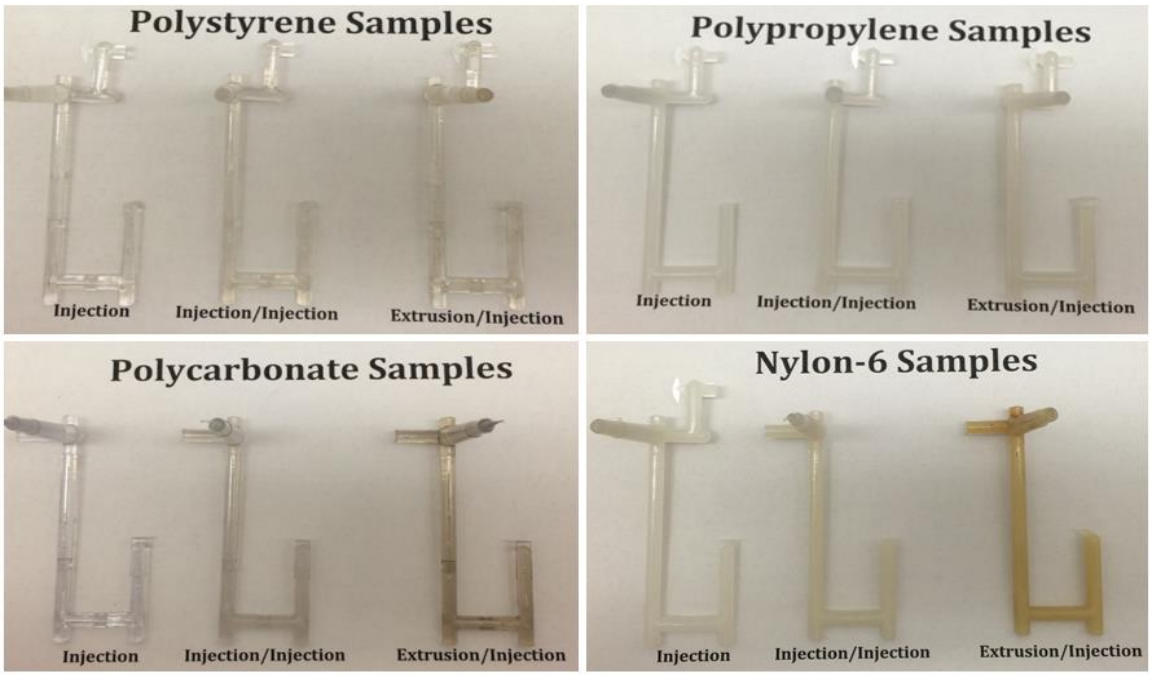

Figure 19. Color changes observed in injection molded samples.

The color change after successive occurrences of processing was due to a slight reduction in molecular weight resulting from the combination of temperature and mechanical shear that the materials encounter during processing.[116] This slight molecular weight reduction did not significantly decrease the thermal or mechanical properties.

Fornes and coworkers experienced a similar phenomenon by melt processing Nylon-6 composites. They observed a color change that occurred after processing due to polymer degradation.[116] Yoon and coworkers prepared polycarbonate composites using two different twin-screw extruders. They observed that a higher reduction in molecular weight resulted in a more dramatic color change.[117]

4.5 Thermogravimetric analysis of thermoplastic materials

The thermal stability of all of the thermoplastic materials was investigated by TGA in a nitrogen atmosphere. Figure 20 displays the TGA thermograms of the polystyrene samples. The thermal properties of the polystyrene samples are summarized in Table 9. The onset of degradation temperature of the virgin polystyrene pellet was observed at 413°C. The injection molded followed by injection molded sample showed an onset of degradation at 409°C, and the extrusion followed by injection molded sample showed an onset of degradation at 412°C. There was no appreciable reduction in the onset of degradation temperature after two occurrences of injection molding (injection/injection), as well as no appreciable reduction in the onset of degradation temperature after extrusion followed by injection molding (extrusion/injection).

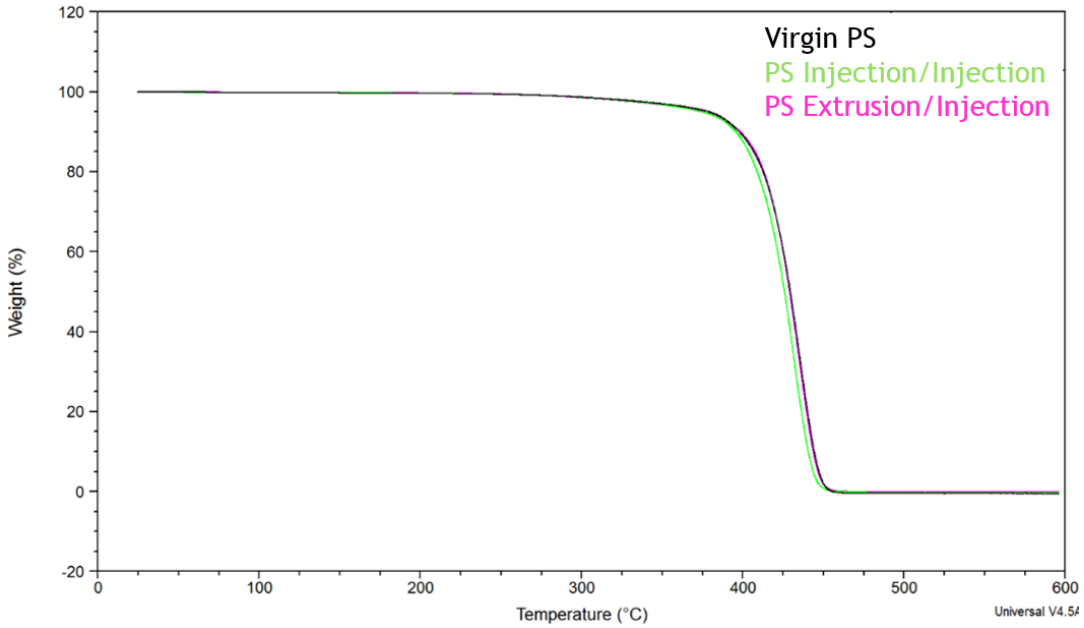

Figure 20. TGA thermograms of the polystyrene samples: virgin polystyrene (—), polystyrene injection/injection (—), and polystyrene extrusion/injection (—).

Figure 21 displays the TGA thermograms of the polypropylene samples. The thermal properties of the polypropylene samples are summarized in Table 9. The onset of degradation of the virgin polypropylene pellet was observed at 458°C. The injection molding followed by injection molding sample showed an onset of degradation at 420°C, and the extrusion followed by injection molding sample showed an onset of degradation at 434°C. There was a 38°C reduction in the onset of degradation temperature after two occurrences of injection molding (injection/injection), as well as 24°C reduction in the onset of degradation temperature after extrusion followed by injection molding (extrusion/injection). The reduction in the onset of degradation temperature was further investigated by percent crystallinity and capillary rheometry.

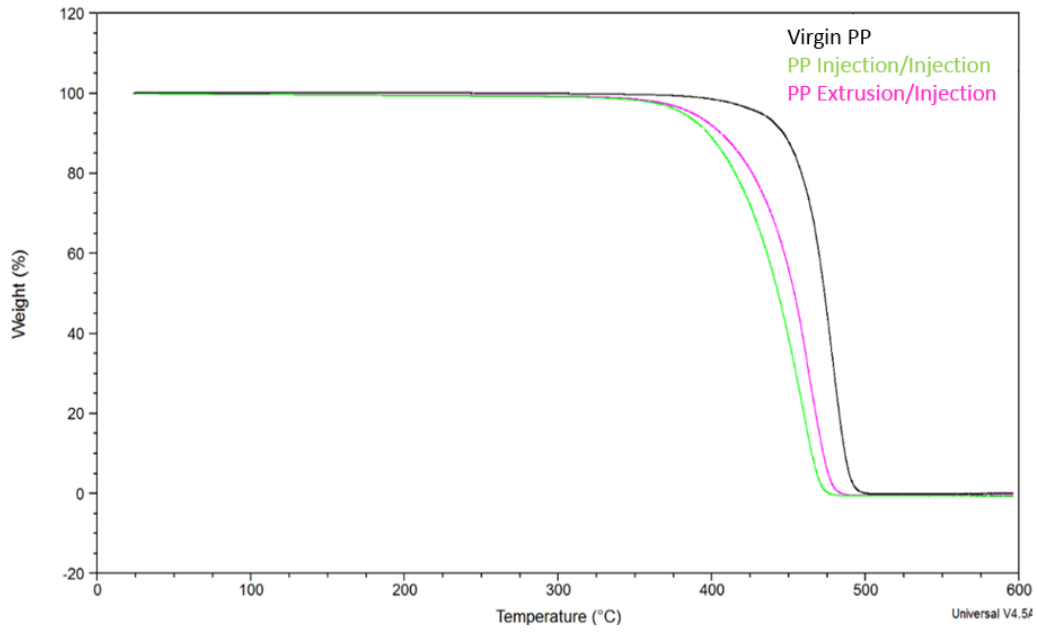

Figure 21. TGA thermograms of the polypropylene samples: virgin polypropylene (—), polypropylene injection/injection (—), and polypropylene extrusion/injection (—).

Figure 22 displays the TGA thermograms of the polycarbonate samples. The thermal properties of the polycarbonate samples are summarized in Table 9. According to the TGA thermograms, the polycarbonate material was approximately 25% filled. The onset of degradation temperature of the virgin polycarbonate pellet was observed at 481°C. The injection molding followed by injection molding sample showed an onset of degradation at 493°C, and the extrusion followed by injection molding sample showed an onset of degradation at 478°C. There was no appreciable reduction in the onset of degradation temperature after two occurrences of injection molding (injection/injection), as well as no appreciable reduction in the onset of degradation temperature after extrusion followed by injection molding (extrusion/injection).

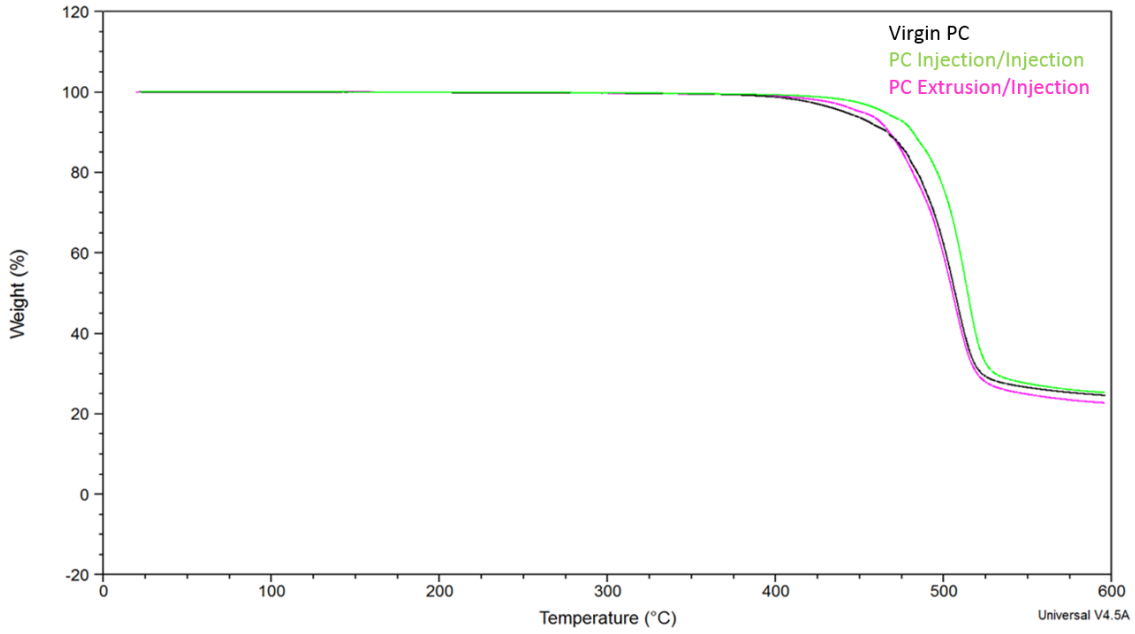

Figure 22. TGA thermograms of the polycarbonate samples: virgin polycarbonate (—), polycarbonate injection/injection (—), and polycarbonate extrusion/injection (—).

Figure 23 displays the TGA thermograms of the Nylon-6 samples. The thermal properties of the Nylon-6 samples are summarized in Table 9. The onset of degradation temperature of the virgin Nylon-6 pellet was observed at 436°C. The injection molding followed by injection molding sample showed an onset of degradation at 423°C, and the extrusion followed by injection molding sample showed an onset of degradation at 426°C. There was no appreciable reduction in the onset of degradation temperature after two occurrences of injection molding (injection/injection), as well as no appreciable reduction in the onset of degradation temperature after extrusion followed by injection molding (extrusion/injection).

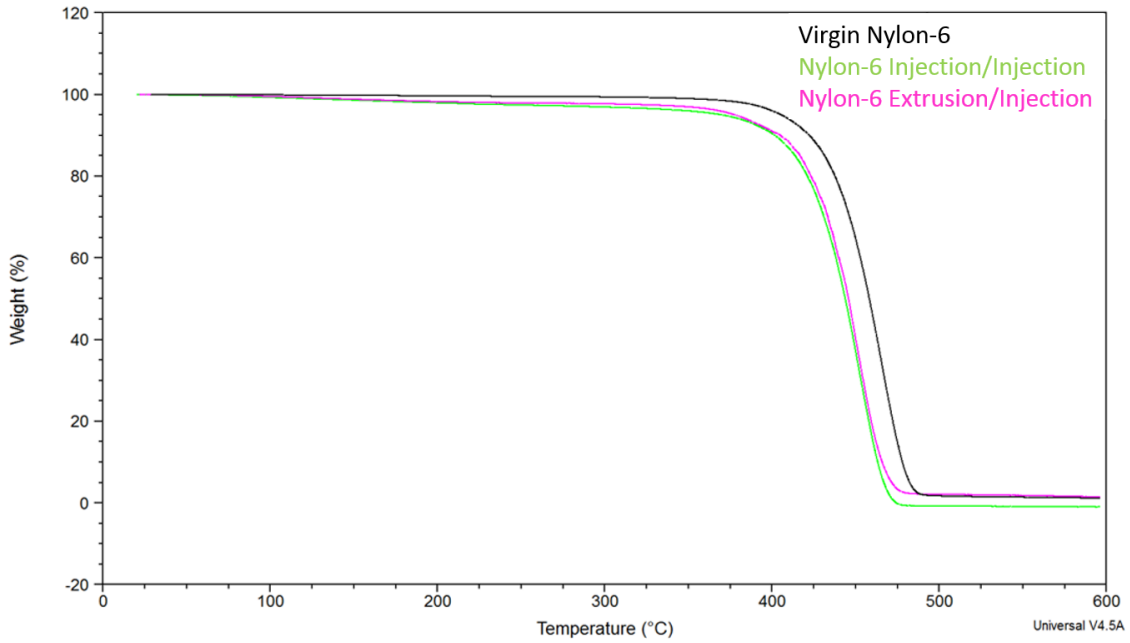

Figure 23. TGA thermograms of the Nylon-6 samples: virgin Nylon-6 (—), Nylon-6 injection/injection (—), and Nylon-6 extrusion/injection (—).

Table 9. Thermal properties of the polystyrene, polypropylene, polycarbonate, and Nylon-6 samples.

Thermoplastic	**Process**	**Onset of Degradation (°C)**	**Residue (%)**
Polystyrene	Virgin	413	-
	Injection/Injection	409	-
	Extrusion/Injection	412	-
Polypropylene	Virgin	458	-
	Injection/Injection	420	-
	Extrusion/Injection	434	-
Polycarbonate	Virgin	481	24.59
	Injection/Injection	493	25.27
	Extrusion/Injection	478	22.71
Nylon-6	Virgin	436	-
	Injection/Injection	423	-
	Extrusion/Injection	426	-

Figure 24 displays the TGA thermograms of the Starex extrusion samples. Table 10 displays the residue percentage of the TiO_2 filler in the extruded Starex material. The extrusion samples contained 5.47% TiO_2 filler as determined by TGA. The onset of degradation temperature of the virgin Starex pellet was observed at 403°C. The unfilled extrusion sample showed an onset of degradation at 403°C, and the filled extrusion sample showed an onset of degradation at 403°C. There was no appreciable reduction in the onset of degradation temperature from the virgin material compared to the unfilled extrusion samples or the filled extrusion samples.

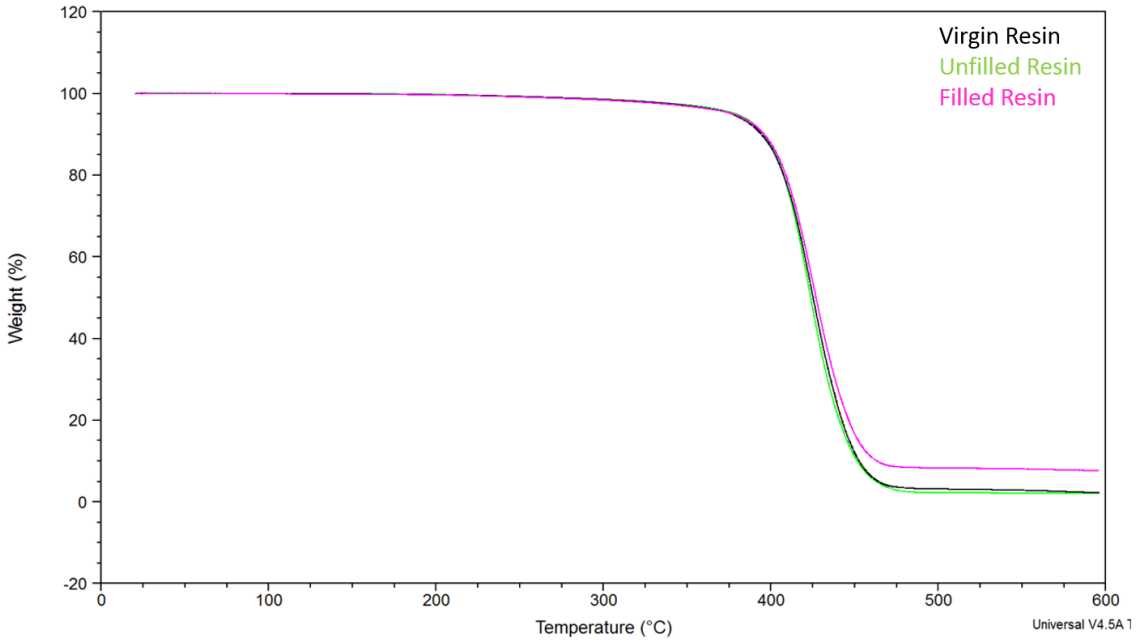

Figure 24. TGA thermograms of the Starex extrusion samples: virgin Starex (—), unfilled Starex (—), and filled Starex (—).

Table 10. Residue percentage of the TiO_2 filler in the extruded Starex material.

Sample	Residue (%)
Virgin Material	2.20
Unfilled Material	2.08
Filled Material	7.67

Figure 25 displays the TGA thermograms of the Starex injection molded samples. Table 11 displays the residue percentage of the TiO_2 filler in the injection molded Starex material. The injection molded samples contained 6.63% TiO_2 filler as determined by TGA. The onset of degradation temperature of the virgin Starex pellet was observed at 403°C. The unfilled injection molded sample showed an onset of degradation at 403°C, and the filled injection molded sample showed an onset of degradation at 401°C. There was no appreciable reduction in the onset of degradation temperature from the virgin material compared to the unfilled injection samples or the filled injection samples.

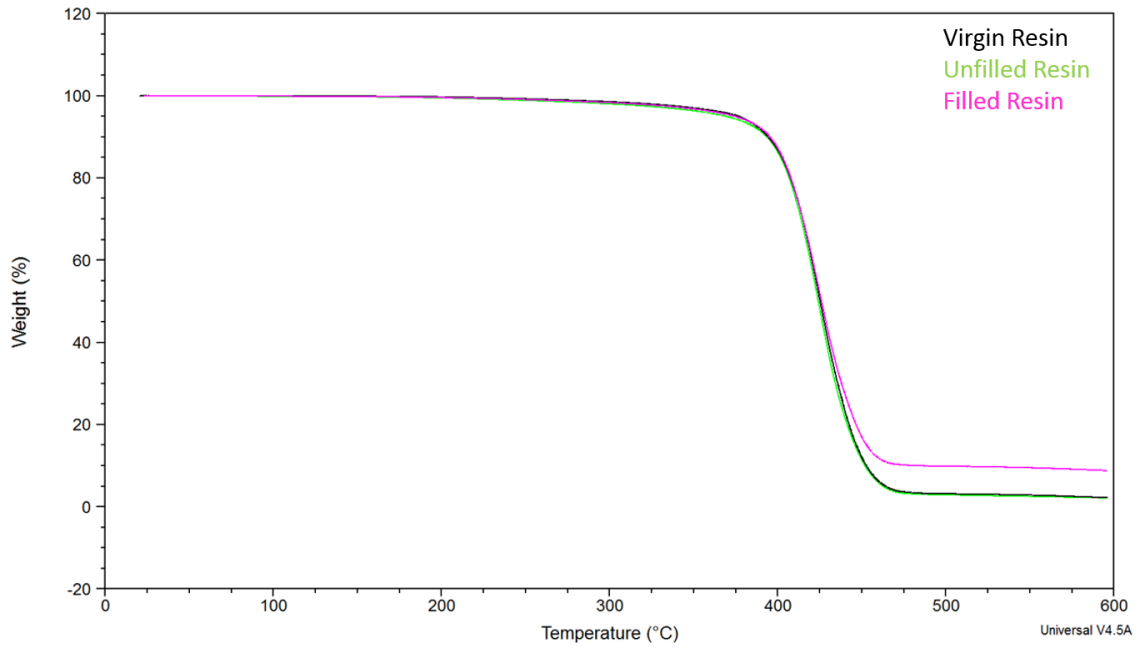

Figure 25. TGA thermograms of the Starex injection samples: virgin Starex (—), unfilled Starex (—), and filled Starex (—).

Table 11. Residue percentage of the TiO_2 filler in the injection molded Starex material.

Sample	Residue (%)
Virgin Material	2.20
Unfilled Material	2.12
Filled Material	8.83

4.6 Differential scanning calorimetry of thermoplastic materials

The thermal behavior of the polystyrene samples was investigated by DSC. The curves only displayed a T_g because polystyrene is amorphous. Figure 26 displays the DSC curves of the polystyrene samples. The T_g of the virgin polystyrene pellet was 89°C. The T_g of the injection molding followed by injection molding sample was 90°C, and the T_g of the extrusion followed by injection molding sample was 92°C. There was no appreciable change in the T_g after two occurrences of injection molding (injection/injection), as well as no appreciable change in the T_g after extrusion followed by injection molding (extrusion/injection).

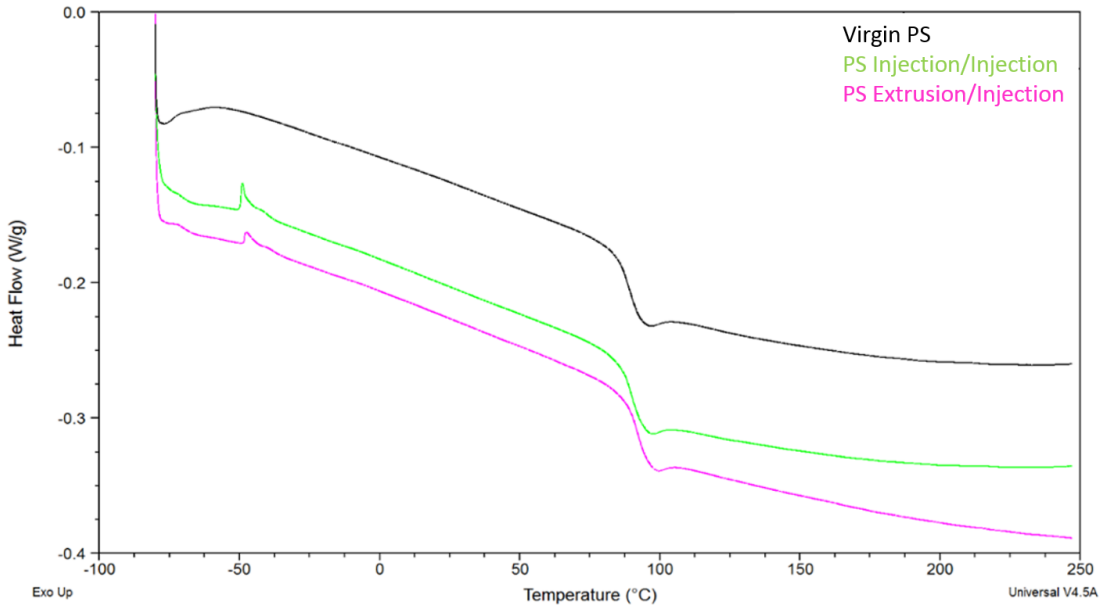

Figure 26. DSC curves of the polystyrene samples: virgin polystyrene (—), polystyrene injection/injection (—), and polystyrene extrusion/injection (—).

The thermal behavior of the polypropylene samples was investigated by DSC. The curves displayed a T_g, T_m, and T_c because polypropylene is semi-crystalline. Figure 27a displays the DSC curves of the polypropylene samples. Figure 27b displays the inset

of the T_g region of the polypropylene DSC curves. Table 12 displays the thermal transition temperatures of the polypropylene samples. There was no appreciable change in the T_g, T_m, or T_c after two occurrences of injection molding (injection/injection), as well as no appreciable change in the T_g, T_m, or T_c after extrusion followed by injection molding (extrusion/injection).

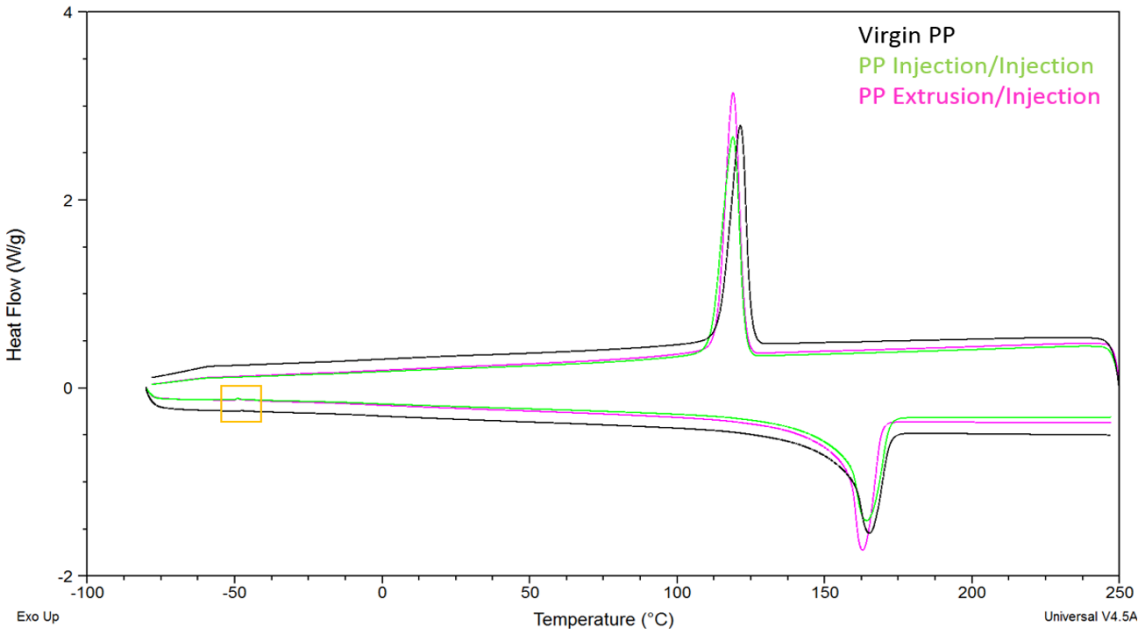

Figure 27a. DSC curves of the polypropylene samples: virgin polypropylene (—), polypropylene injection/injection (—), and polypropylene extrusion/injection (—).

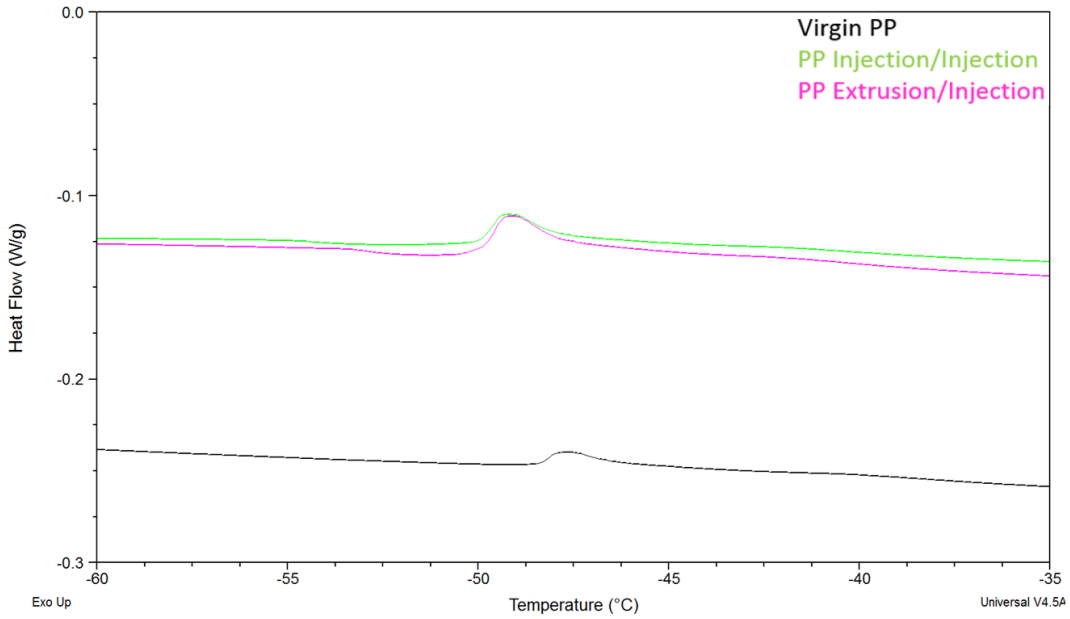

Figure 27b. Inset of the T_g region of the polypropylene DSC curves: virgin polypropylene (—), polypropylene injection/injection (—), and polypropylene extrusion/injection (—).

Table 12. Thermal transition temperatures of the polypropylene samples.

Sample	T_g (°C)	T_m (°C)	T_c (°C)
Virgin	-47	165	122
Injection/Injection	-49	164	119
Extruded/Injection	-49	163	119

The thermal behavior of the polycarbonate samples was investigated by DSC. The curves only displayed a T_g because polycarbonate is amorphous. Figure 28 displays the DSC curves of the polycarbonate samples. The T_g of the virgin polycarbonate pellet was 144°C. The T_g of the injection molding followed by injection molding sample was 143°C, and the T_g of the extrusion followed by injection molding sample was 141°C. There was no appreciable change in the T_g after two occurrences of injection molding (injection/injection), as well as no appreciable change in the T_g after extrusion followed by injection molding (extrusion/injection).

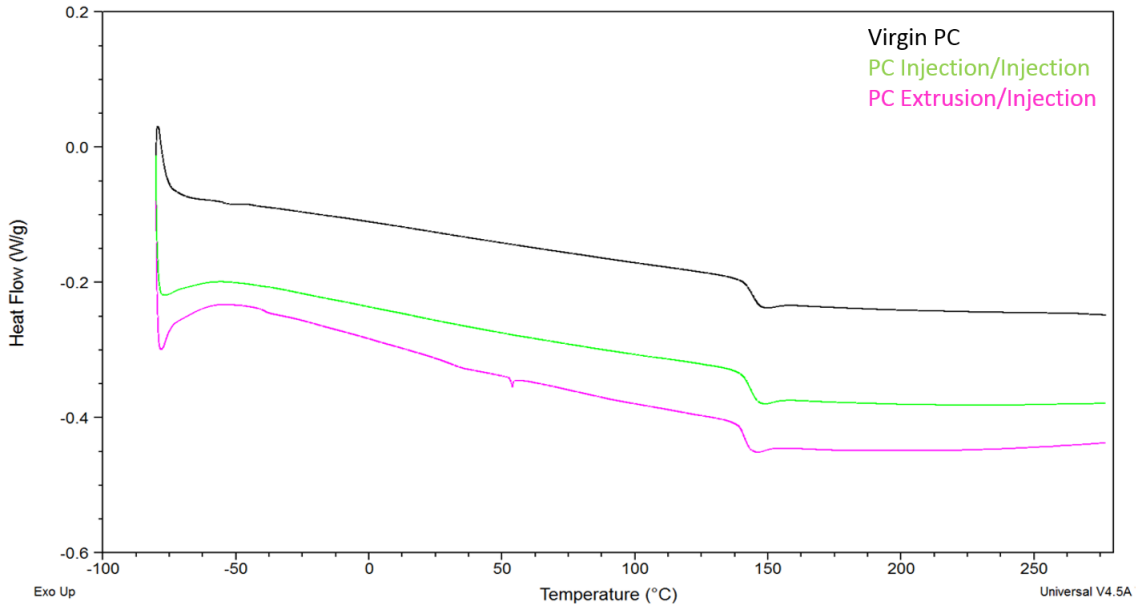

Figure 28. DSC curves of the polycarbonate samples: virgin polycarbonate (—), polycarbonate injection/injection (—), and polycarbonate extrusion/injection (—).

The thermal behavior of the Nylon-6 samples was investigated by DSC. The curves displayed a T_g, T_m, and T_c because Nylon-6 is semi-crystalline. Figure 29a displays the DSC curves of the Nylon-6 samples. Figure 29b displays the inset of the T_g region of the Nylon-6 DSC curves. Table 13 displays the thermal transition temperatures of the Nylon-6 samples. There was no appreciable change in the T_g, T_m, or T_c after two rounds of injection molding (injection/injection), as well as no appreciable change in the T_g, T_m, or T_c after extrusion followed by injection molding (extrusion/injection).

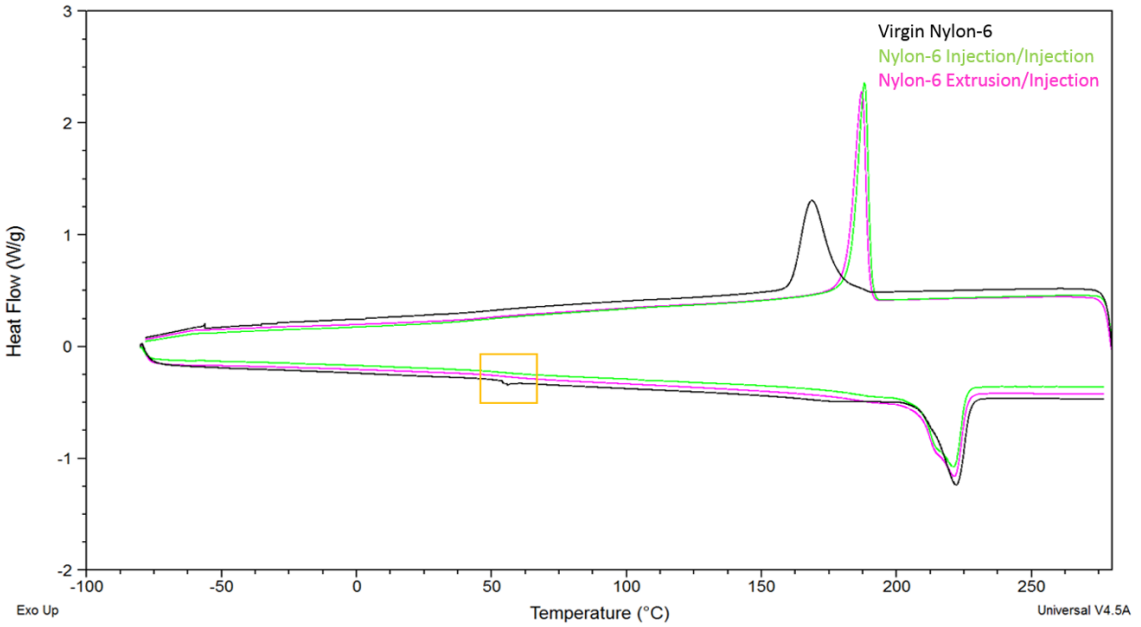

Figure 29a. DSC curves of the Nylon-6 samples: virgin Nylon-6 (—), Nylon-6 injection/injection (—), and Nylon-6 extrusion/injection (—).

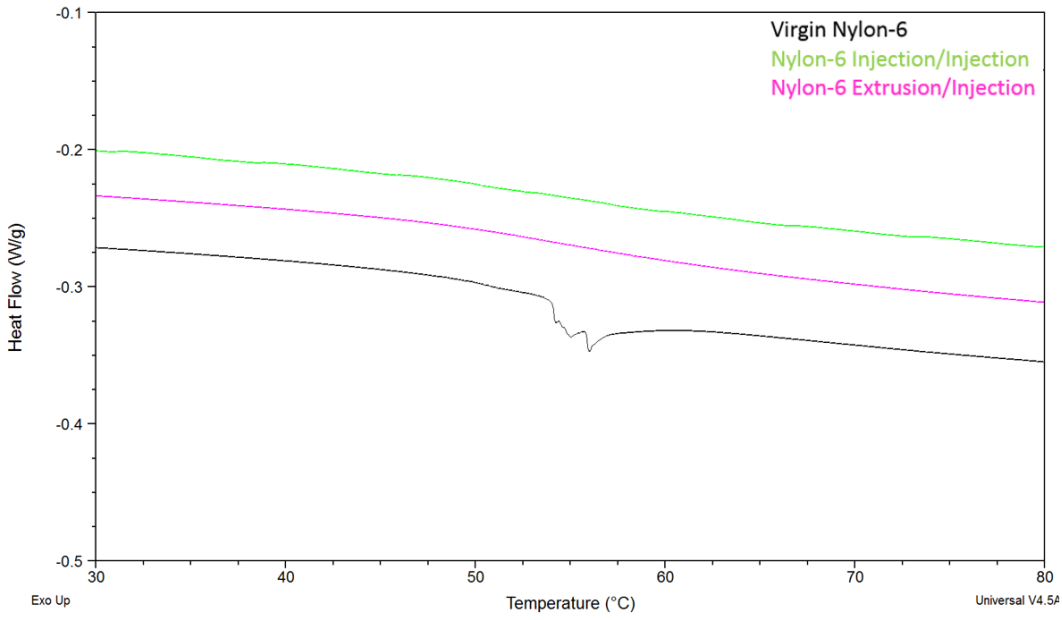

Figure 29b. Inset of the T_g region of the Nylon-6 DSC curves: virgin Nylon-6 (—), Nylon-6 injection/injection (—), and Nylon-6 extrusion/injection (—).

Table 13. Thermal transition temperatures of the Nylon-6 samples.

Sample	T_g (°C)	T_m (°C)	T_c (°C)
Virgin	56	222	169
Injection/Injection	57	221	188
Extruded/Injection	54	221	187

The thermal behavior of virgin Starex was investigated by DSC. The curve only displayed a T_g because Starex is amorphous. Figure 30 displays the DSC curve of the Starex pellet. Two glass transition temperatures were observed on the DSC curve, indicating that the material was indeed a polymer blend or a block copolymer. The first T_g (Peak 1) of virgin Starex was 104°C. This corresponds to ABS that has a T_g of approximately 110°C.[118] The second T_g (Peak 2) of virgin Starex was 129°C. This corresponds to polycarbonate that has a T_g of approximately 150°C.[118] The observed glass transition temperatures of both of the ABS and polycarbonate were decreased compared to the glass transition temperatures of the polymers alone, which is typical when immiscible polymers are blended.[119]

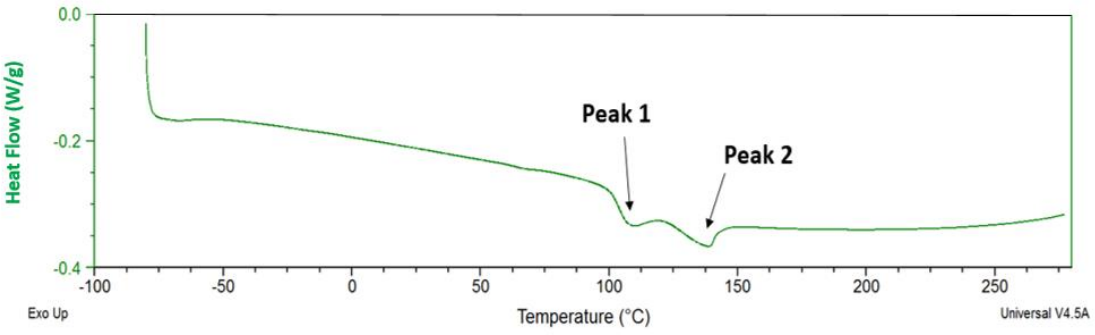

Figure 30. DSC curve of the Starex pellet: Peak 1 is indicative of ABS, while Peak 2 is indicative of polycarbonate.

Plastic blends are used for reducing material depletion for manufacturing optimization. Peydro and coworkers blended high impact polystyrene and ABS together by twin-screw extrusion and performed DSC analysis on the blend. The DSC analysis also revealed two different glass transition temperatures with the blend: one corresponding to high impact polystyrene and the other corresponding to ABS.[120] Chiang and coworkers blended polycarbonate and ABS together at a ratio of 80/20 polycarbonate to ABS and the resulting blend was analyzed by DSC. The polycarbonate/ABS blend exhibited two T_g values from the DSC analysis, similar to what was observed in Figure 30.[119]

4.7 Percent crystallinity of thermoplastic materials

Because there was a 38°C reduction in the onset of degradation temperature for the polypropylene samples after two occurrences of injection molding, as well as 24°C reduction in the onset of degradation temperature after extrusion followed by injection molding, the decrease in the onset of degradation temperature was investigated further. The first method for investigating the decrease in the onset of degradation temperature was evaluating the percent crystallinity. An increase in percent crystallinity after successive occurrences of processing could be the result of a decrease in molecular weight of the base polymer. When plastic materials are processed several times, the long polymer chains that make up the materials may break and get shorter, allowing for greater chain mobility and an increase in crystallization.[114]

The percent crystallinity was calculated for the polypropylene samples by dividing either the heat of melting or heat of recrystallization by the heat of fusion for polypropylene. The heat of melting or heat of recrystallization was determined from the

previous polypropylene DSC curves (Figure 27a). The heat of fusion for polypropylene is 207 J/g and Table 14 displays the percent crystallinity results of the polypropylene samples.[121] The melt temperatures were taken from the second heating cycle. This analysis demonstrates that there was no significant change in crystallinity between the polypropylene samples processed by different procedures.

Table 14. Percent crystallinity of the polypropylene samples.

Sample	T_m (°C)	% Crystallinity Calculated from Melting	T_c (°C)	% Crystallinity Calculated from Recrystallization
Virgin	165.11	53.1	121.47	55.5
Injection/Injection	164.29	55.3	118.93	57.8
Extruded/Injection	162.84	55.9	118.95	58.8

The percent crystallinity was also calculated for the Nylon-6 samples. The percent crystallinity was calculated by dividing either the heat of melting or heat of recrystallization by the heat of fusion for Nylon-6. The heat of melting or heat of recrystallization was determined from the previous Nylon-6 DSC curves (Figure 29a). The heat of fusion for Nylon-6 is 230 J/g and Table 15 displays the percent crystallinity results of the Nylon-6 samples.[121] The melt temperatures were taken from the second heating cycle. There was no significant change in crystallinity between the Nylon-6 samples processed by different procedures.

Table 15. Percent crystallinity of the Nylon-6 samples.

Sample	T_m (°C)	% Crystallinity Calculated from Melting	T_c (°C)	% Crystallinity Calculated from Recrystallization
Virgin	222.14	31.4	168.69	26.7
Injection/Injection	221.05	35.0	188.20	32.4
Extruded/Injection	221.29	36.1	187.20	32.7

4.8 Capillary rheometry of thermoplastic materials

The second method for investigating the decrease in onset of degradation temperature observed in TGA analysis of the polypropylene samples was capillary rheometry. A decrease in viscosity of the polypropylene samples after successive occurrences of processing would be indicative of a decrease in the polypropylene molecular weight. Figure 31 displays the viscosity curves of the polypropylene samples. There was no appreciable change in viscosity of the polypropylene samples as determined by capillary rheometry. From that, it was concluded that there was also no appreciable drop in molecular weight with successive occurrences of processing.

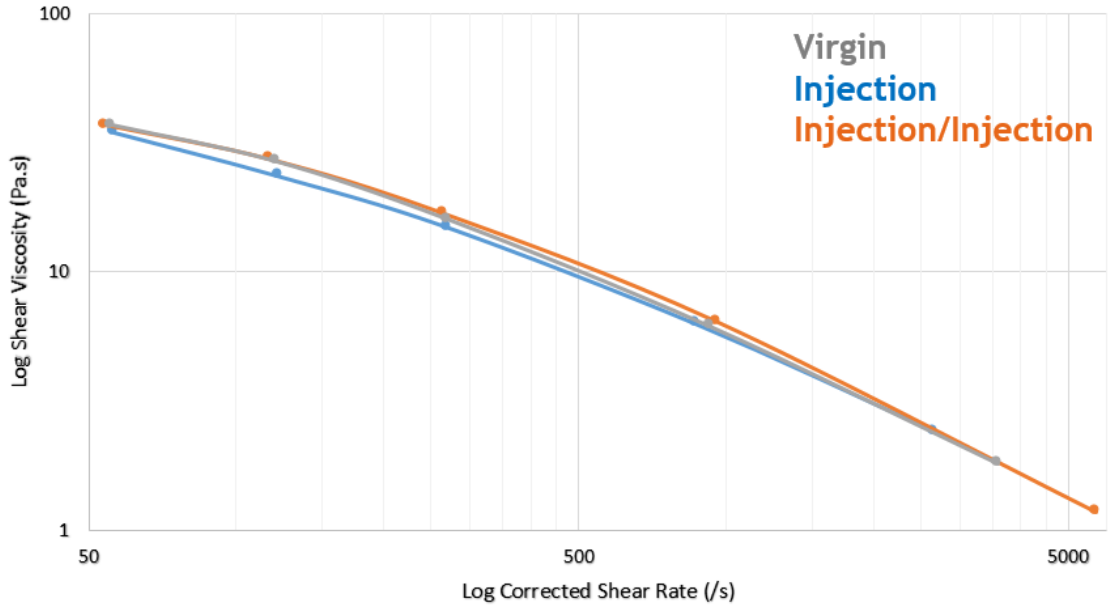

Figure 31. Viscosity curves of the polypropylene samples.

The decrease in the onset of degradation temperature may have occurred from an additive package that was incorporated into the polypropylene material. The additive package may have started to degrade as successive occurrences of processing and grinding occurred, causing the polypropylene material to start degrading sooner. Typical

additives found in a polyolefin formulation are UV stabilizers (blockers, absorbers, and radical scavengers), thermal stabilizers (antioxidants), flame retardants, clarifiers, nucleating agents, and colorants.[122]

4.9 Tensile testing of thermoplastic materials

Table 16 displays the mechanical properties of the polystyrene samples. The values are an average of five specimens per sample. There was no appreciable reduction in yield stress, break stress, or break elongation after two occurrences of injection molding (injection/injection), as well as no appreciable reduction in the yield stress, break stress, or break elongation after extrusion followed by injection molding (extrusion/injection).

Table 16. Mechanical properties of the polystyrene samples.

Sample	Yield Stress (MPa)	Break Stress (MPa)	Break Elongation (%)
1st Injection Test Bar	57.8 (±3.58)	56.8 (±3.0)	5.3 (±0.2)
Injection/Injection	57.1 (±1.5)	56.3 (±1.4)	4.9 (±0.2)
Extruded/Injection	56.8 (±1.6)	55.7 (±1.7)	4.9 (±0.1)

Table 17 displays the mechanical properties of the polypropylene samples. The values are an average of five specimens per sample. There was no appreciable reduction in yield stress, break stress, or break elongation after two occurrences of injection molding (injection/injection), as well as no appreciable reduction in the yield stress, break stress, or break elongation after extrusion followed by injection molding (extrusion/injection).

Table 17. Mechanical properties of the polypropylene samples.

Sample	Yield Stress (MPa)	Break Stress (MPa)	Break Elongation (%)
1st Injection Test Bar	40.9 (±0.5)	46.8 (±1.4)	386.0 (±6.3)
Injection/Injection	40.8 (±0.5)	47.9 (±0.5)	396.3 (±7.1)
Extruded/Injection	40.6 (±0.4)	46.9 (±1.2)	385.5 (±7.8)

Table 18 displays the mechanical properties of the polycarbonate samples. The values are an average of five specimens per sample. There was no appreciable reduction in yield stress after two occurrences of injection molding (injection/injection), but there was a 16.3% reduction in break stress, and a 29.4% reduction in break elongation after two occurrences of injection molding. There was no appreciable reduction in the yield stress after extrusion followed by injection molding, but there was a 14.9% reduction in break stress, and a 15.6% reduction in break elongation after extrusion followed by injection molding (extrusion/injection).

Table 18. Mechanical properties of the polycarbonate samples.

Sample	Yield Stress (MPa)	Break Stress (MPa)	Break Elongation (%)
1st Injection Test Bar	59.3 (±1.0)	73.7 (±1.8)	78.7 (±0.7)
Injection/Injection	61.3 (±0.5)	61.7 (±1.2)	55.6 (±3.8)
Extruded/Injection	61.1 (±0.5)	62.7 (±0.5)	66.4 (±1.2)

The reductions in break stress and break elongation could indicate that the molecular weight of the polycarbonate could have decreased similarly to what occurred in the study by Ronkay and coworkers. They observed that higher break stress and break elongation results could be obtained with virgin polycarbonate material blended with less than 20% regrind.[112] The greater amount of virgin material present in the formulation would result in better mechanical properties. Every instance of processing or grinding of

the material will reduce the molecular weight of the material to a certain extent, and this may result in lower mechanical properties. If there was a decrease in the polycarbonate molecular weight, it was not significant enough to influence the observed polycarbonate thermal properties. The molecular weight of the polycarbonate samples could have been reduced just enough to show a reduction in tensile properties.

Table 19 displays the mechanical properties of the Nylon-6 samples. The values are an average of five specimens per sample. There was no appreciable reduction in yield stress, break stress, or break elongation after two occurrences of injection molding (injection/injection), as well as no appreciable reduction in the yield stress, break stress, or break elongation after extrusion followed by injection molding (extrusion/injection).

Table 19. Mechanical properties of the Nylon-6 samples.

Sample	Yield Stress (MPa)	Break Stress (MPa)	Break Elongation (%)
1st Injection Test Bar	41.6 (±3.1)	52.0 (±3.0)	185.1 (±9.9)
Injection/Injection	45.7 (±1.5)	64.8 (±4.0)	211.8 (±8.5)
Extruded/Injection	56.8 (±2.0)	59.2 (±3.1)	177.1 (±6.9)

Table 20 displays the mechanical properties of the Starex samples. The values are an average of five specimens per sample. The presence of approximately 7 wt% TiO_2 filler did not appear to significantly affect the mechanical properties. There was no appreciable reduction in yield stress, break stress, or break elongation.

Table 20. Mechanical properties of the Starex samples.

Sample	Yield Stress (MPa)	Break Stress (MPa)	Break Elongation (%)
Virgin Material	51.6 (±3.8)	40.8 (±1.688)	21.3 (±2.3)
Unfilled Material	51.7 (±3.0)	41.0 (±3.009)	19.2 (±1.1)
Filled Material	49.8 (±2.2)	41.4 (±2.119)	17.0 (±0.7)

4.10 Scanning electron microscopy of thermoplastic materials

The compounding effectiveness of the Starex and TiO_2 formulation was evaluated by SEM. Figure 32 displays SEM micrographs of the Starex/TiO_2 formulation samples. Micrograph A displays the virgin injection molded test bar break region. Micrograph B displays the extruded unfilled extrudate break region. Micrograph C displays the filled extruded/injection molded test bar break region, and micrograph D displays the inset image indicated in red of micrograph C.

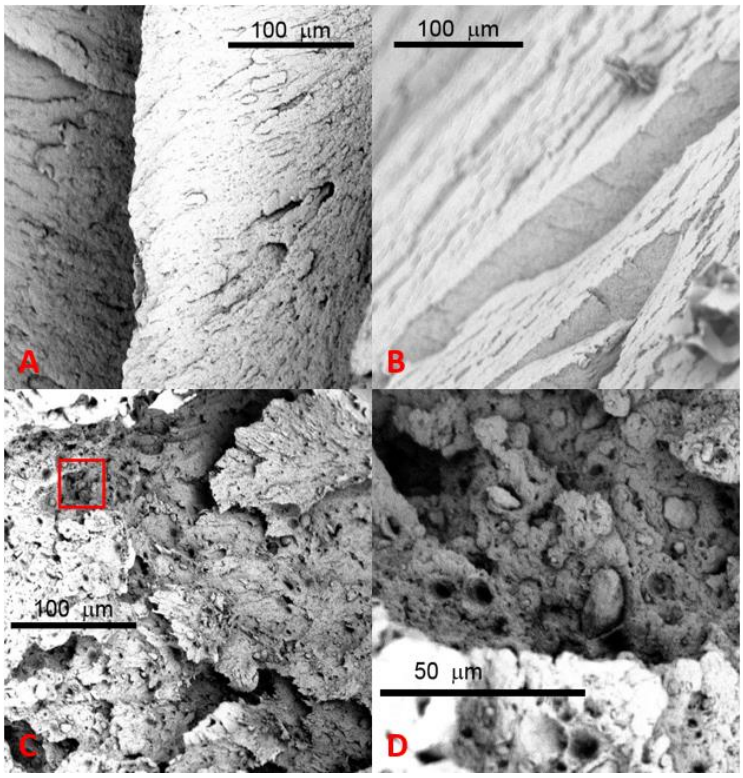

Figure 32. SEM micrographs of the Starex/TiO_2 formulation samples: A) virgin injection molded test bar break region, B) the extruded unfilled extrudate break region, C) filled extruded/injection molded test bar break region, and D) inset image indicated in red box in micrograph C.

Micrographs A and B show the unfilled test bar and extrudate break regions respectively. The images show relatively smooth surfaces because the samples are not filled with TiO_2. The voids that are shown in micrographs A and B are attributed to the actual breaking of the samples by mechanical testing. Micrographs C and D display the break regions of the TiO_2-filled test bar with a relatively rough surface. The surface roughness indicates that the filler debonded and pulled out of the matrix. The rough surface also confirms that the TiO_2 filler was fully embedded into the Starex matrix. This is similar to a study performed by Gerhardt and coworkers that filled poly(lactic acid) with TiO_2.[123] The SEM data further concludes that approximately 7 wt% of TiO_2 did not result in filler agglomeration, which can potentially decrease the mechanical properties of the formulation. The TiO_2 filler appeared to be fully embedded into the Starex matrix. Other researchers have demonstrated through SEM imaging that lower filler concentrations allow the small particles to be encapsulated into the matrix material. They also showed that wide particle size distribution reduces the tendency of the filler to agglomerate.[45,124-126,]

Thermoplastic materials were successfully compounded using the Process 11, a lab-scale twin-screw extruder. The Process 11 did not negatively affect the thermal and mechanical properties of amorphous and semi-crystalline materials to a great extent. The formulations that were prepared by the Process 11 were appropriate for injection molding. The Process 11 effectively compounded a Starex and TiO_2 formulation, dispersing the TiO_2 filler evenly throughout the Starex matrix.

CHAPTER V

5. RESULTS AND DISCUSSION- MODEL COMPONENTS AND FILLED PDMS

5.1 Observations of commercial polysiloxanes and fillers

5.1.1 Observations of commercial polysiloxanes

The commercial PDMS and model copolymer were both transparent, colorless, viscous fluids. The reference silicone was a clear, white, soft, paste-like material. The appearance of the three commercially-available polysiloxanes are presented in Figure 33.

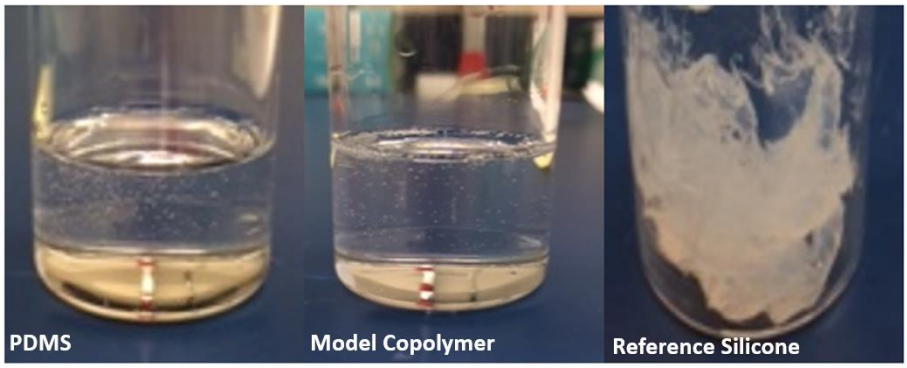

Figure 33. Appearance of the commercial polysiloxanes: PDMS, model copolymer, and reference silicone (left to right).

5.1.2 Observations of commercial fillers

The commercial fillers were all white, flaky, powders. Figure 34 displays the appearance of the three commercial synthetic amorphous silica fillers.

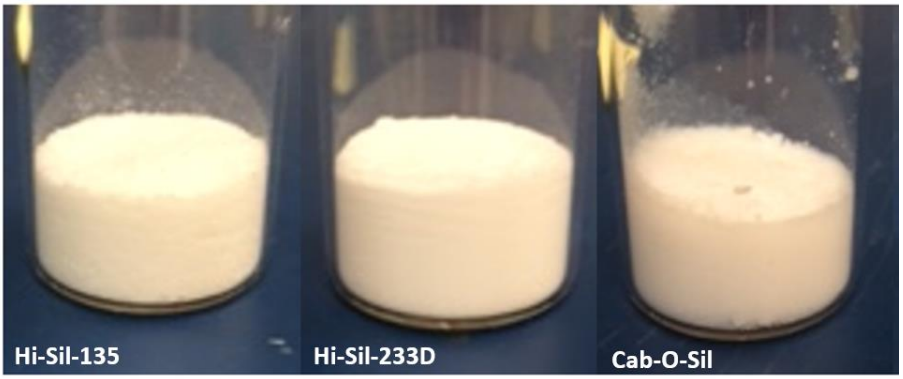

Figure 34. Appearance of the commercial fillers: Hi-Sil-135, Hi-Sil-233D, Cab-O-Sil (left to right).

5.2 Gel permeation chromatography of commercial polysiloxanes

The molecular weight of the commercial polysiloxanes were investigated by GPC in toluene to verify that both polymers contained the molecular weight reported by Gelest. The GPC curves of the commercial polysiloxanes are shown in Figure 35. Table 21 displays the reported molecular weight, the number average molecular weight (M_n), the peak molecular weight (M_p), the weight average molecular weight (M_w), and the polydispersity index (PDI) for the commercial polysiloxanes. The polymers were injected into the Wyatt Technology GPC instrument which evaluated the molecular weight of polymers relative to their hydrodynamic volume.[127]

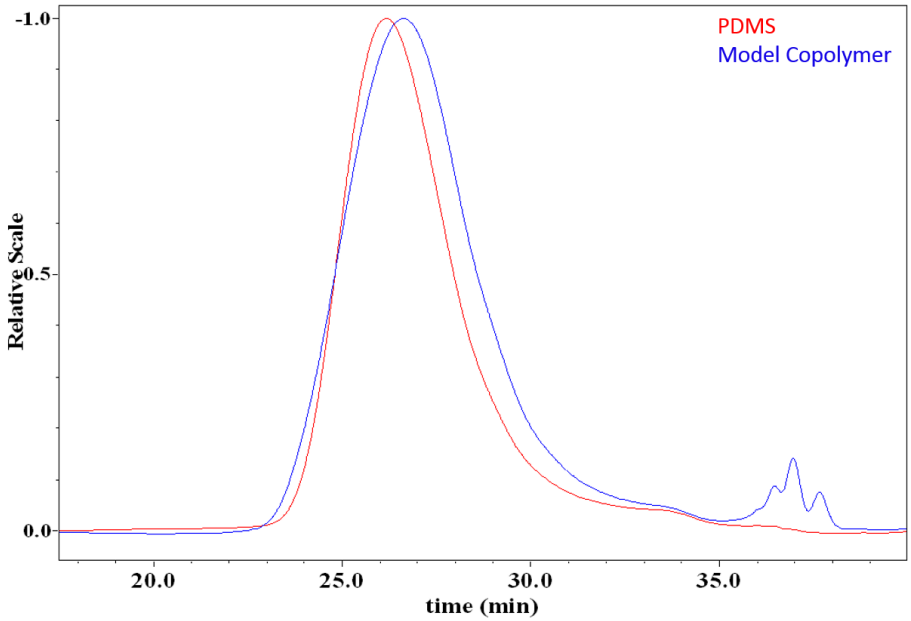

Figure 35. GPC curves of the commercial polysiloxanes: PDMS (—), and model copolymer (—).

Table 21. Molecular weight of the commercial polysiloxanes.

Polysiloxane	**Reported Molecular Weight (g/mol)**	**M_n (g/mol)**	**M_p (g/mol)**	**M_w (g/mol)**	**PDI (M_w/M_n)**
PDMS	28,000	18,096	28,644	28,332	1.57
Model Copolymer	27,000	16,660	24,260	29,149	1.75

The GPC curves were similar to typical curves of PDMS and dimethyl diphenyl polysiloxane copolymers reported in previous studies.[127-131] Polymers are considered to have a narrow molecular weight distribution if the PDI is less than 1.2, whereas they have a broad molecular weight distribution if the PDI is greater than 1.2.[129] The two commercial polysiloxanes contain a relatively broad molecular weight distribution. The smaller peak between 31 and 34 minutes was attributed to oligomers.[128] Smaller amounts of oligomers were observed in PDMS.

5.3 Differential scanning calorimetry of commercial polysiloxanes

The thermal behavior of the commercial polysiloxanes was investigated by DSC. The T_g of PDMS is around -120°C, thus the T_g of these polysiloxanes were not shown.[132,133] The curves only displayed a T_m for the semi-crystalline materials. Figure 36 displays the DSC curves of the commercial polysiloxanes.

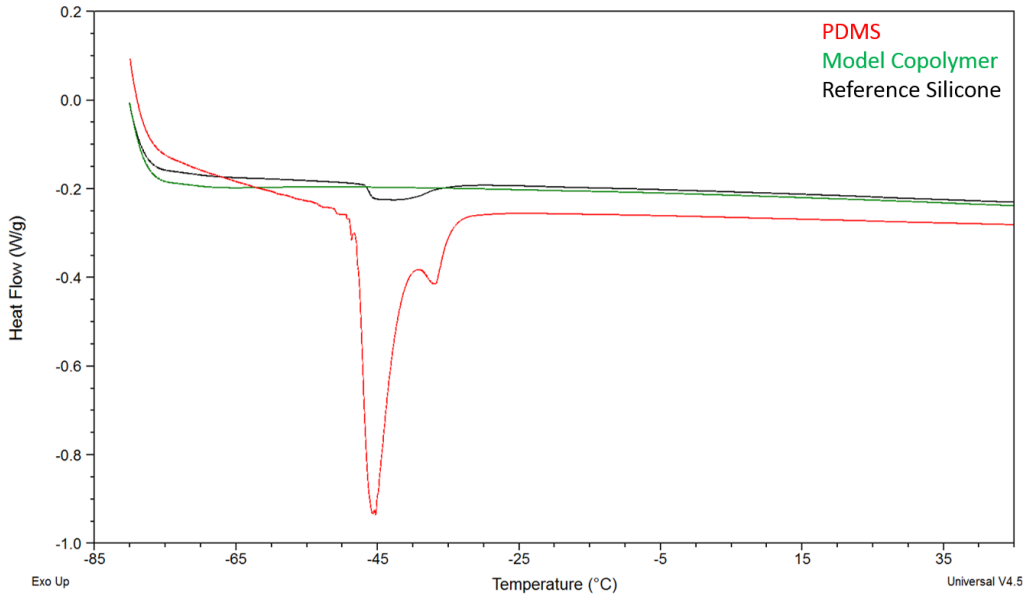

Figure 36. DSC curves of the commercial polysiloxanes: PDMS (—), model copolymer (—), and reference silicone (—).

The DSC curves resemble typical curves of PDMS, dimethyl diphenyl polysiloxane copolymers, and the reference silicone that have been reported in literature.[133-135] The T_m of the commercial PDMS was -43.58°C. The T_m of the reference silicone was -45.03°C. The reference silicone was determined to be a PDMS type polysiloxane due to the T_m. These transitions are similar to other studies.[12] The model copolymer did not exhibit a T_m. This was due to the presence of diphenyl siloxy units. The bulky phenyl groups disrupt crystallization through disturbing the symmetry of the

copolymer and requiring more energy to move the polymer chains that result in crystallization.[12,13]

5.4 Thermogravimetric analysis of commercial polysiloxanes

Polysiloxanes contain incredibly high thermal-oxidative and thermal stability properties. The ionic character and high energy required to break the siloxane bond provides high thermal stability properties to these polymers.[136,137] Polysiloxanes generally degrade through heterolytic cleavage of the polysiloxane main chain, which releases volatile, low molecular weight products. The products are ultimately comprised of six- and eight-membered cyclic oligomeric compounds.[136,138-140] Numerous literature studies have described one of the most common degradation schemes for PDMS to be intramolecular and back-biting depolymerization reactions of the siloxane backbone that results in the formation of the cyclic volatiles being released during decomposition.[141-145] The back-biting mechanism is similar to the secondary reactions that occur during the polysiloxane polymerization process and are shown in Scheme 6.[146]

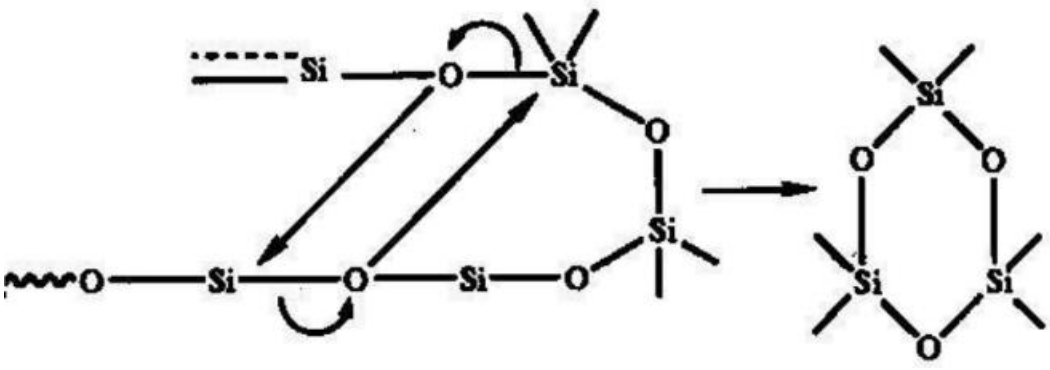

Scheme 6. Back-biting depolymerization mechanism during thermal decomposition.[146]

Variations of solvents, end-group functionalities, and impurities can alter the degradation of PDMS.[146] However, the thermal stability of PDMS can be further

enhanced with the incorporation of numerous functional groups, such as diphenyl-, diethyl-, and divinyl siloxy units to produce various copolymers.[140,146,147] These copolymers also back-bite to release volatile cyclic siloxanes during decomposition.[147] The thermal stability of the commercial polysiloxanes was investigated by TGA in a nitrogen atmosphere and the TGA thermograms are shown in Figure 37. Table 22 displays the temperature at 10% and 50% weight loss, as well as the residue percentage values of the commercial polysiloxanes.

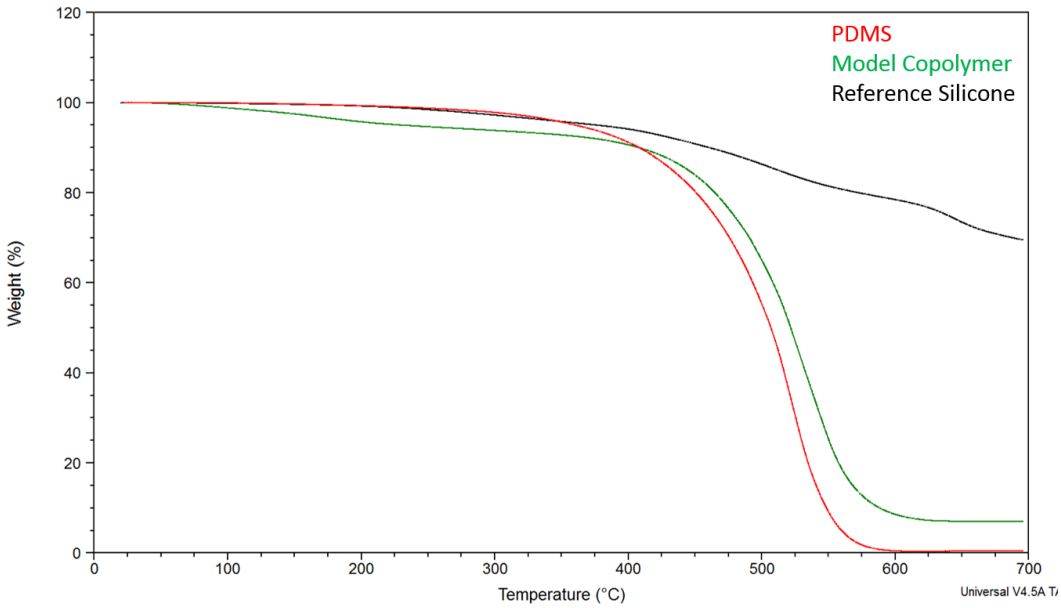

Figure 37. TGA thermograms of the commercial polysiloxanes: PDMS (—), model copolymer (—), and reference silicone (—).

Table 22. Thermal properties of the commercial polysiloxanes.

Polysiloxane	Temperature at 10% Weight Loss (ºC)	Temperature at 50% Weight Loss (ºC)	Residue (%)
PDMS	408	507	0.00
Model Copolymer	409	522	6.99
Reference Silicone	461	-	69.51

The curves in Figure 37 resemble typical TGA curves of PDMS, dimethyl diphenyl polysiloxane copolymers, and the reference silicone that have been reported in multiple papers in literature.[33,136,146-152] The model copolymer's weight decreased from 75°C to 400°C. This decrease was attributed to cyclic siloxane oligomers that are still present in the polymer mixture from the original copolymer synthesis that are being volatilized during the TGA experiment. This decrease was only present in the model dimethyl diphenyl copolymers.[147]

The overall thermal stability of the model copolymer was greater than PDMS. The model copolymer had almost 7% residue left after the experiment compared to PDMS, which completely decomposed. These observations of the copolymer are similar to observations and reports from previous studies. The majority of studies reported that the incorporation of diphenyl groups reduces the backbone chain mobility, making the polymer less able to release the cyclic volatiles. Thus, the thermal stability and percent residue of dimethyl diphenyl copolymers are increased, compared to PDMS.[146,147,151,152]

The commercial polysiloxanes were compared to a commercially-available reference silicone resin to evaluate the potential formulations for their efficacy in applications in which the commercial resin is currently utilized. The reference silicone was determined to be a reinforced PDMS polysiloxane material and according to Table 22, it is filled with about 70% of some unknown filler. The reference silicone was substantially more thermally stable than the commercial polymers, which can be attributed to the interaction between the filler and the polymer backbone. As mentioned earlier, PDMS decomposes by the formation and releasing of cyclic volatile compounds. However, the incorporation of filler disrupts the discharge of the volatile compounds. The

filler aggregates and generates a protective barrier that restricts and delays the release of the volatile compounds, thus increasing the thermal stability of the material.[33,37]

5.5 Scanning electron microscopy of commercial fillers

The particle size of the silica fillers was evaluated by SEM and have been referenced in numerous studies.[153,154,156] The SEM micrographs of the silica filler particles are shown in Figure 38. Micrograph A displays the Hi-Sil-135 filler particles. Micrograph B displays the Hi-Sil-233D filler particles. Micrograph C displays the Cab-O-Sil filler particles.

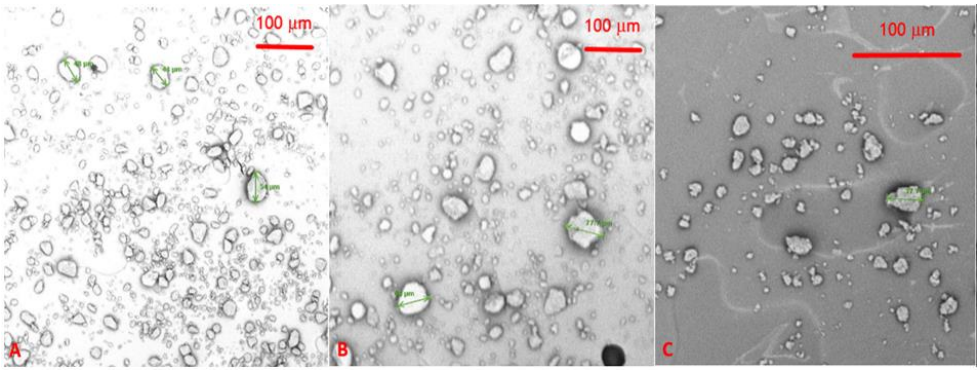

Figure 38. SEM micrographs of the commercial fillers: A) Hi-Sil-135 filler particles, B) Hi-Sil-233D filler particles, and C) Cab-O-Sil filler particles.

The Hi-Sil-135 filler contained filler particles that ranged from 44 µm to 70 µm in size. The Hi-Sil-233D filler contained filler particles that ranged from 53 µm to 78 µm in size. The Cab-O-Sil filler contained filler particles that ranged from 28 µm to 38 µm in size.

5.6 Thermogravimetric analysis of commercial fillers

The purity and water content of the commercial silica fillers were investigated by TGA in a nitrogen atmosphere and Figure 39 displays the TGA thermograms. The curves in Figure 39 resemble typical TGA curves of silica fillers present in literature.[24,155-157] The residue percentage values of the commercial fillers are shown in Table 23.

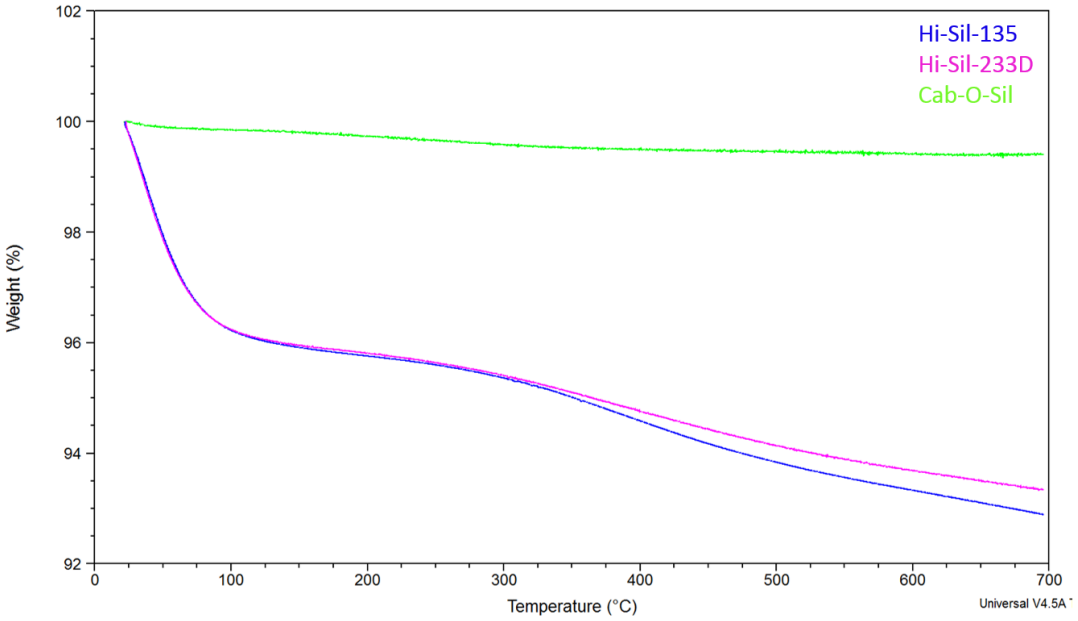

Figure 39. TGA thermograms of the commercial fillers: Hi-Sil-135 (—), Hi-Sil-233D (—), and Cab-O-Sil (—).

Table 23. Thermal properties of the commercial fillers.

Silica Filler	Residue (%)
Hi-Sil-135	92.89
Hi-Sil-223D	93.34
Cab-O-Sil	99.41

Both Hi-Sil fillers lost about 7% of their weight overall. The Cab-O-Sil filler lost less than 1% of its weight. The weight loss in the three silica fillers were the result of the removal of water from the filler. Numerous authors commented that any weight loss that

occurs below 200°C is attributed to the removal of physically adsorbed water on the surface of the fillers. They also discussed that any weight loss from 200°C and above is attributed to the removal of chemically bound water that was trapped in the silica skeleton and the removal of some surface hydroxyl groups.[24,155,157] The removal of water is important because water will physically separate the polymer from the filler surface, allowing chain mobility and a more shear-thinning behavior on the filled systems.[158,48] The less water that is attached to the filler surface will result in superior interactions between the filler and the polymer matrix.[158]

5.7 Observations of filled PDMS

The processing parameters, filler content, and filler type were evaluated to determine the processing conditions needed to obtain the desired yield stress and thixotropic behavior in the filled materials. The first model polymer that was evaluated with the three silica fillers was PDMS. PDMS is the simplest and most readily available polysiloxane.[145] Figure 40 shows the appearance of the filled PDMS premixed materials with the three separate fillers before extrusion.

Figure 40. Appearance of the filled PDMS premixed materials with the three separate fillers before extrusion: Hi-Sil-135, Hi-Sil-233D, and Cab-O-Sil (left to right).

When the fillers were first introduced into the PDMS, the mixtures would thicken into a ball shape. However, as the mixtures were continuously mixed for one minute, the viscosity decreased and the ball began to flow to the bottom of the mixing bowl. The initial increase in viscosity phenomenon could be attributed to the initial interactions between the filler and the polymer matrix. Filler aggregates may also have been formed, and these aggregates reduce the polymer chain mobility and increase the viscosity of the filled materials. As the ball shape began to dissipate, the filler became better dispersed in the liquid polymer. The shearing that occurred during premixing breaks up the aggregates and disperses them throughout the matrix. The destruction of aggregates result in better chain mobility of the polymer, which decreases the viscosity of the mixtures and allows them to flow.[26]

The premixed materials were loaded into the Process 11 twin-screw extruder by hand. During the compounding process of each formulation studied, the temperatures inside the barrel of the extruder increased as compounding progressed. This increase in temperature can be attributed to the abrasive nature of the silica. During twin-screw extrusion, materials are sheared between the screws and barrel to thoroughly mix the abrasive silica into the polymer matrix. The shearing action of the silica against the screws and the barrel creates friction, resulting in heat and raising the temperatures inside the barrel. The barrel temperatures increased as the filler loading increased. As more abrasive filler was added to the formulation, additional shear, friction, and heat were also generated.[159-161]

The compounded PDMS with Hi-Sil-135 filler was a clear, white, soft, paste-like material with little dimensional stability at 20 wt%. At higher filler loading amounts, the

compounded extrudate obtained a higher degree of dimensional stability compared to the 20 wt%-filled material. The torque on the extruder also increased at higher loadings. This was due to the increased viscosity in the materials with greater filler loading amounts. The greater filler loading amounts required more torque to mix the stiffer filled materials. The torque reached up to 0.4 N m for 20 wt% Hi-Sil-135 filler, 1.0 N m for 25 wt% filler, and 3.2 N m for 30 wt% filler. The increase in observed extruder torque was also observed in Sombatsompop and coworkers work with increasing filler amounts.[49]

While compounding the PDMS with Hi-Sil-233D filler, the torque reached up to 0.8 N m. The compounded PDMS with Hi-Sil-233D filler was also a clear, white, soft, paste-like material with greater dimensional stability than the Hi-Sil-135-filled materials. When compounding the PDMS with Cab-O-Sil filler, the torque on the extruder never exceeded 2.5 N m. The compounded PDMS with Cab-O-Sil filler was a light grey, viscous, paste-like material with enhanced dimensional stability compared to all Hi-Sil-filled materials. The appearance of the filled PDMS compounded materials with the three separate fillers after extrusion are shown in Figure 41.

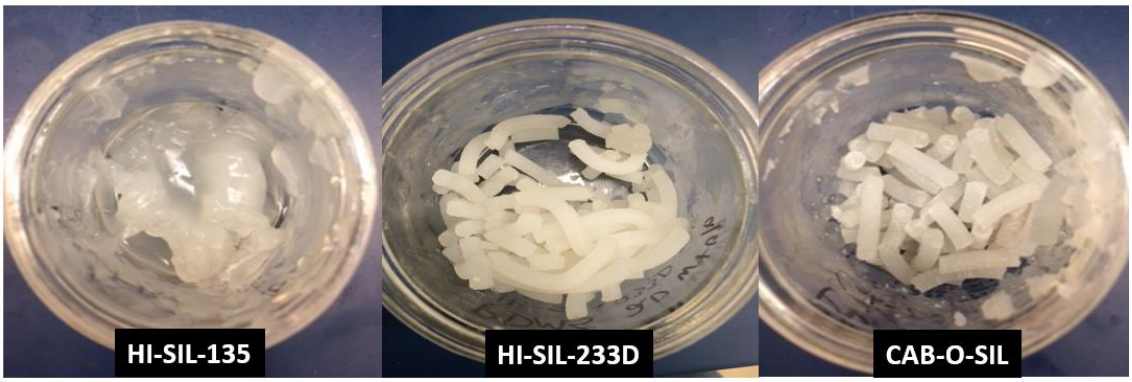

Figure 41. Appearance of the filled PDMS compounded materials with the three separate fillers after extrusion: Hi-Sil-135, Hi-Sil-233D, and Cab-O-Sil (left to right).

5.8 Thermogravimetric analysis of filled PDMS

The thermal stability and the filler dispersion of the PDMS-filled materials were investigated by TGA in a nitrogen atmosphere. The residue percentage values reported by TGA were examined to verify that the residue percentage was similar to the calculated filler loading amount. Three specimens were assessed from each compounded material taken from the beginning of the compounding process, middle of the compounding process, and end of the compounding process. This was to ensure that the filler was consistently dispersed at the desired calculated filler loading amount throughout the compounding process.

Various extrusion parameters were evaluated using the commercial PDMS and the three fillers. A temperature study was conducted by compounding the PDMS compounded with the Hi-Sil fillers at three different processing temperatures in order to determine which processing temperature achieved the best distribution of filler and the most thermally stable compounded extrudate materials. It is well documented that higher processing temperatures will decrease the viscosity of materials. The polymer chains are more mobile at elevated temperatures, decreasing the viscosity and allowing better mixing in the extruder.[162 -167]

Figure 42 displays the TGA thermograms of the filled PDMS compounded with 20 wt% Hi-Sil-135 filler at 30°C, 40°C, and 50°C compared to the PDMS polymer. The curves in Figure 42 resemble typical TGA curves of silica-filled PDMS materials.[33,139,168] The temperature at 10% and 50% weight loss, as well as the residue percentage values of the filled PDMS compounded with 20 wt% Hi-Sil-135 filler at varied extrusion temperatures compared to the PDMS polymer are shown in Table 24. The values in Table

24 are median values of the three specimens per compounded material taken at the beginning of the compounding process, middle of the compounding process, and end of the compounding process.

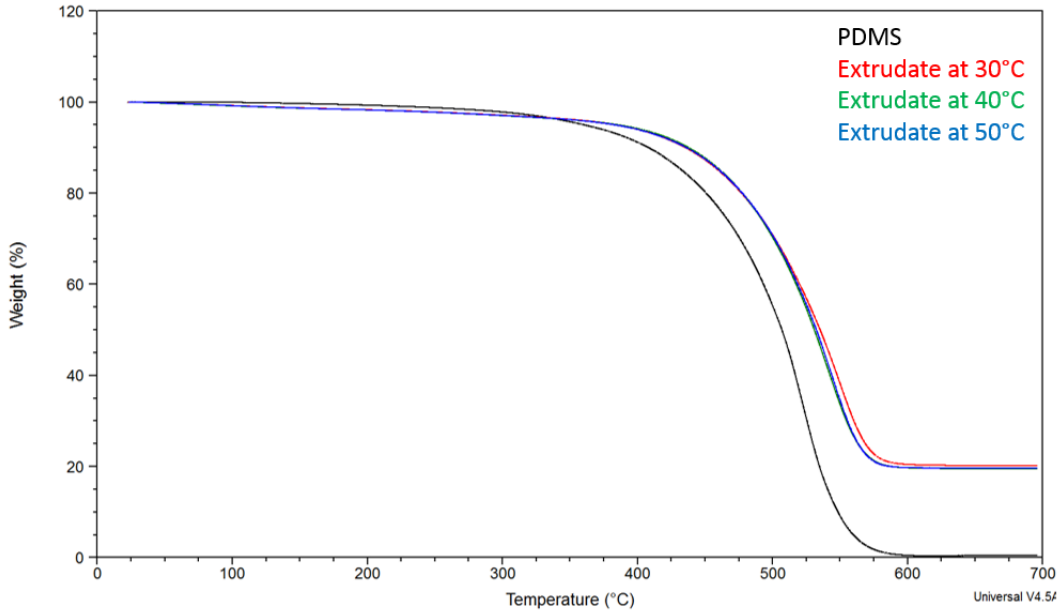

Figure 42. TGA thermograms of the filled PDMS compounded with 20 wt% Hi-Sil-135 filler at varied extrusion temperatures compared to the PDMS polymer: PDMS polymer (—), extrudate at 30°C (—), extrudate at 40°C (—), and extrudate at 50°C (—).

Table 24. Thermal properties of the filled PDMS compounded with 20 wt% Hi-Sil-135 filler at varied extrusion temperatures compared to the PDMS polymer.

Polysiloxane	**Extrusion Temperature (°C)**	**Temperature at 10% Weight Loss (°C)**	**Temperature at 50% Weight Loss (°C)**	**Residue (%)**
PDMS Polymer	-	408	507	0.00
Extrudate at 30°C	30	436	535	20.14 (±0.04)
Extrudate at 40°C	40	438	531	19.37 (±0.11)
Extrudate at 50°C	50	436	532	19.81 (±0.21)

The filled materials possessed greater thermal stability compared to the unfilled PDMS polymer. However, there was no appreciable difference in thermal stability among the materials processed at the three different temperatures. The residue percentage values were approximately equivalent to the calculated filler loading amount. The values were within 2% of each other, indicating an even distribution of filler throughout the compounded materials.

It is commonly reported in literature that the incorporation of additives, such as fillers can increase the thermal stability of polysiloxane materials.[21,34,36-38,47-50,139,147,150,158,169-171] The enhanced thermal stability for the PDMS compounded with Hi-Sil-135 filler could be attributed to the addition of the silica filler. Thermal stability in filled materials is attributed to the ability of the surface functional groups of the filler to interact with the polymer backbone through hydrogen bonding. Silica fillers have large surface areas with an abundance of silanol groups that interact with the polysiloxane backbone. The interaction strength and thermal stability can be enhanced with additional silanol groups on the filler that can interact with the polymer.[21,26,27,29,34,48,139,172] The polymer-filler interaction effects the polymer chains by creating a steric hindrance on the chains and hampering their mobility. This results in an enhancement of thermal stability compared to unfilled polymers.[21,31,49,169-171]

The viscosity of the PDMS with Hi-Sil-135 filler was lower than expected and could flow relatively easily. As a result of the lower viscosity, a loading study was conducted on the PDMS compounded with Hi-Sil-135 filler at 20 wt%, 25 wt%, and 30 wt% loading levels to determine if additional filler would enhance the viscosity and the

thermal stability of the filled materials. Multiple studies have noted that elevated filler loadings can enhance the thermal stability of filled materials.[26,27,29,31,37,59,173]

Figure 43 displays the TGA thermograms of the filled PDMS compounded with 20 wt%, 25 wt%, and 30 wt% Hi-Sil-135 filler at 30°C compared to the PDMS polymer. The temperature at 10% and 50% weight loss, as well as the residue percentage values of the filled PDMS compounded with varied filler amounts of Hi-Sil-135 filler at 30°C compared to the PDMS polymer are shown in Table 25. The values in Table 25 are median values of the three specimens per compounded material taken at the beginning of the compounding process, middle of the compounding process, and end of the compounding process.

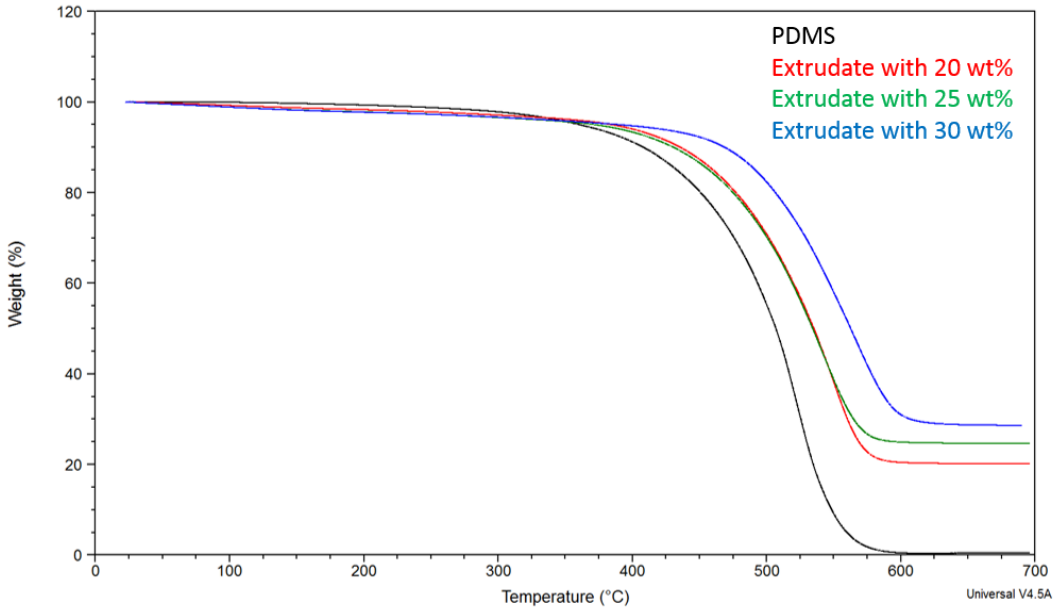

Figure 43. TGA thermograms of the filled PDMS compounded with varied filler amounts of Hi-Sil-135 filler at 30°C compared to the PDMS polymer: PDMS polymer (—), extrudate with 20 wt% filler (—), extrudate with 25 wt% filler (—), and extrudate with 30 wt% filler (—).

Table 25. Thermal properties of the filled PDMS compounded with varied filler amounts of Hi-Sil-135 filler at 30°C compared to the PDMS polymer.

Polysiloxane	Filler Loading Level (wt%)	Temperature at 10% Weight Loss (°C)	Temperature at 50% Weight Loss (°C)	Residue (%)
PDMS Polymer	-	408	507	0.00
Extrudate with 20 wt%	20	436	535	20.14 (±0.04)
Extrudate with 25 wt%	25	431	534	24.60 (±0.32)
Extrudate with 30 wt%	30	469	563	28.48 (±2.11)

The filled materials possessed greater thermal stability compared to the unfilled PDMS polymer. Minimal enhancement in thermal stability was observed comparing the 20 wt% and 25 wt%-filled materials. However, there was a 30°C enhancement in thermal stability in the 30 wt%-filled material. The residue percentage values were approximately equivalent to the calculated filler loading amount. The values were within 2% of each other, indicating an even distribution of filler throughout the compounded materials.

The enhanced thermal stability of the materials with higher silica loading can be attributed to higher filler amounts. It is commonly reported that additional filler can further interact with the polymer backbone to hinder the mobility of the polymer chains.[21,31,49,169-171] Additional filler can also further aggregate to create a stronger and thicker protective silica barrier to hinder the release of the cyclic volatiles and enhance the thermal stability.[37,173] However, further enhancement of filler can begin to cluster up and create agglomerates that disrupt the polymer-filler interactions and reduce the thermal stability of the filled materials.[26,31,59,173] According to Figure 43, agglomeration does not appear to be present for the PDMS compounded with 30 wt% Hi-Sil-135-filler.

The TGA thermograms of the filled PDMS compounded with 20 wt% Hi-Sil-233D filler at 30°C, 40°C, and 50°C compared to the PDMS polymer are displayed in

Figure 44. The temperature at 10% and 50% weight loss, as well as the residue percentage values of the filled PDMS compounded with 20 wt% Hi-Sil-233D filler at varied extrusion temperatures compared to the PDMS polymer are shown in Table 26. The values in Table 26 are median values of the three specimens per compounded material taken at the beginning of the compounding process, middle of the compounding process, and end of the compounding process.

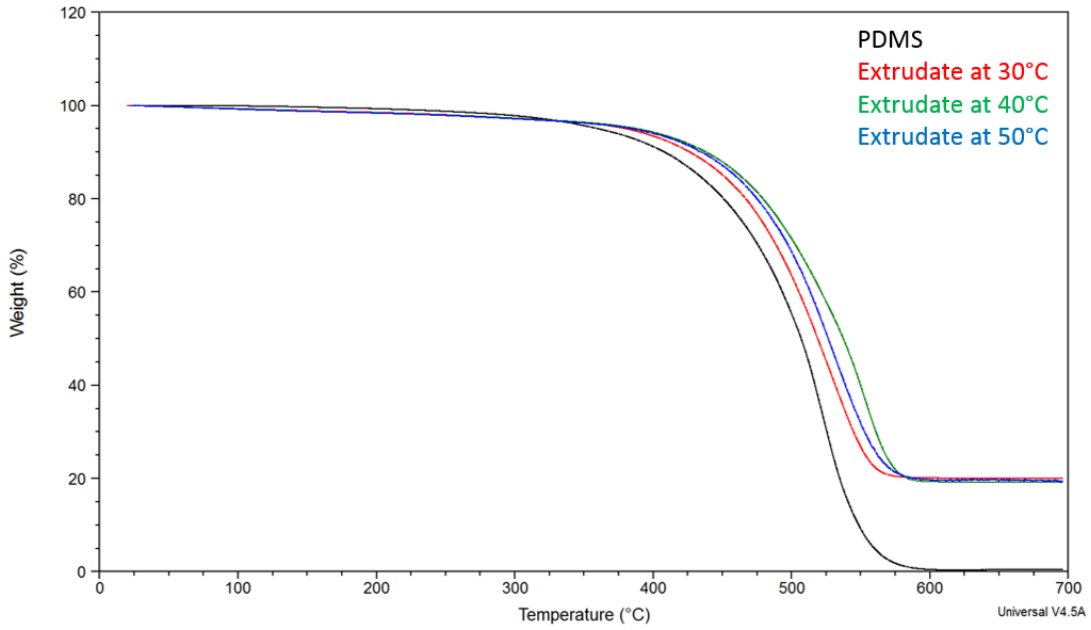

Figure 44. TGA thermograms of the filled PDMS compounded with 20 wt% Hi-Sil-233D filler at varied extrusion temperatures compared to the PDMS polymer: PDMS polymer (—), extrudate at 30°C (—), extrudate at 40°C (—), and extrudate at 50°C (—).

Table 26. Thermal properties of the filled PDMS compounded with 20 wt% Hi-Sil-233D filler at varied extrusion temperatures compared to the PDMS polymer.

Polysiloxane	Extrusion Temperature (°C)	Temperature at 10% Weight Loss (ºC)	Temperature at 50% Weight Loss (ºC)	Residue (%)
PDMS Polymer	-	408	507	0.00
Extrudate at 30°C	30	427	519	19.99 (±0.12)
Extrudate at 40°C	40	438	538	19.15 (±0.27)
Extrudate at 50°C	50	435	527	19.52 (±1.14)

The filled materials possessed greater thermal stability compared to the unfilled PDMS polymer. However, there was no appreciable difference in thermal stability among the materials processed at the three different temperatures, expect for a slight thermal enhancement in the material processed at 40°C. The residue percentage values were approximately equivalent to the calculated filler loading amount. The values were within less than 1% of each other, indicating an even distribution of filler throughout the compounded materials.

Figure 45 shows the TGA thermograms of the filled PDMS compounded with 20 wt% Cab-O-Sil filler at 30°C compared to the PDMS polymer. The temperature at 10% and 50% weight loss, as well as the residue percentage values of the filled PDMS compounded with 20 wt% Cab-O-Sil filler at 30°C compared to the PDMS polymer are shown in Table 27. Extrudate A was a specimen from the beginning of the compounding process, extrudate B was a specimen from the middle of the compounding process, and extrudate C was a specimen from the end of the compounding process.

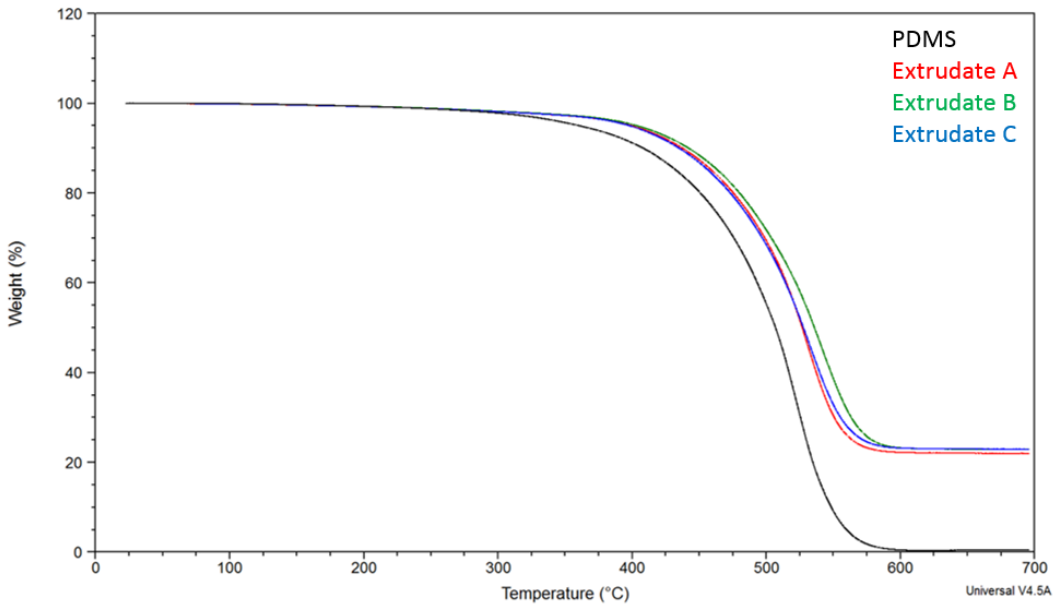

Figure 45. TGA thermograms of the filled PDMS compounded with 20 wt% Cab-O-Sil filler at 30°C compared to the PDMS polymer: PDMS polymer (—), extrudate A (—), extrudate B (—), and extrudate C (—).

Table 27. Thermal properties of the filled PDMS compounded with 20 wt% Cab-O-Sil filler at 30°C compared to the PDMS polymer.

Polysiloxane	**Temperature at 10% Weight Loss (ºC)**	**Temperature at 50% Weight Loss (ºC)**	**Residue (%)**
PDMS Polymer	408	507	0.00
Extrudate A	437	527	21.96
Extrudate B	442	536	22.87
Extrudate C	435	528	22.92

The filled materials possessed greater thermal stability compared to unfilled PDMS polymer. There was no appreciable difference in thermal stability among the three specimens. The residue percentage values were approximately equivalent to the calculated filler loading amount. The values were within less than 3% of each other,

indicating an even distribution of filler throughout the compounded materials. However, the residue percentage values were slightly higher than the calculated filler loading amount.

The increase in the residue percentage values could be attributed to the Cab-O-Sil filler. The Cab-O-Sil filler is a fumed silica with a higher surface area compared to both Hi-Sil precipitated silica fillers. Higher surface area fillers have an abundance of silanol groups to enhance the interactions with the polymer backbone.[139,27,31] Thus, the Cab-O-Sil filler obtained a stronger interaction with the PDMS that resulted in higher residue that remained after TGA analysis. The higher residue values were composed of unreleased polymer fused with the filler. Shim and Isayev reinforced PDMS with precipitated and fumed silica. They observed that both types of silica, despite their differences in dimensions were dispersed similarly in the PDMS matrix. They also recognized that the fumed silica had a stronger interaction with the PDMS than the precipitated silica when comparing rheological properties.[32]

5.9 Oscillatory rheometry of filled PDMS

The yield stress of the commercial PDMS-filled materials were analyzed by oscillatory rheometry. The yield stress of the silica-filled materials were determined by the point at which the storage modulus and loss modulus curves intersect. Thus, an oscillatory stress sweep from 3 Pa to 5,000 Pa was applied to the Hi-Sil-135-filled and the Hi-Sil-233D-filled formulations. An oscillatory stress sweep from 3 Pa to 10,000 Pa was applied to the Cab-O-Sil-filled formulations and the reference silicone. A temperature and loading study were conducted on the PDMS compounded with Hi-Sil-

135-filler. Table 28 displays the yield stress values of the filled PDMS compounded with Hi-Sil-135 filler at varied extrusion temperatures compared to the reference silicone.

Table 28. Yield stress of the filled PDMS compounded with 20 wt% Hi-Sil-135 filler at varied extrusion temperatures compared to the reference silicone.

Polysiloxane	Extrusion Temperature (°C)	Yield Stress (Pa)
Reference Silicone	-	1,340
PDMS	30	21
PDMS	40	33
PDMS	50	21

These silica-filled materials exhibit similar rheological behavior to other silica-filled materials.[174-176] The yield stress values were significantly lower than the reference silicone for all of the PDMS materials filled with 20 wt% Hi-Sil-135 filler. This could be attributed to the filled materials not obtaining the desired percolation threshold. Various authors have stated that low silica concentration levels do not approach the percolation threshold and therefore cannot obtain an accurate yield stress.[40,177] It is also known that low filler loadings can act as a plasticizer and decrease viscosity. The filler amount was too low to generate an aggregated network structure and disrupt the mobility of the polymer chains.[39,178,179]

However, as the filler loading increased, the percolation threshold was likely achieved. At 25 wt% and 30 wt% filler loadings, the yield stress values for these PDMS-filled materials dramatically increased and exceeded the reference silicone. Table 29 displays the yield stress values of the filled PDMS compounded with varied filler amounts of Hi-Sil-135 filler at 30°C compared to the reference silicone.

Table 29. Yield stress of the filled PDMS compounded with varied filler amounts of Hi-Sil-135 filler at 30°C compared to the reference silicone.

Polysiloxane	Filler Loading Level (wt%)	Yield Stress (Pa)
Reference Silicone	-	1,340
PDMS	20	21
PDMS	25	2,674
PDMS	30	3,366

It was observed that the yield stress, storage modulus, and loss modulus increased as the filler loading level increased. This phenomenon is referenced in numerous studies and is attributed to the additional amount of filler generating an aggregated network structure that enhances the interactions between the polymer matrix and the filler that hinders the polymer chain mobility.[29,31,39,41,43,66,69,70,177,180-182]

Table 30 displays the yield stress values of the filled PDMS compounded with 20 wt% Hi-Sil-233D filler at varied extrusion temperatures compared to the reference silicone.

Table 30. Yield stress of the filled PDMS compounded with 20 wt% Hi-Sil-233D filler at varied extrusion temperatures compared to the reference silicone.

Polysiloxane	Extrusion Temperature (°C)	Yield Stress (Pa)
Reference Silicone	-	1,340
PDMS	30	2,122
PDMS	40	1,340
PDMS	50	2,383

The yield stress values of the Hi-Sil-233D-filled materials were similar to the reference silicone and significantly higher than the Hi-Sil-135-filled materials. The storage and loss moduli also were enhanced with the Hi-Sil-233D-filled materials

compared to the Hi-Sil-135-filled materials. The differences in yield stress, storage modulus, and loss modulus between the Hi-Sil-filled materials can be attributed to the surface area of the fillers. The Hi-Sil-233D filler particles consist of larger surface areas of 151 m^2/g on average compared to 150 m^2/g for Hi-Sil-135. Larger surface area fillers contain a much greater abundance of silanol groups that enhance particle aggregation and interactions between the filler-polymer matrix.[29,34,48,139,172] The Hi-Sil-135 filler also contained more water, per the TGA results shown in Table 23.

The yield stress of the PDMS compounded with 20 wt% Cab-O-Sil filler at 30°C was evaluated by oscillatory rheometry. The yield stress obtained for the PDMS-filled material was 8,453 Pa. The yield stress for the Cab-O-Sil-filled material was six times higher than the reference silicone. The yield stress enhancement can be attributed to the greater surface area of Cab-O-Sil. The surface area of Cab-O-Sil is 200 m^2/g, which is much larger than both Hi-Sil fillers. Larger surface areas enhance particle aggregation and interactions between the filler and the polymer matrix, resulting in increased yield stress values.[21,27,31,39,41]

5.10 Flow rheology of filled PDMS

The thixotropic behavior of the PDMS-filled materials were characterized by studying the flow rheology of the filled polysiloxane systems. Three different PDMS-filled materials were compared to the reference silicone. Figure 46 displays the first stage of the flow test for the reference silicone compared to the filled PDMS materials.

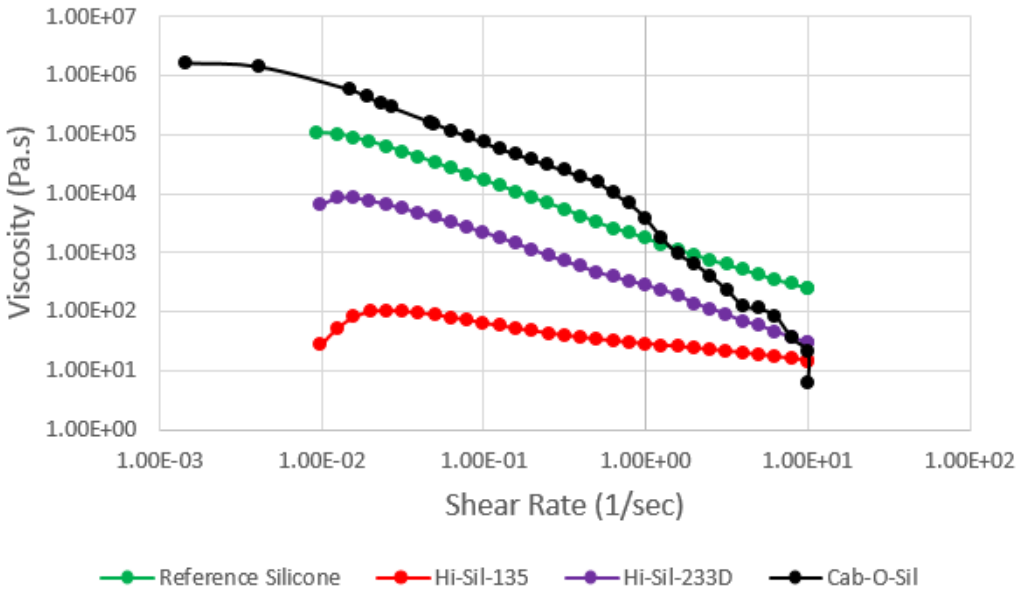

Figure 46. First stage of the flow rheology analysis for the reference silicone compared to the filled PDMS materials compounded with 20 wt% of various filler at 30°C: reference silicone (•), Hi-Sil-135 (•), Hi-Sil-233D (•), and Cab-O-Sil (•).

The viscosity of the filled materials decreased as the shear rate increased, which was attributed to the destruction of the filler network structure by the increasing shear rates. The viscosity of the Cab-O-Sil-filled material was higher at the beginning of the flow test until higher shear rates were reached and the viscosity dropped dramatically. This can be attributed to the Cab-O-Sil-filled material obtaining a higher percolation threshold than the other filled materials, although the internal aggregated network structure of the Cab-O-Sil-filled material was destroyed considerably at higher shear rates.[75,66] The viscosity of the Hi-Sil-135 and Hi-Sil-233D-filled materials were both lower than the reference silicone material. This can be attributed to both Hi-Sil-filled materials obtaining a lower percolation threshold than the reference silicone.[75,66]

The second stage of the flow test for the reference silicone compared to the filled PDMS materials are shown in Figure 47. The viscosity of the filled materials increased as the shear rate decreased, which was attributed to the reconstruction of the filler network structure over time.

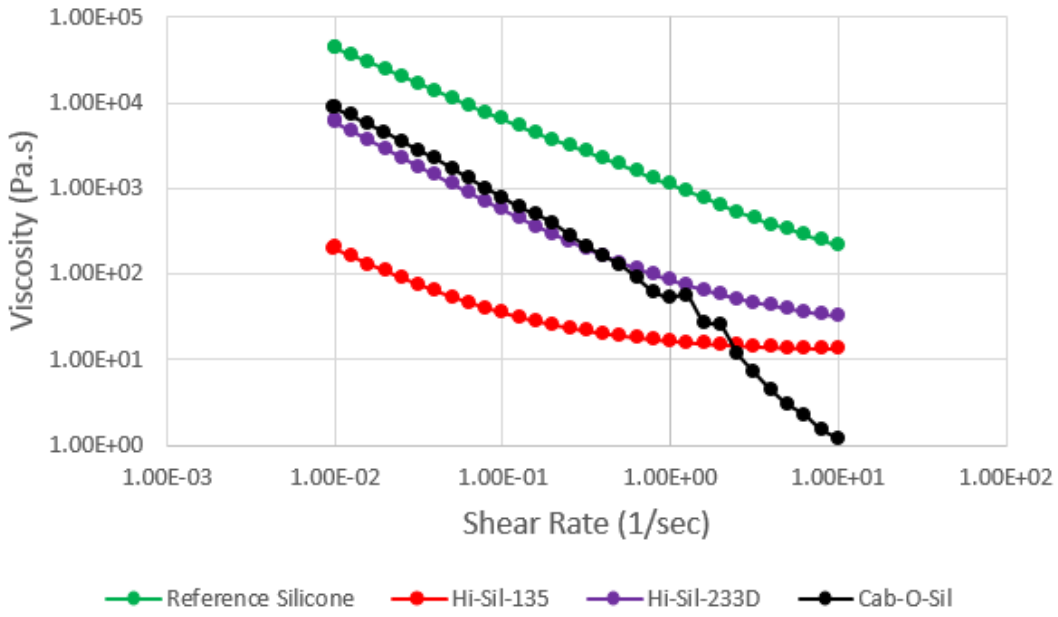

Figure 47. Second stage of the flow rheology analysis for the reference silicone compared to the filled PDMS materials compounded with 20 wt% of various filler at 30°C: reference silicone (•), Hi-Sil-135 (•), Hi-Sil-233D (•), and Cab-O-Sil (•).

Figure 48 displays the thixotropic loops of the flow test for the reference silicone compared to the filled PDMS materials. The Cab-O-Sil-filled material possessed a greater thixotropic behavior than the other filled materials. This indicates that the Cab-O-Sil-filled material required more time to reconstruct its network structure.[80,183,184] The Cab-O-Sil filler bears a higher surface area than both Hi-Sil fillers, which enhances filler-particle aggregation and interactions between the filler and the polymer matrix to enhance the thixotropic behavior.[21,27,31,39,41] The Hi-Sil-135 and Hi-Sil-233D-filled materials

displayed a shear-thinning behavior, rather than a thixotropic behavior. The shear-thinning behavior was indicated by the up and down curves almost overlaying each other. This could be attributed to the permanent deformation of the network structure in these filled materials and/or inadequate time to recover.[80]

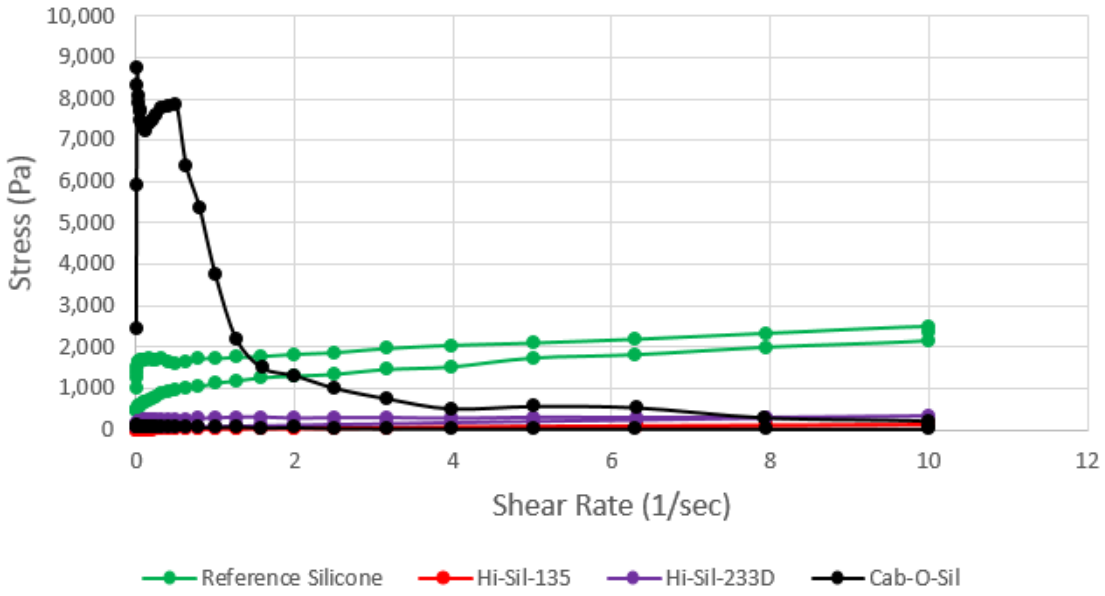

Figure 48. Thixotropic loops of the flow rheology analysis for the reference silicone compared to the filled PDMS materials compounded with 20 wt% of various filler at 30°C: reference silicone (•), Hi-Sil-135 (•), Hi-Sil-233D (•), and Cab-O-Sil (•).

A loading study was conducted on the PDMS and Hi-Sil-135 filler, and were compared to the reference silicone. Figure 49 displays the first stage of the flow test for the reference silicone compared to the filled PDMS materials with varied filler amounts of Hi-Sil-135 filler.

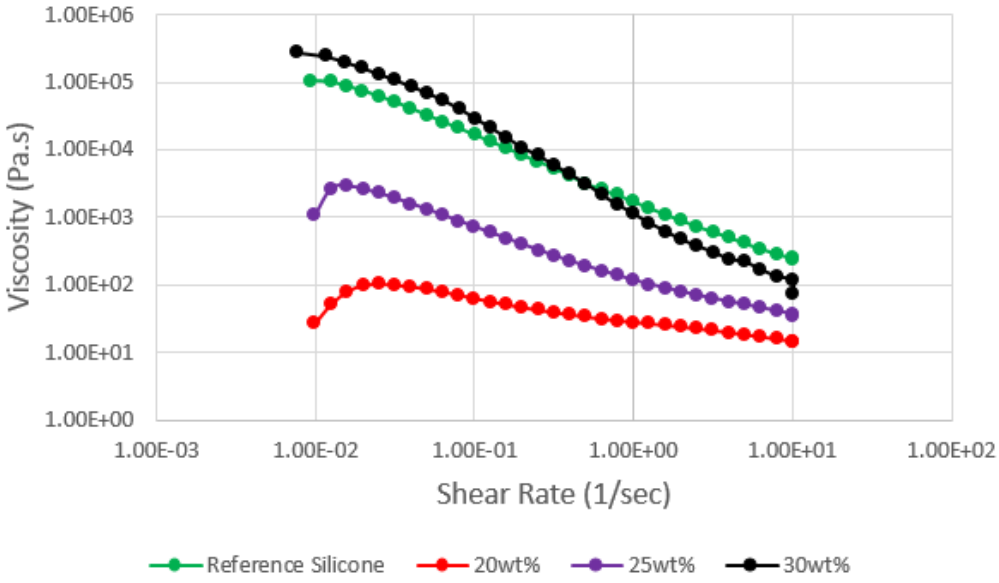

Figure 49. First stage of the flow rheology analysis for the reference silicone compared to the filled PDMS materials compounded with varied filler amounts of Hi-Sil-135 filler at 30°C: reference silicone (•), 20 wt% (•), 25 wt% (•), and 30 wt% (•).

The viscosity of the filled materials increased with increasing filler amount. The viscosity of the PDMS compounded with 30 wt% Hi-Sil-135 filler was higher at the beginning of the flow test until sufficiently high shear rates were reached and the viscosity dropped dramatically due to the considerable destruction of the network structure.[75,66] The viscosity of the PDMS compounded with 20 wt% and 25 wt% Hi-Sil-135 filler were both lower than the reference silicone material due to these materials obtaining a lower percolation threshold than the reference silicone.[75,66]

The second stage of the flow test for the reference silicone compared to the filled PDMS materials with varied filler amounts of Hi-Sil-135 filler are shown in Figure 50. The viscosity of the filled materials increased as the shear rate decreased.

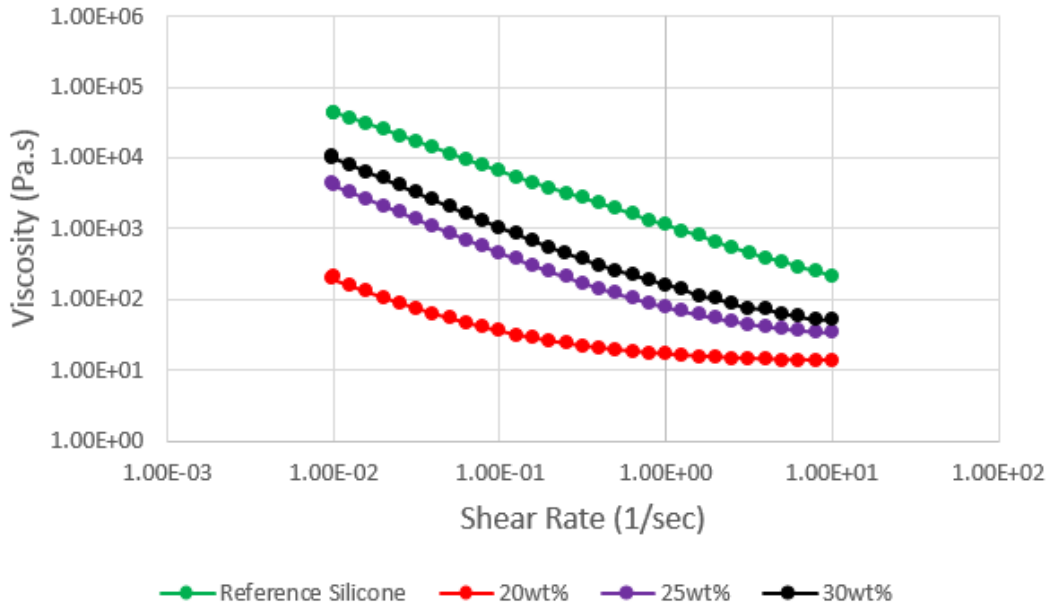

Figure 50. Second stage of the flow rheology analysis for the reference silicone compared to the filled PDMS materials compounded with varied filler amounts of Hi-Sil-135 filler at 30°C: reference silicone (•), 20 wt% (•), 25 wt% (•), and 30 wt% (•).

Figure 51 displays the thixotropic loops of the flow test for the reference silicone compared to the filled PDMS materials with varied filler amounts of Hi-Sil-135 filler. The PDMS compounded with 30 wt% Hi-Sil-135 filler displayed a greater thixotropic behavior than the other filled materials, indicating that the material required more time to reconstruct its network structure.[80,183,184] The additional amount of filler generates an aggregated network structure that hinders the polymer chains mobility to a greater extent.[31,39] The PDMS compounded with 20 wt% and 25 wt% Hi-Sil-135 filler displayed a shear-thinning behavior than a thixotropic behavior, as indicated by the up and down curves almost overlaying each other. This could be attributed to the permanent deformation of the network structure in these filled materials and/or inadequate time to recover.[80]

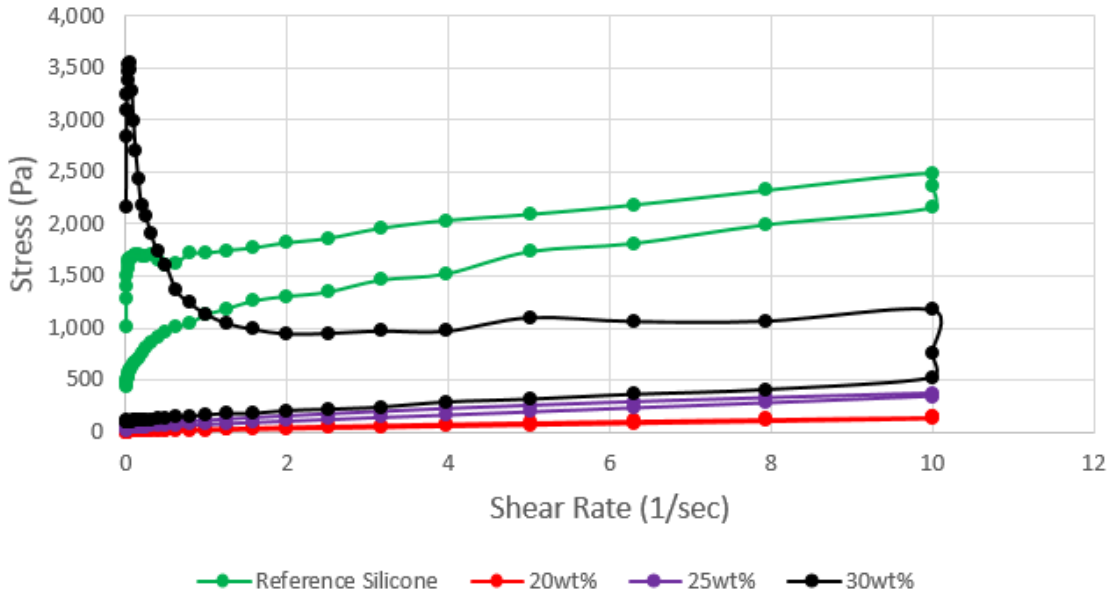

Figure 51. Thixotropic loops of the flow rheology analysis for the reference silicone compared to the filled PDMS materials compounded with varied filler amounts of Hi-Sil-135 filler at 30°C: reference silicone (•), 20 wt% (•), 25 wt% (•), and 30 wt% (•).

The reference silicone and model polysiloxanes displayed thermal properties that were consistent with previous studies evaluated of these materials. The reference silicone and the PDMS both demonstrated some degree of low-temperature crystallization that was absent in the model copolymer. The molecular weight analysis indicated that the PDMS and the model copolymer contained a mixture of high molecular weight polymer and cyclic oligomers. Thermogravimetric analysis of the three fillers studied indicated that the Hi-Sil fillers contained up to 7% water, while the Cab-O-Sil filler possessed less than 1% water. SEM analysis indicated that the Cab-O-Sil filler consisted of much smaller particles than the Hi-Sil fillers.

The thermal stability, yield stress, and thixotropic behavior were all dependent on the type of filler and not dependent on the polymer utilized in the system. When the

PDMS was filled with the Hi-Sil fillers, lower yield stresses were achieved compared to the PDMS polymer that was filled with Cab-O-Sil filler. When the PDMS was filled with greater amounts of Hi-Sil-135 filler, greater yield stresses were achieved compared to the PDMS that was filled with lesser loading amounts of Hi-Sil-135 filler. Thus, the properties of the filled polysiloxane materials were more dependent on the type of filler and filler amount, and less on the nature of the polysiloxane polymer.

CHAPTER VI

6. RESULTS AND DISCUSSION- FILLED MODEL COPOLYMER

6.1 Observations of filled model copolymer

The processing parameters, filler content, and filler type were evaluated to determine the processing conditions needed to obtain the desired yield stress and thixotropic behavior in the filled materials using a commercially-available model polysiloxane copolymer. Once these parameters were determined, they were applied to four experimentally-synthesized polysiloxanes to produce potentially viable compounded materials. The commercially-available model polysiloxane copolymer was evaluated with the three silica fillers. The model copolymer was similar to the synthesized polysiloxanes, however the model copolymer contained lower diphenyl content and lower molecular weight.

Much like with PDMS, the model copolymer was premixed with Hi-Sil-135, Hi-Sil-233D, or Cab-O-Sil silica fillers. When the fillers were first introduced into the mixtures, the mixtures would thicken and begin to form into a ball, similar to the filled PDMS materials. As mixing progressed, the viscosity of the materials decreased and they began to flow to the bottom of the mixing vessel. This phenomenon could be attributed to the interactions between the filler and the polymer matrix. It can also be attributed to the construction of aggregates that begin to reduce the chain mobility of the polymer, thus

increasing the viscosity of the material. As the filler was dispersed, the shearing of the mixer dismantled the aggregates and dispersed the filler throughout the polysiloxane matrix. The destruction of aggregates allows more apparent chain mobility which decreases the viscosity of the materials, allowing them to flow.[26]

Throughout every compounded formulation, the temperatures of the extruder increased as compounding progressed. The increase in temperature was attributed to the abrasive nature of the silica. During twin-screw extrusion, shearing of the screws and barrel creates friction that results in heat that raises the temperatures inside the barrel. The barrel temperatures increased as the filler loading increased due to the abrasive filler that generated additional shear, friction, and heat.[159-161]

When compounding the model copolymer with Hi-Sil-135 filler, the torque of the screws on the extruder never exceeded 0.4 N m. The model copolymer compounded with Hi-Sil-135 filler was a clear, white, soft, paste-like material with little dimensional stability. At higher filler loading amounts, the compounded extrudate obtained a higher degree of dimensional stability compared to the 20 wt% filled materials. The torque on the extruder also increased at higher filler loadings. This was due to the enhanced viscosity in the higher filled materials that required more torque and shear to mix them. The torque of the filled materials reached up to 0.4 N m with 20 wt% filler, 0.9 N m with 25 wt% filler, and 0.8 N m with 30 wt% filler. A study performed by Sombatsompop and coworkers also saw an increase in torque values with additional filler.[49]

While compounding the model copolymer with Hi-Sil-233D filler, the torque reached up to 0.8 N m. The model copolymer compounded with Hi-Sil-233D filler was a clear, white, soft, paste-like material with greater dimensional stability compared the Hi-

Sil-135-filled materials. When compounding the model copolymer with Cab-O-Sil filler, the torque on the extruder never exceeded 3.2 N m. The model copolymer compounded with Cab-O-Sil filler was a light grey, viscous, paste-like material with enhanced dimensional stability compared to all Hi-Sil-filled materials. The appearance of the filled model copolymer compounded materials with the three fillers after extrusion are shown in Figure 52.

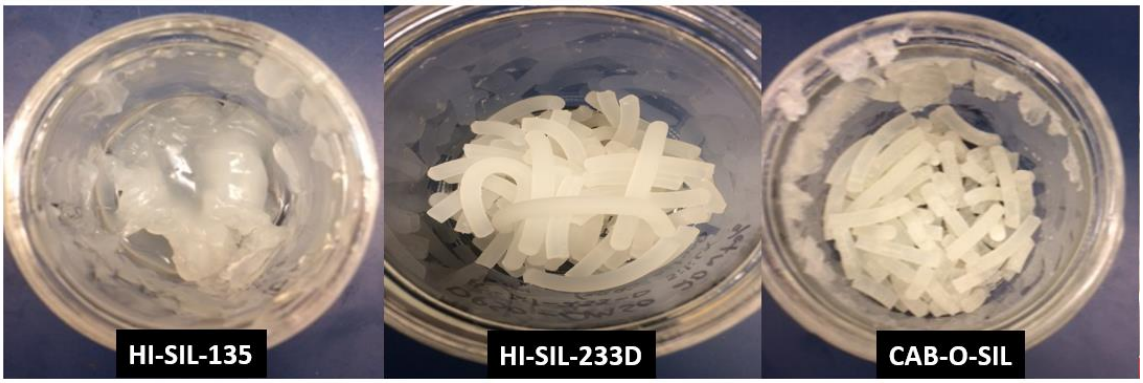

Figure 52. Appearance of the filled model copolymer compounded materials with the three separate fillers after extrusion: Hi-Sil-135, Hi-Sil-233D, and Cab-O-Sil (left to right).

6.2 Thermogravimetric analysis of filled model copolymer

The thermal stability and the filler dispersion of the filled model copolymer filled materials were investigated by TGA in a nitrogen atmosphere for the model copolymer-filled materials. Three specimens were assessed from the compounded extrudate material taken at the beginning of the compounding process, middle of the compounding process, and end of the compounding process. The residue percentage values were examined to verify an even distribution of filler by ensuring that the residue percentage values were approximately equivalent to the calculated filler loading amount. Various studies were performed using the commercial model copolymer and the three fillers. The first study

was a temperature study which consisted of the model copolymer compounded with the fillers at three different processing temperatures in order to determine which processing temperature achieved the best distribution of filler and the most thermally stable compounded extrudate materials.

Figure 53 displays the filled model copolymer compounded with 20 wt% Hi-Sil-135 filler at 30°C, 40°C, and 50°C compared to the model copolymer. The curves in Figure 53 resemble typical TGA curves of silica-filled polysiloxane materials.[33,139,168] The temperature at 10% and 50% weight loss, as well as the residue percentage values of the filled model copolymer compounded with 20 wt% Hi-Sil-135 filler at varied extrusion temperatures compared to the model copolymer are shown in Table 31. The values in Table 31 are median values of the three specimens per compounded material taken at the beginning of the compounding process, middle of the compounding process, and end of the compounding process.

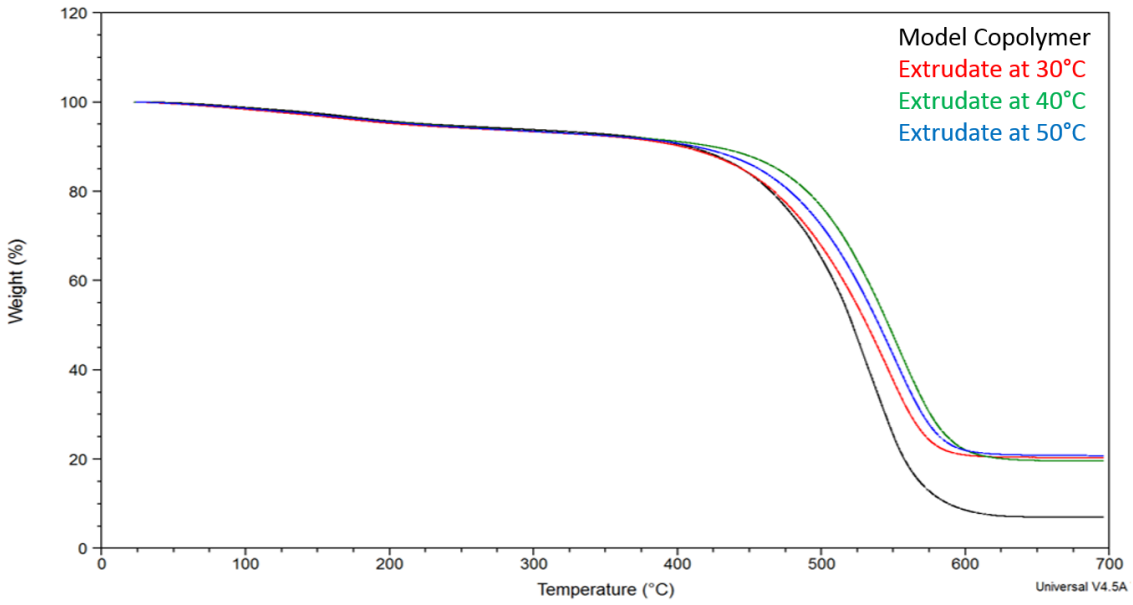

Figure 53. TGA thermograms of the filled model copolymer compounded with 20 wt% Hi-Sil-135 filler at varied extrusion temperatures compared to the model copolymer: model copolymer (—), extrudate at 30°C (—), extrudate at 40°C (—), and extrudate at 50°C (—).

Table 31. Thermal properties of the filled model copolymer compounded with 20 wt% Hi-Sil-135 filler at varied extrusion temperatures compared to the model copolymer.

Polysiloxane	Extrusion Temperature (°C)	Temperature at 10% Weight Loss (°C)	Temperature at 50% Weight Loss (°C)	Residue (%)
Model Copolymer	-	409	522	6.99
Extrudate at 30°C	30	403	532	20.09 (±0.27)
Extrudate at 40°C	40	425	547	19.56 (±1.22)
Extrudate at 50°C	50	413	540	20.32 (±0.41)

The filled materials possessed greater thermal stability compared to the unfilled model copolymer. There was a slight thermal stability enhancement in the material processed at 40°C. The residue percentage values were approximately equivalent to the

calculated filler loading amount. The values were within 1% of each other, indicating an even distribution of filler throughout the compounded materials.

The enhanced thermal stability of the filled materials was attributed to the addition of the silica filler. The surface functional groups of the filler interact with the polymer backbone to create a steric hindrance on the polymer chains and hamper their mobility.[21,31,49,169- 171] The thermal stability enhancement of the filled materials was also attributed to the filler particles participating in aggregation.[34] Aggregates can interact with the polymer matrix to create a protective barrier that disrupts the release of cyclic volatiles during decomposition.[33,36-38,139]

The viscosity of the model copolymer compounded with Hi-Sil-135 filler was lower than expected and could flow relatively easily. As a result of the lower viscosity, a loading study was also conducted on the model copolymer compounded with Hi-Sil-135 filler at 20 wt%, 25 wt%, and 30 wt% loading levels to determine if additional filler would enhance the viscosity and the thermal stability of the filled materials.

Figure 54 displays the filled model copolymer compounded with 20 wt%, 25 wt%, and 30 wt% Hi-Sil-135 filler at 30°C compared to the model copolymer. The temperature at 10% and 50% weight loss, as well as the residue percentage values of the filled model copolymer compounded with varied filler amounts of Hi-Sil-135 filler at 30°C compared to the model copolymer are shown in Table 32. The values in Table 32 are median values of the three specimens per compounded material taken at the beginning of the compounding process, middle of the compounding process, and end of the compounding process.

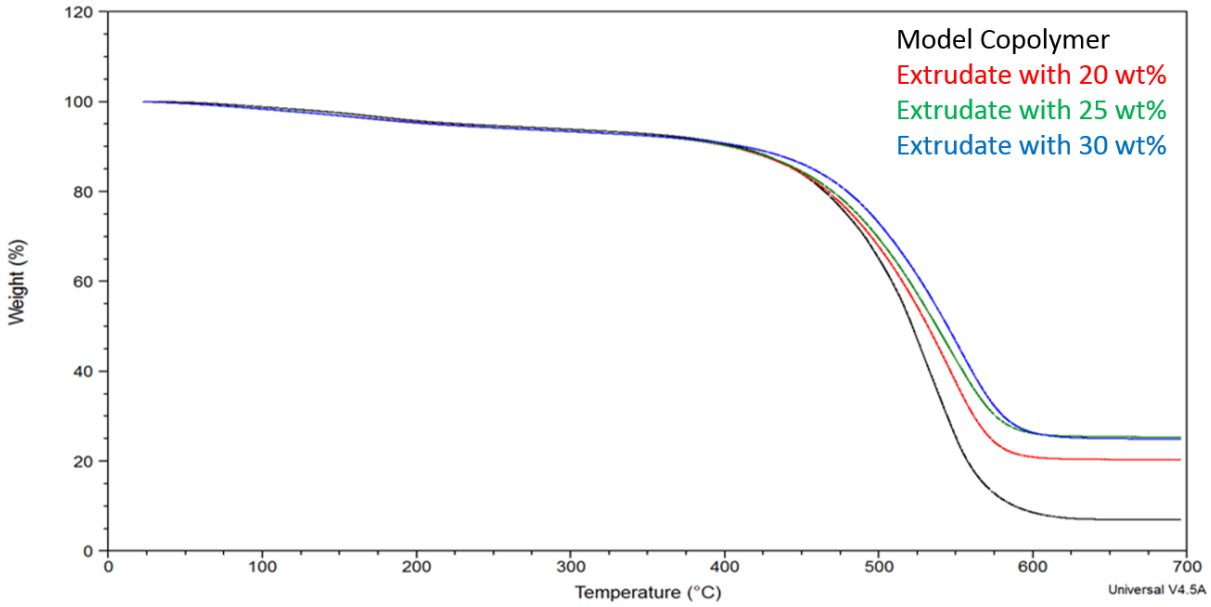

Figure 54. TGA thermograms of the filled model copolymer compounded with varied filler amounts of Hi-Sil-135 filler at 30°C compared to the model copolymer: model copolymer (—), extrudate with 20 wt% filler (—), extrudate with 25 wt% filler (—), and extrudate with 30 wt% filler (—).

Table 32. Thermal properties of the filled model copolymer compounded with varied filler amounts of Hi-Sil-135 filler at 30°C compared to the model copolymer.

Polysiloxane	Filler Loading Level (wt%)	Temperature at 10% Weight Loss (ºC)	Temperature at 50% Weight Loss (ºC)	Residue (%)
Model Copolymer	-	409	522	6.99
Extrudate with 20 wt%	20	403	532	20.09 (±0.27)
Extrudate with 25 wt%	25	404	538	25.14 (±0.16)
Extrudate with 30 wt%	30	412	545	24.50 (±0.37)

The filled materials possessed greater thermal stability compared to the unfilled model copolymer. The thermal stability of the filled materials increased with increasing filler amount. The enhanced thermal stability of these materials was attributed to the higher filler amounts. As the filler content increases, aggregates can generate a stronger

and thicker protective barrier to hinder the release of cyclic volatiles and enhance the thermal stability.[37,173]

The residue percentage values were approximately equivalent to the calculated filler loading amount. The values were within 1% of each other, indicating an even distribution of filler throughout the compounded materials. However, the residue percentage value for the 30 wt% filled material was lower than the calculated filler loading amount. This could be attributed to the increased amount of filler which can increase the viscosity of the material and hinder the dispersion of the silica particles throughout the polymer matrix. Additionally, the increased amount of filler can aggregate more rapidly to produce agglomerates. The agglomerates can reduce the space in the polymer matrix that also prevent proper dispersion of the silica particles during premixing and extrusion.[185,186]

The TGA thermograms of the filled model copolymer compounded with 20 wt% Hi-Sil-233D filler that were compounded at 30°C, 40°C, and 50°C compared to the model copolymer are displayed in Figure 55. The temperature at 10% and 50% weight loss, as well as the residue percentage values of the filled model copolymer compounded with 20 wt% Hi-Sil-233D filler at varied extrusion temperatures compared to the model copolymer are shown in Table 33. The values in Table 33 are median values of the three specimens per compounded material taken at the beginning of the compounding process, middle of the compounding process, and end of the compounding process.

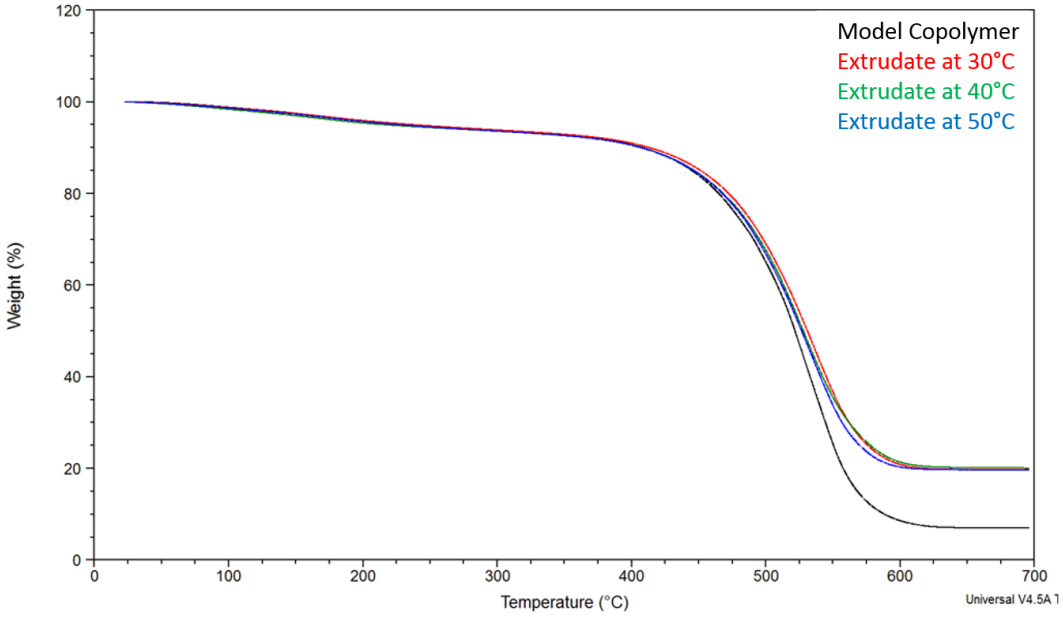

Figure 55. TGA thermograms of the filled model copolymer compounded with Hi-Sil-233D filler at varied extrusion temperatures compared to the model copolymer: model copolymer (—), extrudate at 30°C (—), extrudate at 40°C (—), and extrudate at 50°C (—).

Table 33. Thermal properties of the filled model copolymer compounded with 20 wt% Hi-Sil-233D filler at varied extrusion temperatures compared to the model copolymer.

Polysiloxane	Extrusion Temperature (°C)	Temperature at 10% Weight Loss (°C)	Temperature at 50% Weight Loss (°C)	Residue (%)
Model Copolymer	-	409	522	6.99
Extrudate at 30°C	30	413	531	19.81 (±0.12)
Extrudate at 40°C	40	407	528	20.09 (±0.17)
Extrudate at 50°C	50	406	527	19.65 (±0.07)

The filled materials possessed greater thermal stability compared to the unfilled model copolymer. There was no appreciable difference in thermal stability among the materials processed at the three different temperatures. The residue percentage values were approximately equivalent to the calculated filler loading amount. The values were

within 1% of each other, indicating an even distribution of filler throughout the compounded materials.

The TGA thermograms of the filled model copolymer compounded with 20 wt% Cab-O-Sil filler at 30°C, 40°C, and 50°C compared to the model copolymer are displayed in Figure 56. The temperature at 10% and 50% weight loss, as well as the residue percentage values of the filled model copolymer compounded with 20 wt% Cab-O-Sil filler at varied extrusion temperatures compared to the model copolymer are shown in Table 34. The values in Table 34 are median values of the three specimens per compounded material taken at the beginning of the compounding process, middle of the compounding process, and end of the compounding process.

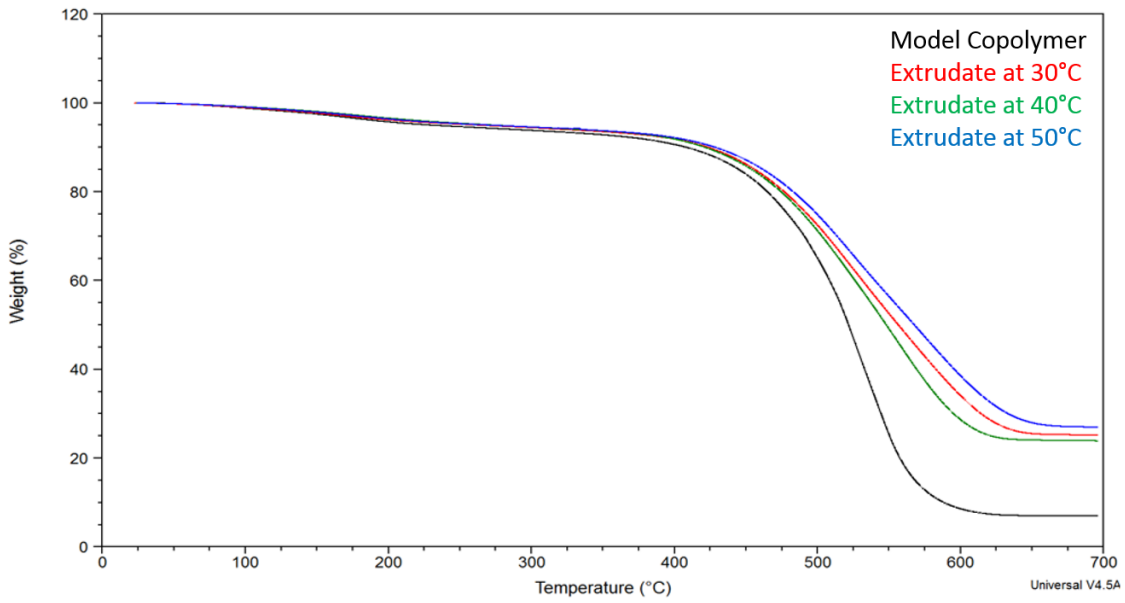

Figure 56. TGA thermograms of the filled model copolymer compounded with 20 wt% Cab-O-Sil filler at varied extrusion temperatures compared to the model copolymer: model copolymer (—), extrudate at 30°C (—), extrudate at 40°C (—), and extrudate at 50°C (—).

Table 34. Thermal properties of the filled model copolymer compounded with 20 wt% Cab-O-Sil filler at varied extrusion temperatures compared to the model copolymer.

Polysiloxane	Extrusion Temperature (°C)	Temperature at 10% Weight Loss (ºC)	Temperature at 50% Weight Loss (ºC)	Residue (%)
Model Copolymer	-	409	522	6.99
Extrudate at 30°C	30	423	557	25.18 (±2.08)
Extrudate at 40°C	40	421	548	23.68 (±0.34)
Extrudate at 50°C	50	428	568	25.38 (±1.59)

The filled materials possessed greater thermal stability compared to the unfilled model copolymer. There was a slight thermal enhancement in the material processed at 50°C. The residue percentage values were slightly higher than the calculated filler loading amount. The increase in the residue percentage values could be attributed to the higher surface area of the Cab-O-Sil filler compared to the Hi-Sil fillers. Higher surface area fillers have an abundance of silanol groups to enhance the interactions with the polymer backbone.[27,31,139] The Cab-O-Sil filler also contained less water bound to the filler surface, as demonstrated by the TGA analysis of the fillers alone. The compounded materials with the Hi-Sil fillers will lose this filler surface water during TGA, while materials compounded with Cab-O-Sil will not, resulting in higher residue percentage values.

6.3 Oscillatory rheometry of filled model copolymer

The yield stress of the commercial model copolymer-filled materials were analyzed by oscillatory rheometry. The yield stress of the silica-filled materials were determined by the point at which the storage modulus and loss modulus curves intersect. An oscillatory stress sweep from 3 Pa to 5,000 Pa was applied to the Hi-Sil-135-filled

and the Hi-Sil-233D-filled formulations. An oscillatory stress sweep from 3 Pa to 10,000 Pa was applied to the Cab-O-Sil-filled formulations and the reference silicone. A temperature and loading study were conducted on the model copolymer compounded with Hi-Sil-135 filler. Table 35 displays the yield stress values for the filled model copolymer compounded with 20 wt% Hi-Sil-135 filler at varied extrusion temperatures compared to the reference silicone.

Table 35. Yield stress of the filled model copolymer compounded with 20 wt% Hi-Sil-135 filler at varied extrusion temperatures compared to the reference silicone.

Polysiloxane	Extrusion Temperature (°C)	Yield Stress (Pa)
Reference Silicone	-	1,340
Model Copolymer	30	12
Model Copolymer	40	12
Model Copolymer	50	-

The yield stress values were significantly lower than the reference silicone for all of the model copolymer materials filled with 20 wt% Hi-Sil-135 filler. This indicates that the percolation threshold for these filled materials was not reached. Various authors have stated that low silica levels do not reach the desired percolation threshold to generate an aggregated network structure and therefore, the materials cannot reach an accurate yield stress.[39,40,177-179]

It was also observed that the loss modulus was greater than the storage modulus for the model copolymer compounded with 20 wt% Hi-Sil-135 filler processed at 50°C. This phenomenon indicated that the filled material exhibits more viscous, rather than elastic behavior. This behavior indicates that, at best, a weak aggregated network

structure was present in the system and that the percolation threshold was not achieved to obtain a yield stress value.[40,73,74]

The yield stress values for the filled model copolymer compounded with varied filler amounts of Hi-Sil-135 filler at 30°C compared to the reference silicone are shown in Table 36. It was observed that the yield stress increased as the Hi-Sil-135 filler loading level increased. This was attributed to additional filler beginning to generate a partial aggregated network structure.[29,31,39,41,43,66,69,70,177,180-182]

Table 36. Yield stress of the filled model copolymer compounded with varied filler amounts of Hi-Sil-135 filler at 30°C compared to the reference silicone.

Polysiloxane	Filler Loading Level (wt%)	Yield Stress (Pa)
Reference Silicone	-	1,340
Model Copolymer	20	12
Model Copolymer	25	753
Model Copolymer	30	475

Table 37 displays the yield stress values of the filled model copolymer compounded with 20 wt% Hi-Sil-233D filler at varied extrusion temperatures compared to the reference silicone.

Table 37. Yield stress of the filled model copolymer compounded with 20 wt% Hi-Sil-233D filler at varied extrusion temperatures compared to the reference silicone.

Polysiloxane	Extrusion Temperature (°C)	Yield Stress (Pa)
Reference Silicone	-	1,340
Model Copolymer	30	1,339
Model Copolymer	40	1,892
Model Copolymer	50	533.3

The yield stress values of the Hi-Sil-233D-filled materials were fairly similar to the reference silicone and significantly higher than the Hi-Sil-135-filled materials. However, the model copolymer compounded with Hi-Sil-233D filler at 50°C obtained a significantly lower yield stress than the other Hi-Sil-233D-filled materials. This again indicates that the percolation threshold was not obtained or that agglomeration was present in this filled material. The differences in yield stress values between both Hi-Sil-filled materials can be attributed to the surface area of the fillers. The Hi-Sil-233D filler consist of a larger surface area of 151 m^2/g compared to 150 m^2/g for Hi-Sil-135 filler. Larger surface area fillers contain an abundance of silanol groups that enhances aggregation and the interactions between the filler and polymer matrix, resulting in a greater reinforcing effect and a higher yield stress.[29,48,34,139,172] The Hi-Sil-135 filler also contained more water, per the TGA results shown in Table 23.

Table 38 displays the yield stress values of the filled model copolymer compounded with 20 wt% Cab-O-Sil filler at varied extrusion temperatures compared to the reference silicone.

Table 38. Yield stress of the filled model copolymer compounded with 20 wt% Cab-O-Sil filler at varied extrusion temperatures compared to the reference silicone.

Polysiloxane	**Extrusion Temperature (°C)**	**Yield Stress (Pa)**
Reference Silicone	-	1,340
Model Copolymer	30	5,985
Model Copolymer	40	5,334
Model Copolymer	50	8,454

The yield stress of the Cab-O-Sil-filled materials were four to six times higher than the reference silicone. The yield stress enhancement can be attributed to the higher

surface area of the Cab-O-Sil filler compared to the Hi-Sil fillers. The smaller particles of Cab-O-Sil can pack closer together and cover a greater surface area to significantly enhance aggregation and, in turn, significantly increase yield stress.[21,27,31,39,41]

6.4 Flow rheology of filled model copolymer

The thixotropic behavior of the model copolymer-filled materials was characterized by studying the flow rheology of the filled polysiloxane systems. Three different model copolymer-filled materials were compared to the reference silicone. Figure 57 displays the first stage of the flow test of the reference silicone compared to the filled model copolymer materials.

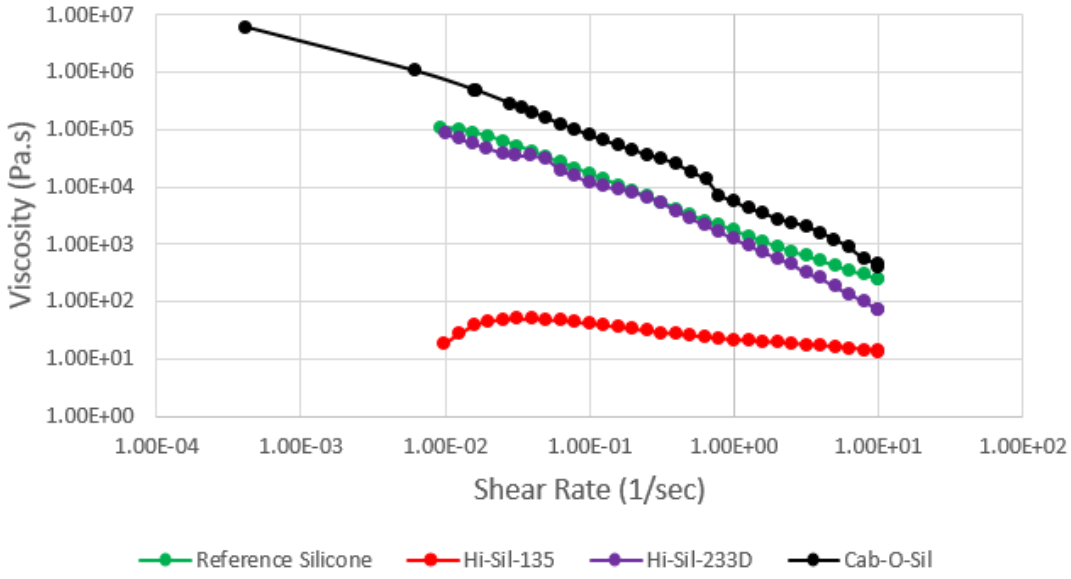

Figure 57. First stage of the flow rheology analysis for the reference silicone compared to the filled model copolymer materials compounded with 20 wt% of various filler at 30°C: reference silicone (•), Hi-Sil-135 (•), Hi-Sil-233D (•), and Cab-O-Sil (•).

The viscosity of the filled materials decreased as the shear rate increased, which was attributed to the destruction of the filler network structure by the increasing shear

rates.[66,75] The Cab-O-Sil-filled material achieved the highest viscosity of the tested materials. This was attributed to the higher surface area of the Cab-O-Sil filler resulting in better interactions with the polysiloxane backbone compared to the Hi-Sil fillers.[21,27,31,39,41] The viscosity of the Hi-Sil-233D-filled material was similar to the reference silicone. The viscosity of the Hi-Sil-135-filled material was the lowest of the tested materials due to the lower percolation threshold.[66,75]

The second stage of the flow test for the reference silicone compared to the filled model copolymer materials are shown in Figure 58. The viscosity of the filled materials increased as the shear rate decreased, which was again attributed to the reconstruction of the filler network structure over time.[80]

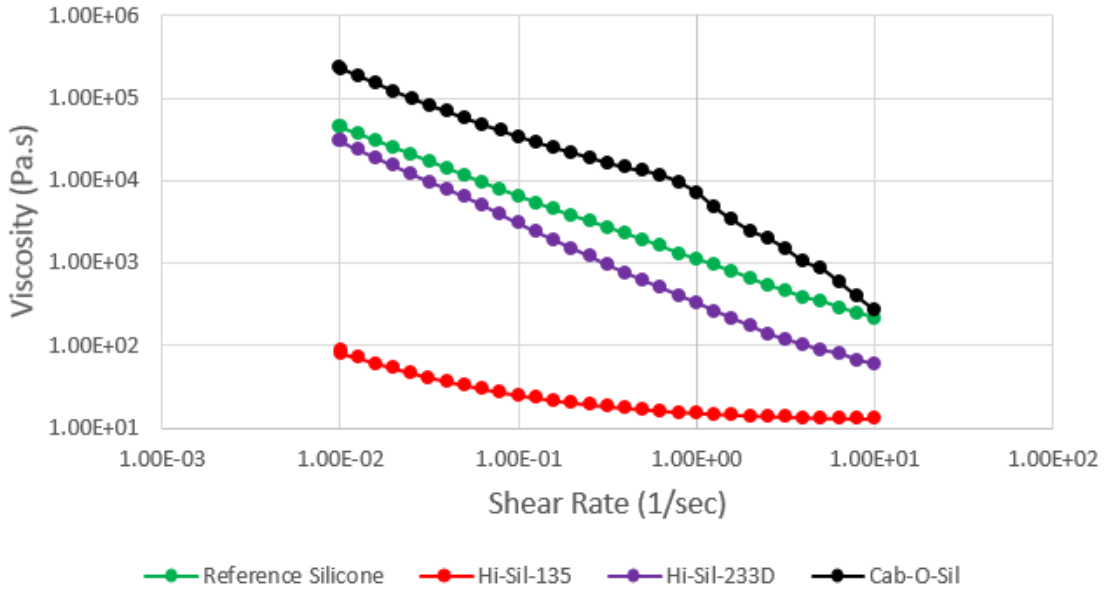

Figure 58. Second stage of the flow rheology analysis for the reference silicone compared to the filled model copolymer materials compounded with 20 wt% of various filler at 30°C: reference silicone (•), Hi-Sil-135 (•), Hi-Sil-233D (•), and Cab-O-Sil (•).

Figure 59 displays the thixotropic loops of the flow test for the reference silicone compared to the filled model copolymer materials. The Cab-O-Sil-filled material obtained a greater thixotropic behavior compared to the other filled materials. This indicates that the Cab-O-Sil-filled material required more time to reconstruct its network structure compared to the Hi-Sil-filled materials.[80,183,184] The Cab-O-Sil filler bears a higher surface area which enhances aggregation and thixotropic behavior.[21,26,27,31,39,41,187] The Hi-Sil-135-filled material demonstrated a more shear-thinning behavior than a thixotropic behavior. This shear-thinning behavior was indicated by the up and down curves almost overlaying each other. This could be attributed to the permanent deformation of the network structure, the lower percolation threshold in this filled material, or inadequate time to recover.[66,75,80]

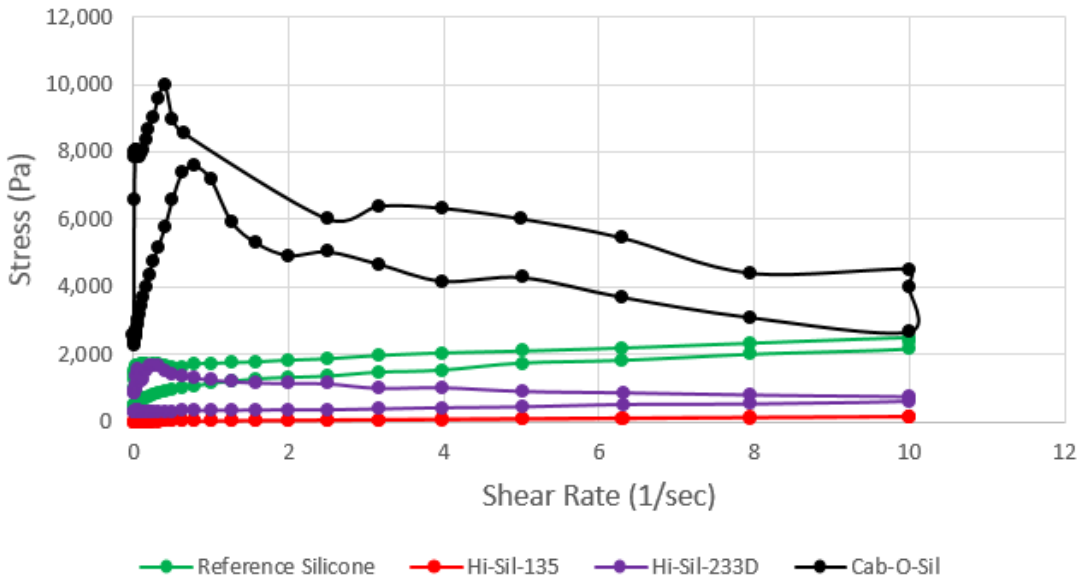

Figure 59. Thixotropic loops of the flow rheology for the reference silicone compared to the filled model copolymer materials compounded with 20 wt% of various filler at 30°C: reference silicone (•), Hi-Sil-135 (•), Hi-Sil-233D (•), and Cab-O-Sil (•).

A loading study was conducted on the model copolymer compounded with Hi-Sil-135 filler and were compared to the reference silicone. Figure 60 displays the first stage of the flow test for the reference silicone compared to the filled model copolymer materials with varied filler amounts Hi-Sil-135 filler.

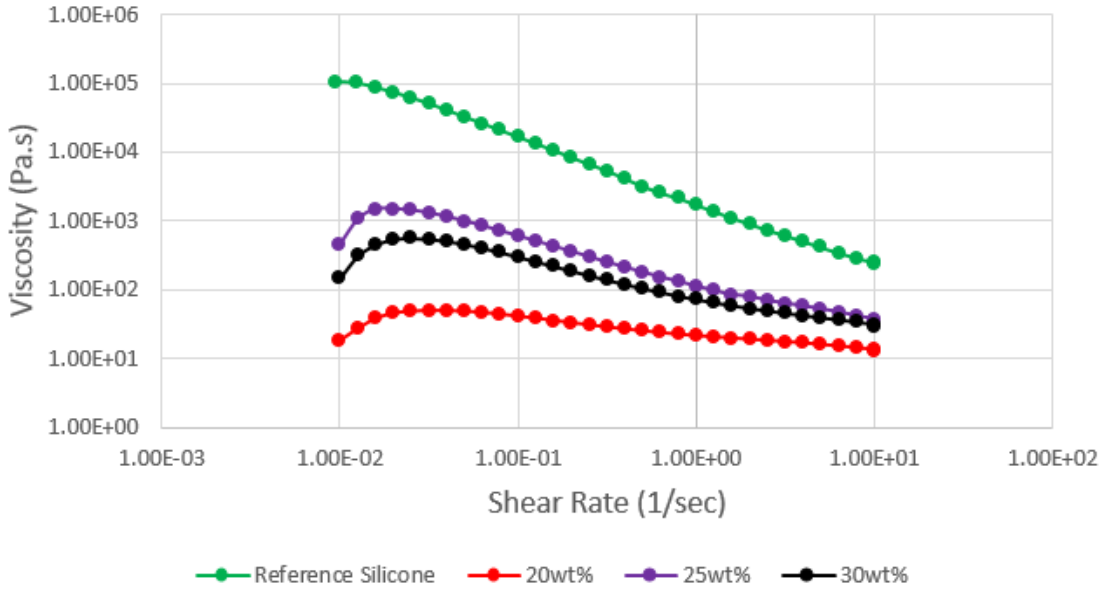

Figure 60. First stage of the flow rheology analysis the reference silicone compared to the filled model copolymer materials compounded with varied filler amounts of Hi-Sil-135 filler at 30°C: reference silicone (•), 20 wt% (•), 25 wt% (•), and 30 wt% (•).

The viscosity of the filled materials increased with increasing filler amount until 30 wt% filler, when the viscosity decreased. This could be attributed to agglomeration. Additional filler can aggregate more rapidly to produce agglomerates. The agglomerates can reduce the space in the polymer matrix that prevents proper dispersion of the silica particles. The open space in the polymer matrix can reduce the viscosity of the filled material.[185,186] The viscosity for all of the Hi-Sil-135-filled materials were lower than the reference silicone.

The second stage of the flow test for the reference silicone compared to the filled model copolymer materials with varied filler amounts of Hi-Sil-135 filler are shown in Figure 61. The viscosity of the filled materials increased as the shear rate decreased.[80]

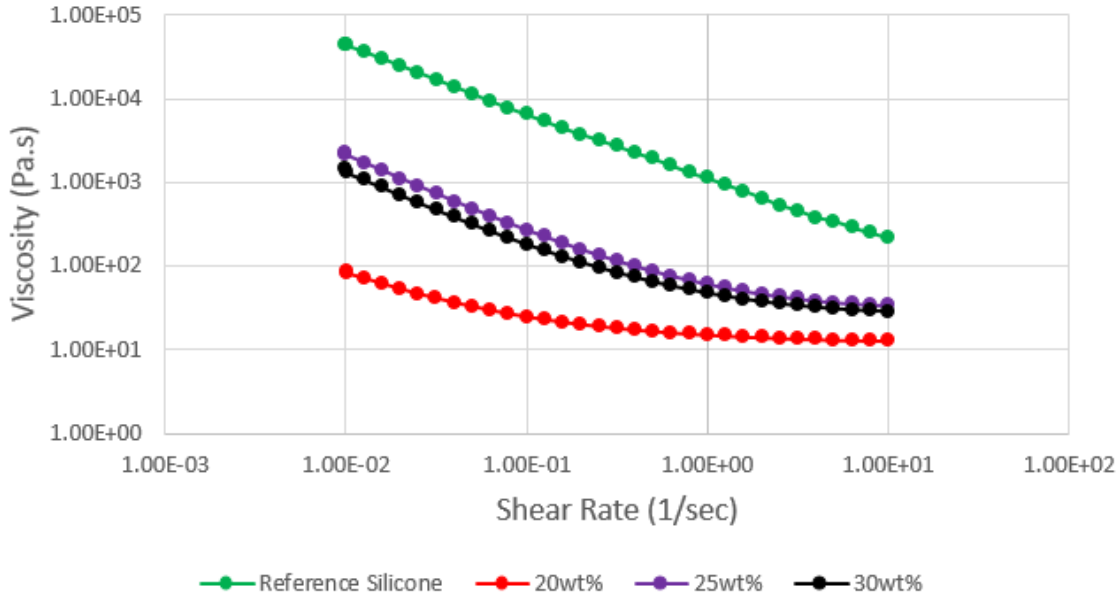

Figure 61. Second stage of the flow rheology analysis for the reference silicone compared to the filled model copolymer materials compounded with varied filler amounts of Hi-Sil-135 filler at 30°C: reference silicone (•), 20 wt% (•), 25 wt% (•), and 30 wt% (•).

Figure 62 displays the thixotropic loops of the flow test for the reference silicone compared to the filled model copolymer materials with varied filler amounts of Hi-Sil-135 filler. The reference silicone possessed a greater thixotropic behavior compared to the Hi-Sil-135-filled materials, indicating that the reference silicone required more time to reconstruct its network structure.[80,183,184] The Hi-Sil-135-filled materials possessed a more shear-thinning behavior than a thixotropic behavior at all loading levels. This was attributed to the permanent deformation of the network structure, the lower the percolation threshold in these filled materials, or inadequate time to recover.[66,75,80]

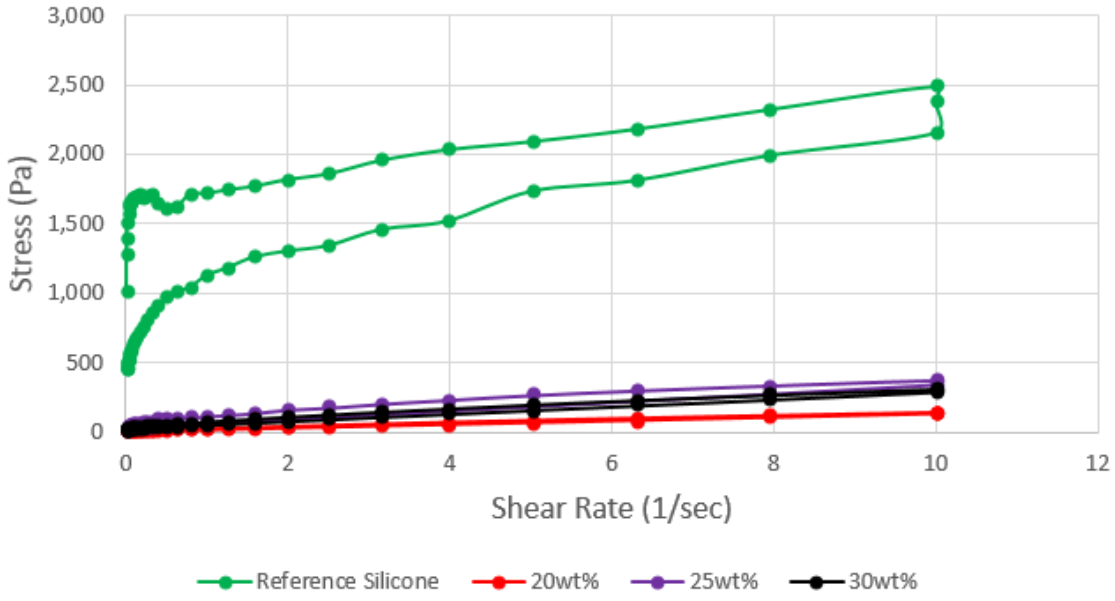

Figure 62. Thixotropic loops of the flow rheology analysis for the reference silicone compared to the filled model copolymer materials compounded with varied filler amounts of Hi-Sil-135 filler at 30°C: reference silicone (•), 20 wt% (•), 25 wt% (•), and 30 wt% (•).

The thermal stability, yield stress, and thixotropic behavior were all dependent on the type of filler and not dependent on the polymer utilized in the system. When the model copolymer was filled with the Hi-Sil fillers, they achieved lower yield stresses than the model copolymer filled with Cab-O-Sil. When the model copolymer was filled with a greater amount of Hi-Sil-135, greater yield stresses were achieved than model copolymer that was filled with lesser loading amounts of Hi-Sil-135. PDMS displayed the same phenomena when filled with these fillers as well. Thus, the properties of the filled polysiloxane materials were more dependent on the type of filler and filler amount, and less on the nature of the polysiloxane polymer.

Various temperature and loading studies were performed on the model copolymer-filled materials in order to determine to determine the appropriate processing

parameters, filler content, and filler type to obtain the appropriate yield stress and thixotropic behavior in the filled materials. These parameters were evaluated and chosen to be applied to the four experimentally-synthesized vinyl-terminated polysiloxanes. From the model copolymer studies, the synthesized polysiloxanes were filled with 20 wt% Cab-O-Sil filler at 40°C. The Cab-O-Sil-filled materials resulted in the most thermally-stable filled materials with the greatest yield stress values. The processing temperature of 40°C resulted in the most consistently thermally stable materials, as well as resulted in the best distribution of filler.

CHAPTER VII

7. RESULTS AND DISCUSSION- FILLED SYNTHESIZED POLYSILOXANES

7.1 Observations of synthesized polysiloxanes

The synthesized polysiloxanes were all opaque, colorless, viscous fluids. The appearance of one of the synthesized polysiloxanes (DiMeDiPh$_{5.3}$DiEt$_5$-720) is shown in Figure 63.

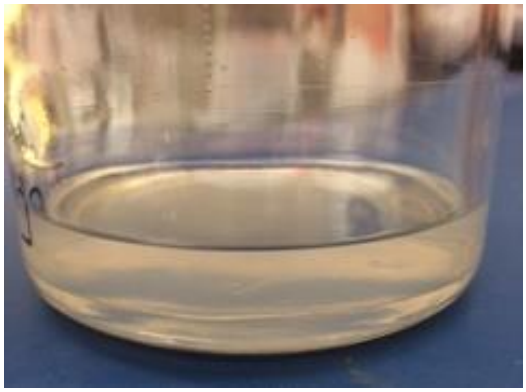

Figure 63. Appearance of one of the synthesized polysiloxanes (DiMeDiPh$_{5.3}$DiEt$_5$-720).

7.2 Gel permeation chromatography of synthesized polysiloxanes

The molecular weight of the synthesized polysiloxanes were determined by GPC. The GPC curves are shown in Figure 64. Table 39 displays the number average molecular weight (M_n), the peak molecular weight (M_p), the weight average molecular weight (M_w), and the polydispersity index (PDI) for the synthesized polysiloxanes.

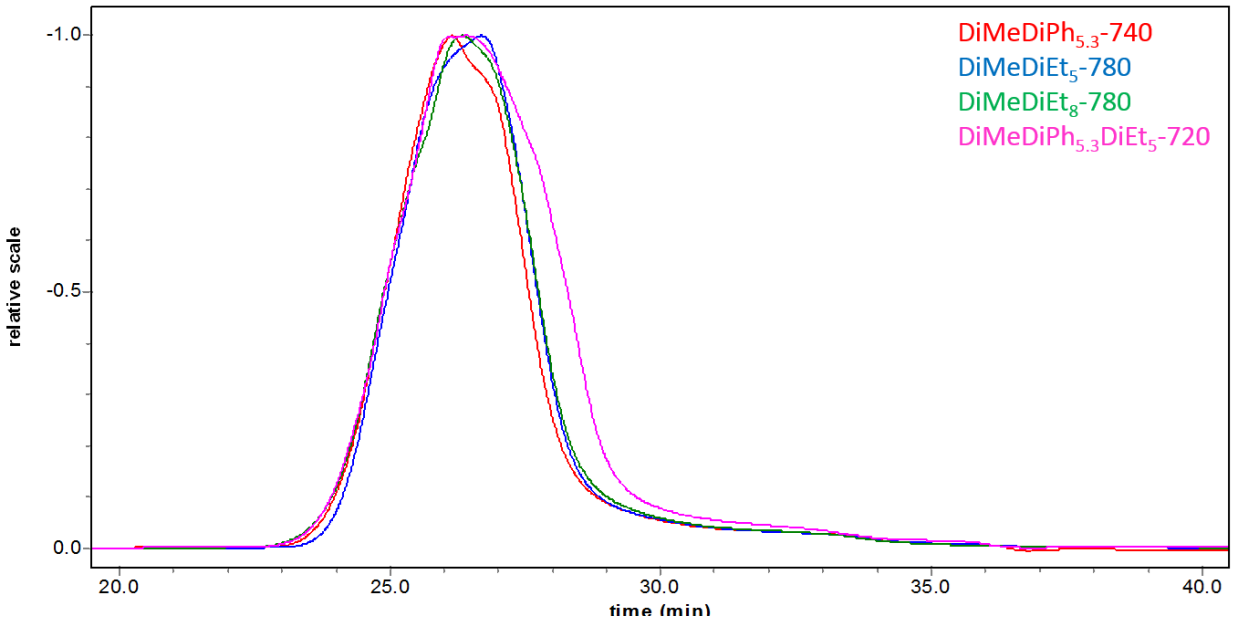

Figure 64. GPC curves of the synthesized polysiloxanes: DiMeDiPh$_{5.3}$-740 (—), DiMeDiEt$_5$-780 (—), DiMeDiEt$_8$-780 (—), and DiMeDiPh$_{5.3}$DiEt$_5$-720 (—).

Table 39. Molecular weight of the synthesized polysiloxanes.

Polysiloxane	M_n (g/mol)	M_p (g/mol)	M_w (g/mol)	PDI (M_w/M_n)
DiMeDiPh$_{5.3}$-740	41,190	55,850	65,540	1.59
DiMeDiEt$_5$-780	36,390	39,600	51,040	1.42
DiMeDiEt$_8$-780	35,890	47,490	59,470	1.66
DiMeDiPh$_{5.3}$DiEt$_5$-720	43,930	48,790	60,650	1.38

The GPC curves were similar to typical curves of dimethyl-, diphenyl-, and diethyl-containing polysiloxanes reported in other studies.[127-131] The four synthesized polysiloxanes all possessed PDIs greater than 1.2, indicative of the most probable distribution resulting from polysiloxane equilbration.[129]

7.3 Differential scanning calorimetry of synthesized polysiloxanes

The thermal behavior of the synthesized polysiloxanes was investigated by DSC. Figure 65 displays the DSC curves of the synthesized polysiloxanes.

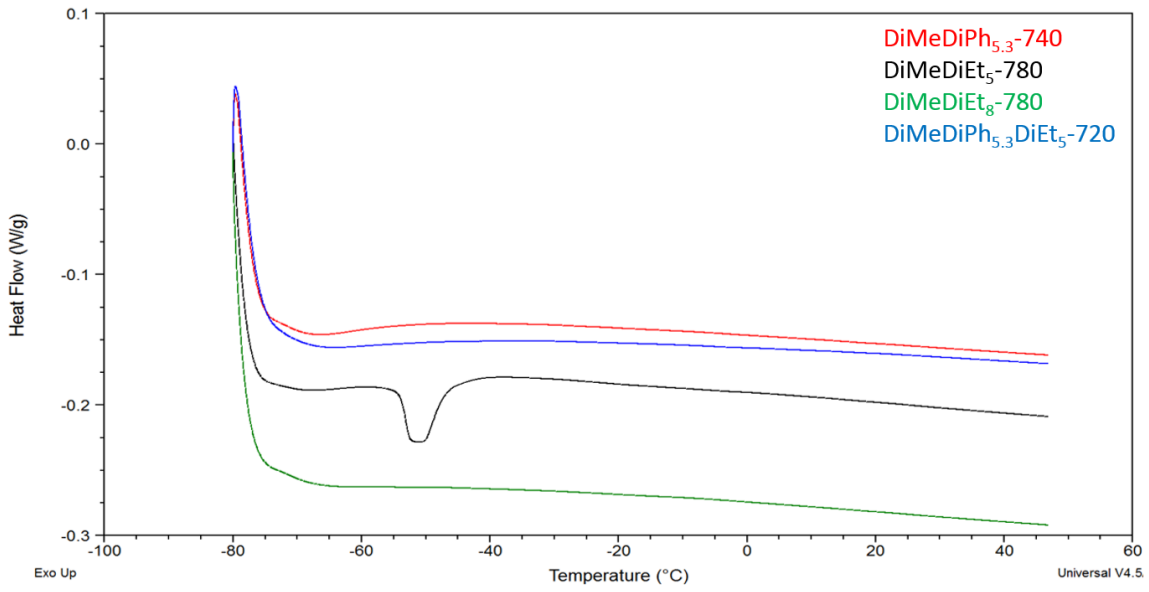

Figure 65. DSC curves of the synthesized polysiloxanes: DiMeDiPh$_{5.3}$-740 (—), DiMeDiEt$_5$-780 (—), DiMeDiEt$_8$-780 (—), and DiMeDiPh$_{5.3}$DiEt$_5$-720 (—).

The DSC curves resemble typical curves of dimethyl-, diphenyl-, and diethyl-containing polysiloxanes that have been reported in literature.[135] The synthesized polysiloxanes were expected to possess no low-temperature crystallization in order to maintain their desirable surface and high temperature properties. The DSC analysis confirms that three of the four synthesized polysiloxanes did not exhibit low-temperature crystallization. This was due to the presence of the diphenyl- and diethyl-siloxy units which disrupts crystallization.[12,13] However, low-temperature crystallization did occur in the DiMeDiEt$_5$-780 copolymer. The T_m was -50.42°C. As a result of the presence of crystallization in the DiMeDiEt$_5$-780 copolymer, the DiMeDiEt$_8$-780 copolymer was synthesized with higher diethyl content to prevent crystallization.[12,13] The DSC analysis confirms that no crystallization was present in the DiMeDiEt$_8$-780 copolymer.

7.4 Thermogravimetric analysis of synthesized polysiloxanes

The thermal stability of the synthesized polysiloxanes was investigated by TGA TGA in a nitrogen atmosphere Figure 66 shows the. The curves in Figure 66 resemble typical TGA curves of dimethyl-, diphenyl-, and diethyl-containing polysiloxanes in multiple studies.[136,146,147,151,152] The temperature at 10% and 50% weight loss, as well as the residue percentage values of the synthesized polysiloxanes are displayed in Table 40.

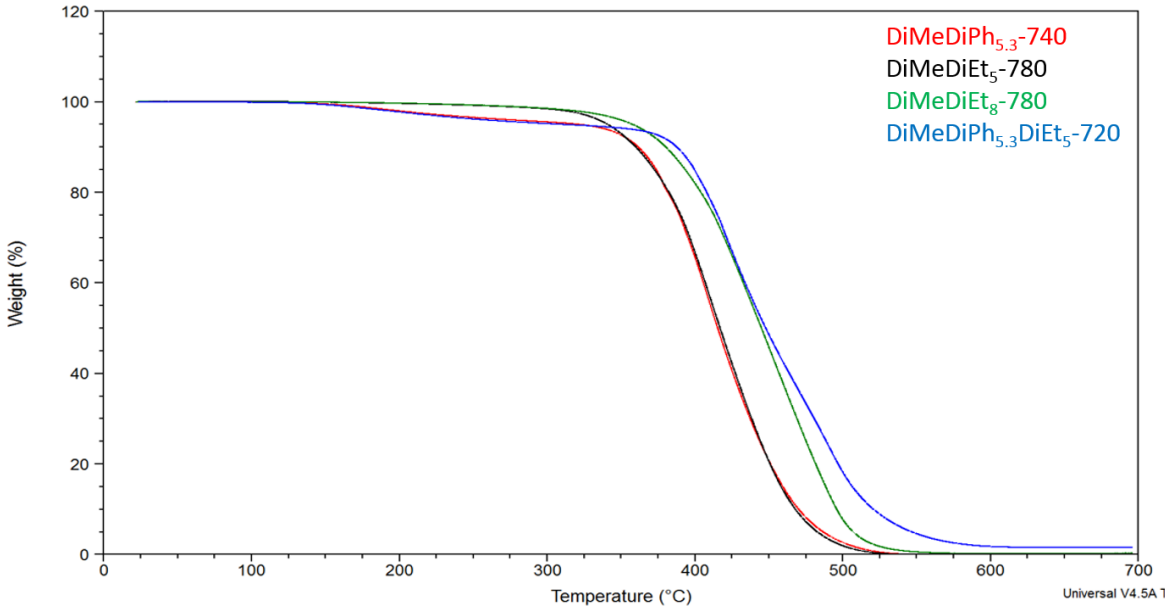

Figure 66. TGA thermograms of the synthesized polysiloxanes: DiMeDiPh$_{5.3}$-740 (—), DiMeDiEt$_5$-780 (—), DiMeDiEt$_8$-780 (—), and DiMeDiPh$_{5.3}$DiEt$_5$-720 (—).

Table 40. Thermal properties of the synthesized polysiloxanes.

Polysiloxane	Temperature at 10% Weight Loss (°C)	Temperature at 50% Weight Loss (°C)	Residue (%)
DiMeDiPh$_{5.3}$-740	361	416	0.06
DiMeDiEt$_5$-780	360	417	0.02
DiMeDiEt$_8$-780	380	445	0.27
DiMeDiPh$_{5.3}$DiEt$_5$-720	388	448	1.51

The DiMeDiEt$_8$-780 and DiMeDiPh$_{5.3}$DiEt$_5$-720 polysiloxanes were the most thermally stable of the four copolymers. The increased thermal stability was attributed to the higher diphenyl- and diethyl-content levels, which was similar to the observations of Zhu and coworkers.[151] Higher diphenyl and diethyl content reduces the chain mobility and hinders the ability of the polymers to release cyclic volatiles, thus increasing the thermal stability of the polymers.[146,147,151,152] The dimethyl- and diphenyl-containing copolymers showed a slight reduction in weight from 75°C to 400°C that was attributed to the release of the cyclic oligomers still present in the polymer mixture from synthesis. This decrease typically occurred in dimethyl- and diphenyl-containing copolymers.[147]

7.5 Observations of filled synthesized polysiloxanes

As mentioned in Chapter VI, the model copolymer was filled with the three separate fillers to determine the appropriate processing parameters, filler content, and filler type in order to apply the parameters to the four experimentally-synthesized vinyl-terminated polysiloxanes. The model copolymer filled Cab-O-Sil filler materials resulted in the most thermally stable materials, obtained the highest yield stress, and achieved the greatest thixotropic behavior compared to the other fillers evaluated. The Cab-O-Sil filler also contained smaller particles, a larger surface area, and was 99.41% pure silica with little water content, whereas the Hi-Sil fillers may contain impurities and moisture.[19] It was decided that the synthesized polysiloxanes would be filled with 20 wt% Cab-O-Sil filler at 40°C. The processing temperature of 40°C resulted in the most consistent thermally stable materials, as well as in the best distribution of filler in the model copolymer studies. The filled synthesized polysiloxane materials were compared to the

commercial reference silicone in terms of yield stress determined from oscillatory rheometry and thixotropy determined from flow rheology analysis.

During premixing, Cab-O-Sil filler was added to the synthesized polysiloxanes and stirred until all of the desired amount of filler was premixed. The mixtures would form into a ball, similar to the model polysiloxane materials. As mixing progressed, the viscosity of the materials decreased and began to flow. This phenomenon could be attributed to the interactions between the filler and the polymer matrix as well as to filler aggregation. The shearing of the mixer disrupted the polymer-filler interactions and the filler aggregates. This resulted in the filled materials being able to flow more easily as mixing progressed.[131]

The premixed synthesized polysiloxanes with Cab-O-Sil were loaded into the Process 11 twin-screw extruder by hand, and the resulting compounded extrudate was collected. Throughout every compounded formulation, the temperatures of the extruder increased as compounding progressed. During twin-screw extrusion, shearing of the screws and barrel creates friction that results in heat and raises the temperatures inside the barrel. The increase in temperature was attributed to the abrasive nature of the silica which generated additional shear, friction, and heat.[159-161]

When compounding the synthesized polysiloxanes with Cab-O-Sil filler, the torque on the extruder never exceeded 3.0 N m. The compounded synthesized polysiloxane materials were light grey, viscous, paste-like materials with enhanced dimensional stability compared to unfilled synthesized polysiloxanes, similar to the compounded model copolymer with Cab-O-Sil. The appearance of the filled

$DiMeDiPh_{5.3}DiEt_5$-720 synthesized polysiloxane compounded material with 20 wt% Cab-O-Sil at 40°C is shown in Figure 67.

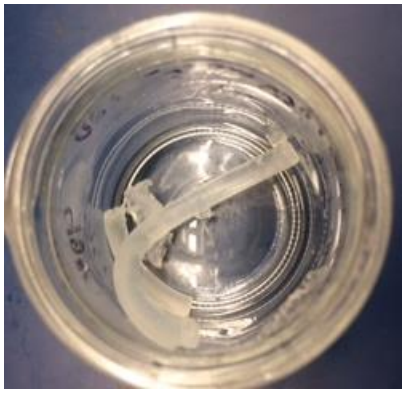

Figure 67. Appearance of the filled $DiMeDiPh_{5.3}DiEt_5$-720 synthesized polysiloxane compounded material with 20 wt% Cab-O-Sil at 40°C.

7.6 Thermogravimetric analysis of filled synthesized polysiloxanes

The thermal stability and filler dispersion of the Cab-O-Sil-filled synthesized polysiloxanes were investigated by TGA in a nitrogen atmosphere. The residue percentage values were examined to verify an even distribution of filler by ensuring that the residue percentage values were approximately equivalent to the calculated filler loading amount. The TGA thermograms of the synthesized polysiloxanes compounded with 20 wt% Cab-O-Sil filler at 40°C are displayed in Figure 68. The temperature at 10% and 50% weight loss, as well as the residue percentage values of the synthesized polysiloxanes compounded with 20 wt% Cab-O-Sil filler at 40°C are shown in Table 41. The values in Table 41 are median values of the three specimens per compounded material taken at the beginning of the compounding process, middle of the compounding process, and end of the compounding process.

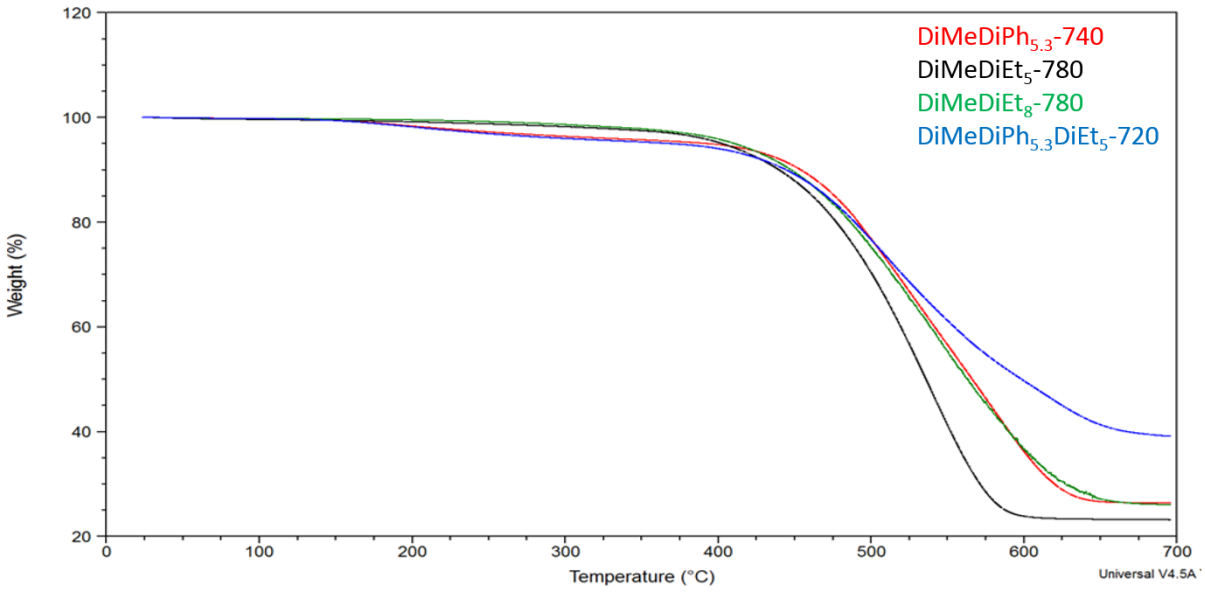

Figure 68. TGA thermograms of the synthesized polysiloxanes compounded with 20 wt% Cab-O-Sil filler at 40°C: DiMeDiPh$_{5.3}$-740 (—), DiMeDiEt$_5$-780 (—), DiMeDiEt$_8$-780 (—), and DiMeDiPh$_{5.3}$DiEt$_5$-720 (—).

Table 41. Thermal properties of the synthesized polysiloxanes compounded with 20 wt% Cab-O-Sil filler at 40°C.

Polysiloxane	**Temperature at 10% Weight Loss (ºC)**	**Temperature at 50% Weight Loss (ºC)**	**Residue (%)**
DiMeDiPh$_{5.3}$-740	454	566	26.38 (±1.03)
DiMeDiEt$_5$-780	440	536	23.17 (±0.11)
DiMeDiEt$_8$-780	448	563	26.04 (±1.27)
DiMeDiPh$_{5.3}$DiEt$_5$-720	444	598	39.11 (±1.69)

The filled materials possessed greater thermal stability compared to the unfilled synthesized polysiloxanes. The residue percentage values were slightly higher than the calculated filler loading amount. The values varied from the calculated filler loading amount by 3% to 19%. The increase in the residue percentage values were attributed to

the higher surface area of the Cab-O-Sil filler. Higher surface area fillers have an abundance of silanol groups to enhance the interaction with the polymer backbone.[27,31,139] The higher residue values can be attributed to unreleased polymer that became fused with filler during the degradation process. Additionally, the greater amount of residue in the filled synthesized polysiloxanes compared to the calculated filler loading amount could be attributed to the higher diphenyl- and diethyl-content levels in the synthesized polysiloxanes.[151] Unfilled DiMeDiPh$_{5.3}$DiEt$_5$-720 had the highest residue percentage value, and the combination of diphenyl and diethyl content may be a contributing factor to the 39% residue observed in the filled material. Higher diphenyl and diethyl content reduces the chain mobility and hinders the ability of the polymers to release cyclic volatiles, thus increasing the thermal stability of these materials.[151]

7.7 Oscillatory rheometry of filled synthesized polysiloxanes

The yield stress of the Cab-O-Sil-filled synthesized polysiloxane materials was analyzed by oscillatory rheometry. The yield stress of the silica-filled materials was determined by the point at which the storage modulus and loss modulus curves intersect. An oscillatory stress sweep from 3 Pa to 10,000 Pa was applied to the Cab-O-Sil-filled formulations and the reference silicone. The yield stress values of all filled materials were compared to the reference silicone to evaluate their efficacy in applications where the reference silicone is currently used.

Table 42 displays the yield stress values of the synthesized polysiloxanes compounded with 20 wt% Cab-O-Sil filler at 40°C. The yield stress of the Cab-O-Sil-filled materials were six times higher than the reference silicone. The yield stress enhancement was attributed to the higher surface area of the Cab-O-Sil filler. The smaller

particles of Cab-O-Sil can pack closer together and cover a greater surface area that enhances aggregation and polymer-filler interactions, resulting in an enhanced yield stress.[21,27,31,39,41]

Table 42. Yield stress of the synthesized polysiloxanes compounded with 20 wt% Cab-O-Sil filler at 40°C.

Polysiloxane	**Yield Stress (Pa)**
Reference Silicone	1,340
$DiMeDiPh_{5.3}$-740	8,452
$DiMeDiEt_5$-780	8,454
$DiMeDiEt_8$-780	8,454
$DiMeDiPh_{5.3}DiEt_5$-720	8,453

7.8 Flow rheology of filled synthesized polysiloxanes

A flow rheology study was conducted on the Cab-O-Sil-filled synthesized polysiloxane materials and compared to the reference silicone. Figure 69 displays the first stage of the flow test for the reference silicone compared to the filled synthesized polysiloxane materials.

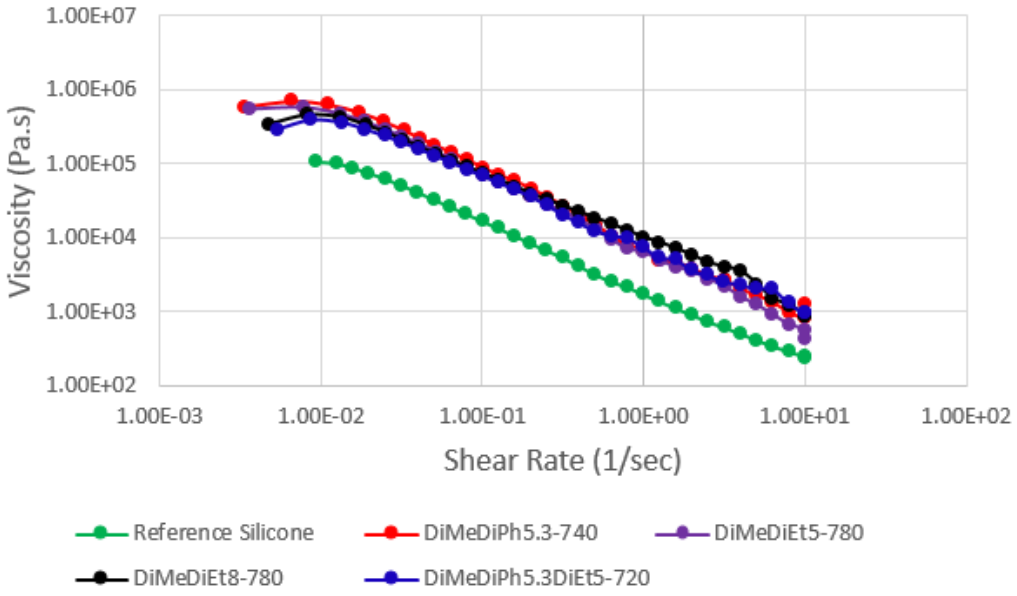

Figure 69. First stage of the flow rheology analysis for the reference silicone compared to the filled synthesized polysiloxane materials: reference silicone (•), DiMeDiPh$_{5.3}$-740 (•), DiMeDiEt$_5$-780 (•), DiMeDiEt$_8$-780 (•), and DiMeDiPh$_{5.3}$DiEt$_5$-720 (•).

The viscosity of the filled materials decreased as the shear rate increased, which was attributed to the destruction of the filler network structure by the increasing shear rates. The viscosity of the Cab-O-Sil-filled materials was significantly higher than the reference silicone. This was attributed to the higher surface area of the Cab-O-Sil filler that provided greater polymer-filler interactions.

The second stage of the flow test for the reference silicone compared to the filled synthesized polysiloxane materials are shown in Figure 70. The viscosity of the filled materials increased as the shear rate decreased, which was attributed to the reconstruction of the filler network structure over time.[80]

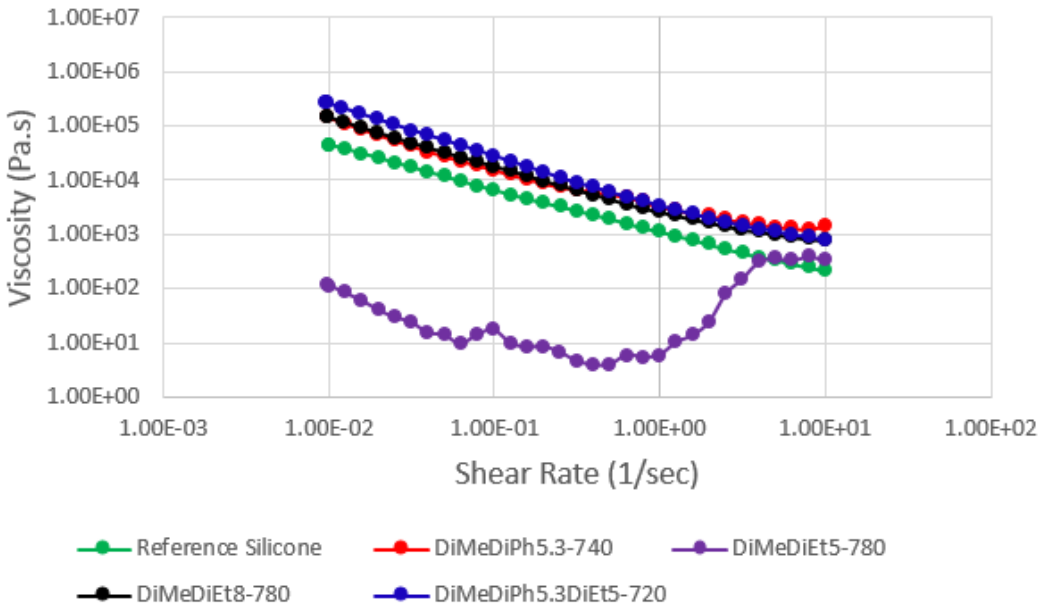

Figure 70. Second stage of the flow rheology analysis for the reference silicone compared to the filled synthesized polysiloxane materials: reference silicone (•), DiMeDiPh$_{5.3}$-740 (•), DiMeDiEt$_5$-780 (•), DiMeDiEt$_8$-780 (•), and DiMeDiPh$_{5.3}$DiEt$_5$-720 (•).

Figure 71 displays the thixotropic loops of the flow test for the reference silicone compared to the filled synthesized polysiloxane materials.

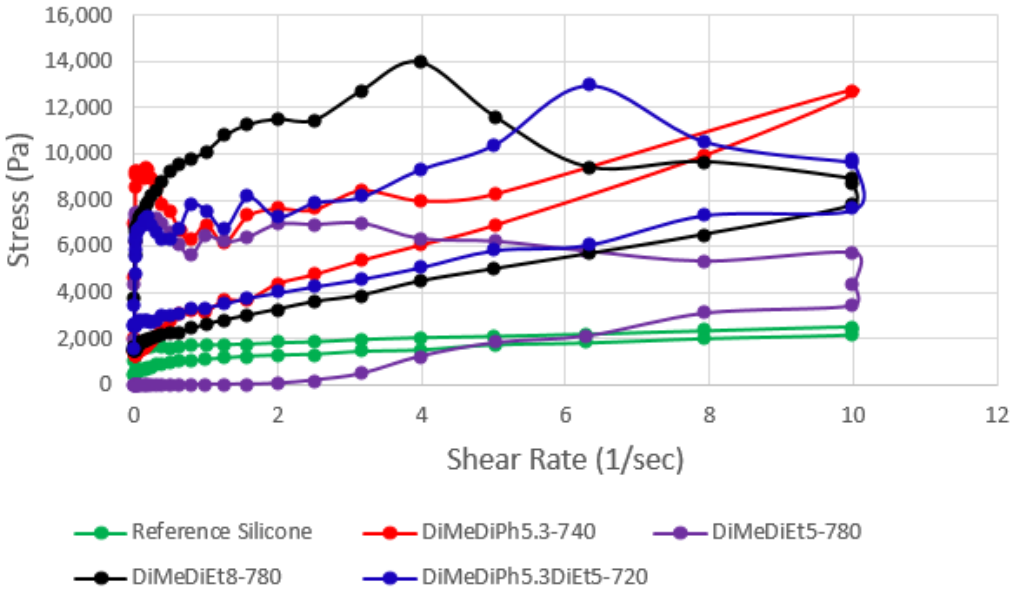

Figure 71. Thixotropic loops of the flow rheology analysis for the reference silicone compared to the filled synthesized polysiloxane materials: reference silicone (•), DiMeDiPh$_{5.3}$-740 (•), DiMeDiEt$_5$-780 (•), DiMeDiEt$_8$-780 (•), and DiMeDiPh$_{5.3}$DiEt$_5$-720 (•).

The Cab-O-Sil-filled materials obtained a significantly greater thixotropic behavior than the reference silicone. This indicates that the Cab-O-Sil-filled materials required more time to reconstruct their network structures.[80,183,184] The Cab-O-Sil filler's higher surface area enhances the thixotropic behavior.[21,26,27,31,39,41,187] However, as a result of the enhanced rheological properties, these filled materials could possibly be too stiff to replace the reference silicone. Similar rheological properties to the reference silicone were observed with other fillers studied. The Hi-Sil-233D-filled materials could prove to be a more suitable replacement for the commercial reference silicones in certain applications, rather than those filled with Cab-O-Sil.

From observations on the filled PDMS, model copolymer, and synthesized polysiloxanes, it was concluded that the thermal stability, yield stress, and thixotropic

behavior were all dependent on the filler type and degree of filler loading to a significantly greater extent than the chemical characteristics of polymer. Addition of filler to a polysiloxane resulted in enhanced thermal stability in all cases. The Cab-O-Sil-filled materials always resulted in significantly higher yield stresses and greater degrees of thixotropy compared to the reference silicone, no matter the type of monomers used to synthesize the polysiloxane or the molecular weight of the polymers chosen for compounding.

CHAPTER VIII

8. CONCLUSIONS

The Process 11 was utilized to compound thermoplastic materials for determining the effects of processing and recycling on the thermal and mechanical properties of the materials. The Process 11 was also utilized to compound an amorphous Starex material with TiO_2 to determine the compounding effectiveness of the extruder by thermal, mechanical, and optical analysis. It was concluded that extrusion by the Process 11 did not negatively affect the thermal and mechanical properties of the amorphous and semi-crystalline thermoplastic materials to a greater extent than injection molding. The formulations extruded by the Process 11 were also deemed appropriate for injection molding. The Process 11 effectively compounded a Starex and TiO_2 formulation, dispersing the TiO_2 filler evenly throughout the Starex matrix.

The Process 11 successfully compounded various model and experimentally-synthesized polysiloxanes with silica fillers to produce well-dispersed extrudate materials. The filled materials were compared to a commercial reference silicone to evaluate the efficacy of these silica-filled polysiloxane materials for use in applications that currently utilize the commercial reference silicone. The filled materials were characterized by TGA to evaluate the distribution of filler. Oscillatory rheometry and flow rheology were utilized to determine the yield stress and to evaluate the thixotropic

behavior, respectively. Various processing parameters, formulations, and fillers were evaluated to achieve these specified properties.

Prior to evaluating the filled materials, the model polymers were first evaluated by GPC to verify that both polymers had the reported molecular weight indicated by Gelest. The thermal behavior of the model polymers and the reference silicone was evaluated by DSC. The PDMS showed a T_m at -43.58°C. The reference silicone also contained a T_m at -45.03°C, from which it was concluded that it was a PDMS-based silicone. The model copolymer did not exhibit a T_m due to the presence of the diphenyl-siloxy units that disrupt low-temperature crystallization. TGA was used to determine the thermal stability of the model polymers compared to the reference silicone. The PDMS completely decomposed, leaving no residue. The model copolymer was more thermally stable compared to the PDMS and resulted in 6.99% residue. The enhanced thermal stability and greater amount of residue of the model copolymer was attributed to the presence of diphenyl- units that reduces the polymer chain mobility and prevents the release of cyclic volatiles during degradation.

The particle size of the three commercial fillers were evaluated by SEM. The fumed silica filler, Cab-O-Sil, contained smaller particles compared to the other two fillers. The two precipitated silica fillers, Hi-Sil-135 and Hi-Sil-233D, contained much larger particles. TGA was used to evaluate the purity and water content of the fillers. Both precipitated silica fillers lost about 7% weight, whereas the Cab-O-Sil filler lost less than 1% of its weight. The weight loss in the fillers were the result of water removal from the filler and some surface hydroxyl groups at elevated analysis temperatures.

Various temperature and loading studies were performed on the PDMS and the model polysiloxane-filled materials in order to determine the appropriate processing parameters, filler content, and filler type to obtain the desired yield stress and thixotropic behavior in the filled materials. These parameters were evaluated and chosen to be applied to the four experimentally-synthesized vinyl-terminated polysiloxanes. The Cab-O-Sil-filled-PDMS and Cab-O-Sil-filled-model copolymer resulted in the most thermally stable materials, attained the highest yield stress values, and achieved the greatest thixotropic behavior. It was determined from the model copolymer studies that the synthesized polysiloxanes should be filled with 20 wt% Cab-O-Sil filler at 40°C.

The Hi-Sil-135-filled materials were clear, white, soft, paste-like materials with little dimensional stability. The Hi-Sil-233D-filled materials were also clear, white, soft, paste-like materials with greater dimensional stability compared to the Hi-Sil-135-filled materials. The Cab-O-Sil-filled materials were light grey, viscous, paste-like materials with enhanced dimensional stability compared to all precipitated silica-filled materials. The enhanced dimensional stability of the Cab-O-Sil-filled materials was attributed to the higher surface area of the Cab-O-Sil fumed silica filler compared to the precipitated silica fillers.

The incorporation of the fillers with the model polymers further enhanced the thermal stability in the filled materials when compared to the unfilled model polymers. The temperature studies performed with the model polymer-filled materials resulted in no appreciable difference in thermal stability among the materials processed at the three different temperatures. However, in some materials, a slight enhancement in thermal stability was observed in some extruded materials compounded at 40°C. Overall, the

materials compounded at 40°C resulted in the most consistent thermally stable materials, as well as resulted in the best distribution of filler.

The loading studies performed with the model polymer-filled materials resulted in increasing thermal stability with increasing filler incorporation. The enhanced thermal stability was attributed to the additional filler creating a protective barrier that hindered the polymer decomposition process. The residue percentage values were approximately equivalent to the calculated filler loading amount in most formulations. The residue percentage values varied less than 3% from the calculated filler loading amount, indicating that filler was evenly distributed throughout the compounded materials in most formulations. Some formulations varied more than 3%, however. The model copolymer filled with 30 wt% of Hi-Sil-135 filler resulted in residue values 5% lower than the calculated filler loading amount. This phenomenon could be attributed to the additional filler increasing the viscosity of the materials and hindering the dispersion of silica. Cab-O-Sil-filled materials resulted in residue values 4% to 7% higher than the calculated filler loading amounts. This can be attributed to the higher surface area of the Cab-O-Sil filler which contained an abundance of silanol groups to enhance interactions with the polymer backbone and prevent decomposition to a greater degree compared to the Hi-Sil fillers.

The yield stress values were evaluated for the filled materials by oscillatory rheometry and compared to the reference silicone. The varied extrusion temperatures did not appear to affect the yield stress values in the filled systems to a significant extent. However, varied loading amounts of filler did affect the yield stress values. The yield stress values for the 20 wt% Hi-Sil-135-filled materials were significantly lower than the reference silicone. This was attributed to the filled materials not attaining the desired

percolation threshold to obtain an accurate yield stress. However, yield stress values increased with an increased amount of Hi-Sil-135 filler. From this data, it was concluded that the desired percolation threshold was reached at 25 wt% in the Hi-Sil-135 formulations. The yield stress values for the Hi-Sil-233D-filled materials were similar to the reference silicone. The yield stress values for the Cab-O-Sil-filled materials were four to six times higher than the reference silicone. The yield stress enhancement was also attributed to the higher surface area of the Cab-O-Sil filler.

The thixotropic behavior of the filled materials was evaluated by flow rheology and compared to the reference silicone. Both Hi-Sil precipitated silica-filled materials resulted in a shear-thinning behavior rather than a thixotropic behavior. This was attributed to the permanent deformation of their network structures and inadequate time to recover. The Cab-O-Sil-filled materials obtained a greater thixotropic behavior compared to the reference silicone and the Hi-Sil precipitated silica-filled materials. The greater thixotropic behavior was attributed to the higher surface area of the Cab-O-Sil filler. The Cab-O-Sil-filled systems resulted in the most thermally stable materials, obtained the highest yield stress values, and achieved the greatest thixotropic behavior. Thus, the Cab-O-Sil filler was utilized when compounding the synthesized polysiloxanes.

Prior to compounding, the synthesized polysiloxanes were first evaluated by GPC to evaluate the molecular weight. All synthesized polysiloxanes possessed a molecular weight of about 60,000 g/mol. The thermal behavior of the synthesized polysiloxanes was evaluated by DSC. The DSC analysis confirmed that three of the four synthesized polysiloxanes did not exhibit low-temperature crystallization. However, low-temperature crystallization was observed in the DiMeDiEt$_5$-780 copolymer. As a result of low-

temperature crystallization, the DiMeDiEt$_8$-780 copolymer was synthesized with higher diethyl- content to prevent crystallization. TGA was used to determine the thermal stability of the synthesized polysiloxanes. The copolymers synthesized with higher diphenyl- and diethyl-content were more thermally stable as a result of the higher substituent levels.

The synthesized polysiloxanes filled with the Cab-O-Sil filler were light grey, viscous, paste-like materials with enhanced dimensional stability similar to the model polysiloxanes filled with Cab-O-Sil. The Cab-O-Sil-filled materials resulted in residue values 3% to 19% higher than the calculated filler loading amount according to TGA. The yield stress values determined by oscillatory rheometry for the Cab-O-Sil-filled materials were four to six times higher than the reference silicone. The flow rheology of Cab-O-Sil-filled materials demonstrated a greater thixotropic behavior compared to the reference silicone. The enhanced percent residue values, yield stress, and thixotropic behavior were attributed to the higher surface area of the Cab-O-Sil filler and greater filler-polymer interactions compared to the Hi-Sil-filled formulations.

From analysis of the filled PDMS, model copolymer, and synthesized polysiloxanes, it was concluded that the thermal stability, yield stress, and thixotropic behavior were mostly dependent on the type of filler and the amount of filler used in each formulation rather than the chemical characteristics of polysiloxane polymer. While the molecular weight and the presence and amount of comonomers varied from formulation to formulation, the behavior of systems with Hi-Sil-135, Hi-Sil-233D, and Cab-O-Sil behaved similarly to their counterparts formulated with different polysiloxanes. The trends observed in the rheological characterization could be predicted based on the type

of filler chosen for each system. Formulations that used Hi-Sil-135 possessed the lowest viscosity at 20 wt% and did not reach a yield stress or demonstrate thixotropic behavior. When formulations contained 20 wt% Hi-Sil-233D possessed yield stresses similar to the reference silicone and demonstrated a moderate thixotropic behavior. The Cab-O-Sil-filled materials almost always resulted in significantly higher yield stresses and a significantly greater thixotropic behavior compared to all the Hi-Sil-filled materials and the reference silicone, no matter the comonomer composition of the polysiloxane or the molecular weight of the polymer.

8.1 Future research

The rheological properties of these Cab-O-Sil-filled materials were drastically higher compared to the reference silicone. As a result of the enhanced rheological properties, these filled materials would likely be too stiff to replace the reference silicone. However, Hi-Sil-233D-filled model copolymer systems obtained the yield stress and thixotropic behavior most similar to the reference silicone. Further compounding of the model polymers with Hi-Sil-233D filler will be investigated and compared to the reference silicone. The Hi-Sil-233D-filled materials could prove to be a more suitable replacement for the commercial reference silicone, rather than the Cab-O-Sil-filled materials. Additional types and amounts of filler, different polysiloxane compositions, and higher polysiloxane molecular weights will also be evaluated in future formulation studies. Further investigation of the chemical characteristics of the surface silanol groups, as well as the amount of silanol groups on each filer type will be performed. Vulcanization of the silica-filled polysiloxanes will also be performed, and the resulting cross-linked materials will be evaluated for their material properties, including but not

limited to thermal properties, mechanical properties, crosslink density, and filler dispersion by SEM.

REFERENCES

1. Dvornic, P. R.; Lenz, R. W. Polysiloxanes. *High Temperature Siloxane Elastomers*; Huthig & Wepf Verlag Basel Publication: New York, 1990; 15-73.
2. Mark, J. E. Physical Properties of Polymers Handbook. *Chapter 54*; Springer Science: New York, 2007; 3-20.
3. Polysiloxanes- by Lachelle Sussman. http://wwwcourses.sens.buffalo.edu/ce435/Polysiloxanes/ (accessed November 2, 2016).
4. Brook, M. A. *Silicon in Organic Organometallic, and Polymer Chemistry*; A Wiley-Interscience Publication: New York, 2000; 1-50.
5. Pauling, L. *The Nature of the Chemical Bond and the Structure of Molecules and Crystals: An Introduction of Modern Structural Chemistry*, 3rd Ed.; Cornell University Press: Ithaca, New York, 1960; 1-30.
6. Oberhammer, H.; Boggs, J. E. Importance of $(p\text{-}d)_{\pi}$ Bonding in the Siloxane Bond. *J. Am. Chem. Soc.* **1980,** *102*, 7241-7244.
7. Wired Chemist. Common Bond Energies and Bond Lengths. http://www.wiredchemist.com/chemistry/data/bond_energies_lengths.html (accessed March 22, 2017).
8. Zhang, Z.; Zhou, N.; Xu, C.; Xie, Z. Polymerization of Octamethylcyclotetrasiloxane with Hexamethyledisilazyl-Lithium as Initiator. *Chinese Journal of Polymer Science.* **2001,** *19*, 7-11.
9. Bohm, P. Functional Silicones and Silicone-Containing Block Copolymers. Ph.D. Dissertation, der Johannes Gutenberg-Universitat Mainz.

10. Ballistreri, A.; Montaudo, G.; Lenz, R. W. Mass Spectral Characterization and Thermal Decomposition Mechanism of Alternating Silarylene-Siloxane Polymers. *Macromolecules.* **1984,** *17*, 1848-1854.
11. Zlatanic, A.; Radojcic, D.; Wan, X.; Messman, J. M.; Dvornic, P. R. Suppression of Crystallization in Polydimethylsiloxanes and Chain Branching in Their Phenyl-Containing Copolymers. *Macromolecules.* **2017** *1*, 1-12.
12. Babu, G. N.; Christopher, S. S.; Newmark, R. A. Poly(dimethylsi1oxane-co-diphenylsiloxanes): Synthesis, Characterization, and Sequence Analysis. *Macromolecules.* **1987**, *20*, (11), 2654-2659.
13. Polk, W. D. Polydimethylsiloxane Containing Block Copolymers: Synthesis and Characterization of Alternating Poly(Arylene Ether Phosphine Oxide)-b-Siloxane and Segmented Nylon 6,6-b-Siloxane Copolymers. Ph.D. Dissertation, Virginia Polytechnic Institute and State University, Blacksburg, Virginia, 2001.
14. van Poll, M.; L.; Zhou, F.; Ramstedt, M.; Hu, L.; Huck; W. T. S. A Self-Assembly Approach to Chemical Micropatterning of Poly(dimethylsiloxane). *Angew. Chem. Int. Ed.* **2007,** *46*, 6634-6637.
15. Momen, G.; Farzaneh, M. SURVEY OF MICRO/NANO FILLER USE TO IMPROVE SILICONE RUBBER FOR OUTDOOR INSULATORS. *Adv. Mater. Sci.* **2011**, *27*, 1-13.
16. Arrighi, V.; Higgins, J. S.; Burgess, A. N.; Floudas, G. Local dynamics of poly(dimethyl siloxane) in the presence of reinforcing filler particles. *Polymer.* **1998**, *39*, (25), 6369-6376.

17. Sukumar, R.; Menon, A. R. R. Organomodified Kaolin as a Reinforcing Filler for Natural Rubber. *J. Appl. Polym. Sci.* **2007**, *107*, 3476-3483.
18. Huber Engineered Materials. Precipitated Silica. https://www.hubermaterials.com/products/silica-and-silicates/precipitated-silica.aspx (accessed March 24, 2017).
19. CABOT. CAB-O-SIL® Fumed Silica for Pharmaceutical and Nutraceutical Applications. file:///C:/Users/Downloads/Brochure-CAB-O-SIL-Fumed-Silica-Pharmaceutical-Nutraceutical-Apps.pdf (accessed February 27, 2017).
20. SIGMA. Fumed Silica. https://www.sigmaaldrich.com/content/dam/sigma-aldrich/docs/Aldrich/Product_Information_Sheet/s5130pis.pdf (accessed February 27, 2017).
21. Gurovich, D.; Macosko, C. W.; Tirrell, M. THE INFLUENCE OF FILLER-FILLER AND FILLER-POLYMER INTERACTIONS ON THE PHYSICAL PROPERTIES OF SILICA-FILLED LIQUID POLYISOPRENE. *Rubber Chemistry and Technology.* **2004**, *76*, 1-12.
22. Bogush, G. H.; Tracy, M. A.; Zukoski IV, C. F. Preparation of monodisperse silica particles: control of size and mass fraction. *J. Non-Cryst. Solids.* **1988,** *104*, 95-106.
23. Traina, M.; Pegoretti, A.; Penati, A. Time–Temperature Dependence of the Electrical Resistivity of High-Density Polyethylene/Carbon Black Composites. *J. Appl. Polym. Sci.* **2007,** *106*, 2065-2074.
24. Zhuravlev, L. T. The surface chemistry of amorphous silica. Zhuravlev model. *Colloids Surf., A.* **2000**, 173, 1-38.

25. Chrissafis, K.; Bikiaris, D. Can nanoparticles really enhance thermal stability of polymers? Part I: An overview on thermal decomposition of addition polymers. *Thermochim. Acta.* **2011**, *523*, 1-24.
26. Cassagnau, P. Melt rheology of organoclay and fumed silica nanocomposites. *Polymer.* **2008,** *49*, 2183-2196.
27. Dorigato, A.; Dzenis, Y.; Pegoretti, A. Filler aggregation as a reinforcement mechanism in polymer nanocomposites. *Mechanics of Materials,* **2013**, *12*, 79-90.
28. Chien, A.; Maxwell, R.; Chambers, D.; Balazs, B.; LeMay, J. Characterization of radiation-induced aging in silica-reinforced polysiloxane composites. *Radiat. Phys. Chem.* **2000**, *59*, 493-500.
29. Dorigato, A.; Pegoretti, A.; Penati, A. Linear low-density polyethylene/silica micro- and nanocomposites: dynamic rheological measurements and modelling. *eXPRESS Polymer Letters,* **2010**, *4*, (2), 115-129.
30. Raghavan, S. R.; Riley, M. W.; Fedkiw, P. S.; Khan, S. A. Composite Polymer Electrolytes Based on Poly(ethylene glycol) and Hydrophobic Fumed Silica: Dynamic Rheology and Microstructure. *Chem. Mater.* **1998**, *10*, (1), 244-251.
31. Luginsland, H-D.; Frohlich, J.; Wehmeier, A. Influence of different silanes on the reinforcement of silica-filled rubber compounds. *Rubber Chemistry and Technology*, **2002**, *75*, 563-579.
32. Shim, S. E.; Isayev, A. I. Rheology and structure of precipitated silica and poly(dimethyl siloxane) system. *Rheologica Acta,* **2004**, *43*, 127-136.
33. Burnside, S. D.; Giannelis, E. P. Synthesis and Properties of New Poly(Dimethylsi1oxane) Nanocomposites. *Chem. Mater.* **1995,** *7*, (9), 1597-1600.

34. Verdejo, R.; Barroso-Bujans, F.; Rodriguez-Perez, M. A.; de Saja, J. A.; Lopez-Manchado, M. A. Functionalized graphene sheet filled silicone foam nanocomposites. *J. Mater. Chem.* **2008**, *18*, 2221-2226.

35. Kim, H.; Lee, B.; Choi, S.; Kim, S.; Kim, H. The effect of types of maleic anhydride-grafted polypropylene (MAPP) on the interfacial adhesion properties of bio-flour-filled polypropylene composites. *Composites Part A: Applied Science and Manufacturing.* **2007**, *38*, 1473-1482.

36. Beyer, G. Nanocomposites: a new class of flame retardants for polymers. *Plastics, Additives and Compounding.* **2002**, *4*, (10), 22-28.

37. Dorigato, A.; Pegoretti, A.; Frache, A. Thermal stability of high density polyethylene–fumed silica nanocomposites. *J. Therm. Anal. Calorim.* **2012**, *109*, 863-873.

38. D' Amato, M.; Dorigato, A.; Fambri, L.; Pegoretti, A. High performance polyethylene nanocomposite fibers. *eXPRESS Polymer Letters.* **2012**, *6*, (12), 954-964.

39. Zhang, Q.; Archer, L. A. Poly(ethylene oxide)/Silica Nanocomposites: Structure and Rheology. *Langmuir*. **2002**, *18*, (26), 10435-10442.

40. Raghavan, S. R. Rheology of Silica Dispersions in Organic Liquids: New Evidence for Solvation Forces Dictated by Hydrogen Bonding. *Langmuir,* **2000**, *16*, (21), 7920-7930.

41. Wang, Y.; Wang, J. Shear Yield Behavior of Calcium Carbonate-Filled Polypropylene. *Polym. Eng.Sci.* **1999**, *39*, (1), 190-198.

42. Le Meins, J.; Moldenaers, P.; Mewis, J. Suspensions in Polymer Melts. 1. Effect of Particle Size on the Shear Flow Behavior. *Ind. Eng. Chem. Res.* **2002**, *41*, (25), 6297-6304.

43. Vermant, J. Quantifying dispersion of layered nanocomposites via melt rheology. *J. Rheol.* **2007**, *51*, 429-450.

44. Ibaseta, N.; Biscans, B. Fractal dimension of fumed silica: Comparison of light scattering and electron microscope methods. *Powder Technol.* **2010**, *203*, 206-210.

45. Bose, S.; Mahanwar, P. A. Influence of particle size and particle size distribution on MICA filled nylon 6 composite. *J. Mater. Sci.* **2005**, *40*, 6423-6428.

46. Thomas, T. P.; Kuruvilla, J.; Sabu, T. Mechanical properties of titanium dioxide-filled polystyrene microcomposites. *Mater. Lett.* **2003**, *58*, 281-289.

47. Jamil, M. S.; Ahmad, I.; Abdullah, I. Effects of Rice Husk Filler on the Mechanical and Thermal Properties of Liquid Natural Rubber Compatibilized High-Density Polyethylene/Natural Rubber Blends. *Journal of Polymer Research.* **2006**, *13*, 315-321.

48. DeGroot, Jr., J. V.; Macosko, C. W. Aging Phenomena in Silica-Filled Polydimethylsiloxane. *J. Colloid Interface Sci.* **1999**, *217*, 86-93.

49. Sombatsompop, N.; Thongsang, S.; Markpin, T.; Wimolmala, E. Fly Ash Particles and Precipitated Silica as Fillers in Rubbers. I. Untreated Fillers in Natural Rubber and Styrene–Butadiene Rubber Compounds. *J. Appl. Polym. Sci.* **2004**, *93*, 2119-2130

50. Wei, L.; Hu, N.; Zhang, Y. Synthesis of Polymer—Mesoporous Silica Nanocomposites. *Materials.* **2010**, *3*, 4066-4079.

51. Chen, J.; Lv, Q.; Wu, D.; Yao, X.; Wang, J.; and Li, Z. Nucleation of a Thermoplastic Polyester Elastomer Controlled by Silica Nanoparticles. *Indust. Eng. Chem. Res.* **2016**, 5279-5286.

52. PolyOne. What is a TPE? http://www.polyone.com/products/thermoplastic-elastomers/tpe-knowledge-center/tpe- faqs (accessed Nov 8, 2016).

53. Doede, C. M.; Panagrossi, A. Polysiloxane Elastomers. *Ind. Eng. Chem.* **1947,** *39*, (11), 1372-1375.

54. Planes, E.; Chazeau, L.; Vigier, G.; Stuhldreier, T. Influence of silica fillers on the ageing by gamma radiation of EDPM nanocomposites. *Compos. Sci. Technol.* **2006**, 1-23.

55. Maxwell, R. S.; Balazs, B. Residual dipolar coupling for the assessment of cross-link density changes in g-irradiated silica-PDMS composite materials. *J. Chem. Phys.* **2002,** *116*, (23), 10492-10502.

56. Huang, X.; Fang, X. L.; Lu, Z.; Chen, S. Reinforcement of polysiloxane with superhydrophobic nanosilica. J. *Mater. Sci.* **2009,** *49*, 4522-4530.

57. Kim, Y. W.; Eom, J. H. Processing of Porous Silicon Carbide Ceramics from Carbon-Filled Polysiloxane by Extrusion and Carbothermal Reduction. *J. Am. Ceram. Soc.* **2008,** *91*, (4), 1361-1364.

58. Tanahashi, M. Development of Fabrication Methods of Filler/Polymer Nanocomposites: With Focus on Simple Melt-Compounding-Based Approach without Surface Modification of Nanofillers. *Materials.* **2010,** *3*, 1593-1619.

59. Pu, Z.; Mark, J. E.; Jethmalani, J. M.; Ford, W. T. Effects of Dispersion and Aggregation of Silica in the Reinforcement of Poly(methyl acrylate) Elastomers. *Chem. Mater.* **1997**, *9*, (11), 2442-2447.

60. Tangram Technology. Extrusion Definitions. http://www.tangram.co.uk/TI-Polymer-Extrusion_Definitions.html (accessed March 19, 2017).

61. Encyclopedia of Chemical Engineering Equipment. Extruders. http://encyclopedia.che.engin.umich.edu/Pages/PolymerProcessing/Extruders/Extruders.html (accessed on October 4, 2016).

62. Shah, A.; Gupta, M. Comparison of the Flow in Co-rotating and Counter-rotating Twin-Screw Extruders. *ANTEC,* **2004,** 443-447.

63. Reiloy USA. L/D Ratio. http://reiloyusa.com/processing-tips/screw-design/ld-ratio/ (accessed on October 4, 2016).

64. Silva, A.; Teixeira, R.; Moutta, R.; Ferreira-Litao, V.; Barros, R. R.; Silva Bon, M. Sugarcane and Woody Biomass Pretreatments for Ethanol Production. *InTech.* **2013,** 47-88.

65. Triad Magnetics. Screw Design and Types in Plastic Extrusion. http://www.thomasnet.com/articles/plastics-rubber/extrusion-screw-design (accessed on October 4, 2016).

66. Galgali, G.; Ramesh, C.; Lele, A. A Rheological Study on the Kinetics of Hybrid Formation in Polypropylene Nanocomposites. *Macromolecules.* **2001**, *34*, (4), 852-858.

67. Incarnato, I.; Scarfato, P.; Scatteia, L.; Acierno, D. Rheological behavior of new melt compounded copolyamide nanocomposites. *Polymer.* **2004**, *45*, 3487-3496.

68. Gahleitner, M. RHEOLOGY AS A QUALITY CONTROL INSTRUMENT. *Pure Appl. Chem.* **1999**, *11*, 1731-1741.

69. Loiseau, A.; Tassin, J. Model Nanocomposites Based on Laponite and Poly(ethylene oxide): Preparation and Rheology. *Macromolecules.* **2006**, *39*, (26), 9185-9191.

70. Zhu, Z.; Thompson, T.; Wang, S.; von Meerwall, E. D.; Halasa, A. Investigating Linear and Nonlinear Viscoelastic Behavior Using Model Silica-Particle-Filled Polybutadiene. *Macromolecules.* **2005**, *38*, (21), 8816-8824.

71. Barnes, H. A; Hutton, J. F.; Walters, K. *An Introduction to Rheology*, 1st Ed.; Elsevier Science Publishers: Amsterdam, The Netherlands, 1989; 1-10.

72. Ghezzehei, T. A.; Or, D. Rheological Properties of Wet Soils and Clays under Steady and Oscillatory Stresses. *Soil Sci. Soc. Am. J.* **2001**, *65*, 624-637.

73. Bao, X.; Ning-Cheng, L.; Raj, R. B.; Rangan, K. P.; Anu, M. Engineering solder paste performance through controlled stress rheology analysis. *Soldering & Surface Mount Technology.* **1989**, *10*, 1-7.

74. Tabilo-Munizaga, G.; Barbosa-Canovas, G. V. Rheology for the food industry. *Journal of Food Engineering.* **2005**, *67*, 147-156.

75. Weiss, K. D.; Carlson, D.; Nixon, D. A. Viscoelastic Properties of Magneto- and Electro-Rheological Fluids. *Journal of Intelligent Material Systems and Structures.* **1994**, *5*, 772-775.

76. Boutelier, D.; Schrank, C.; Cruden, A. Power-law viscous materials for analogue experiments: New data on the rheology of highly-filled silicone polymers. *Journal of Structural Geology.* **2008**, *30*, 341-353.

77. Prashantha, K.; Soulestin, J.; Lacrampe, M. F.; Krawczak, P.; Dupin, G.; Claes, M. Masterbatch-based multi-walled carbon nanotube filled polypropylene nanocomposites: Assessment of rheological and mechanical properties. *Compos. Sci. Technol.* **2009**, *69*, 1756-1763.

78. Chen, P.; Zhang, J.; He, J. Increased Flow Property of Polycarbonate by Adding Hollow Glass Beads. *Polym. Eng. Sci.* **2005**, *45*, (8), 1119-1131.

79. Aztec. Thixotropy Index. http://www.suggest-keywords.com/dGhpeG90cm9weSAgaW5kZXg/ (accessed March 25, 2017).

80. Lee, C. H.; Moturi, V.; Lee, Y. Thixotropic property in pharmaceutical formulations. *J. Controlled Release.* **2009**, *136*, 88-98.

81. Thermo Electron Corporation. Short introduction into rheology. https://www.scribd.com/presentation/161088307/Basics-Rot-Creep-Osc (accessed March 5, 2017).

82. AmSty. Facilities. http://www.amstyrenics.com/facilities (accessed on May 17, 2016).

83. Professional Plastics. USA & Canada Sales. http://www.professionalplastics.com/contact (accessed on March 26, 2017).

84. Sabic. Contact Sabic. https://www.sabic-ip.com/gepapp/Plastics/global/jsp/EmailUs/EmailUs.jsp (accessed on May 17, 2016).

85. Honeywell. Honeywell Celebrates New Global Headquarters During Ribbon Cutting Ceremony. http://www.honeywell.com/newsroom/news/2015/11/honeywell-celebrates-new-global-headquarters-during-ribbon-cutting-ceremony (accessed on May 17, 2016).
86. Lotte Advanced Materials. Global Network. http://www.lotteadms.com/jsp/eng/contactus/sms_worldwide_asia.jsp (accessed on May 17, 2016).
87. TOR Specialty Minerals. Global Locations. http://www.torminerals.com/about-us/global-locations/ (accessed on May 17, 2016).
88. PPG. Contact. http://corporate.ppg.com/Contact.aspx (accessed on October 14, 2016).
89. CABOT. Contact Us. http://www.cabotcorp.com/company/contact-us#customer-service (accessed on October 14, 2016).
90. Gelest. Contact Us. http://www.gelest.com/contact-us/ (accessed on October 14, 2016).
91. ThermoFisher Scientific. About Us. http://corporate.thermofisher.com/en/about-us.html (accessed on May 17, 2016).
92. Thermo Fisher Scientific. Process 11 Parallel Twin-Screw Extruder. https://www.thermofisher.com/order/catalog/product/567-7600 (accessed on October 23, 2016).
93. AEC. ACS Group. http://www.acscorporate.com/aec (accessed on May 17, 2016).
94. Rotogran International Inc. Contact Us. http://rotogran.com/ (accessed on March 26, 2017).

95. Arburg. Germany. https://www.arburg.com/en/company/locations/germany/ (accessed on May 17, 2016).
96. KitchenAid. Contact Us. http://www.kitchenaid.com/contact-us/ (accessed on October 17, 2016).
97. TA Instruments. TA Directory. http://www.tainstruments.com/contact/ta-directory/ (accessed on May 17, 2016).
98. Malvern. About Us. http://www.malvern.com/en/about-us/default.aspx (accessed on June 14, 2016).
99. Sabic. Innovative Plastics: High & Low Shear Rate Rheology. http://www.pod-sabic-ip.com/KBAM/Reflection/Assets/Thumbnail/10606_4.pdf (accessed June 14, 2016).
100. MTS Systems Corporation. Contact Us. http://www.mts.com/en/contact/index.htm (accessed on June 8, 2016).
101. ASTM. Standard Test Method for Tensile Properties of Plastics. http://classes.engr.oregonstate.edu/mime/winter2012/me453-001/Lab1%20-%20Shear%20Strain%20on%20Polymer%20Beam/ASTM%20D638-02a.pdf (accessed on June 8, 2016).
102. Dumbbell Co., LTD. Super Dumbbell Cutters Available. http://www.dumbbell.co.jp/english/super_dumbbell01.html (accessed on March 21, 2017).
103. PhenomWorld. Contact Details. http://www.phenom-world.com/contact#contactdetails (accessed on June 15, 2016).

104. Kurt J. Lesker Company. Contact Us. http://www.lesker.com/contactus/ (accessed on June 15, 2016).

105. Wyatt Technology. Team Wyatt Corporate Headquarters. http://www.wyatt.com/about/team-wyatt.html (accessed on April 1, 2017).

106. Agilent Technologies. Welcome to Agilent.com. http://www.agilent.com/home/more-countries?currPageURL=http://www.agilent.com/en-us/contact-us/page (accessed on April 1, 2017).

107. Phenomenex Inc. Contact Us. http://www.phenomenex.com/Home/ContactUs (accessed on April 1, 2017).

108. Mechanical Engineer's World. Injection Molding. http://www.mechscience.com/injection-moldinginjection-molding-machineinjection-molding-processinjection-molding-on-plastics/ (accessed October 4, 2016).

109. Thomasnet. More about Injection Molded Plastics. http://www.thomasnet.com/about/injection-molded-plastics-60310604.html (accessed May 11, 2016).

110. Association of Plastic Recyclers. Recycling Beyond Bottles. http://www.plasticsrecycling.org/recycling-beyond-bottles (accessed October 9, 2016).

111. Deeproot. Virgin Plastic, Recycled Plastic, and Everything In Between. http://www.deeproot.com/blog/blog-entries/virgin-plastic-recycled-plastic-and-everything-in-between (accessed May 11, 2016).

112. Prospector. Regrinding Plastics. http://knowledge.ulprospector.com/1468/pe-regrinding-plastics/ (accessed May 12, 2016).

113. Ronkay, F. Effect of Recycling on the Rheological, Mechanical and Optical Properties of Polycarbonate. *Acta Polytechnica Hungarica.* **2013,** *10* (1), 209-220.

114. Aurrekoetxea, M.; Sarrionandia, A.; Urrutibeascoa, I.; Maspoch, M. Effects of recycling on the microstructure and the mechanical properties of isotactic polypropylene. *J. Mater. Sci.* **2001,** *36*, 2607-2613.

115. Duigou, A.; Pillin, I.; Bourmaud, A.; Davies, P.; Baley, C. Effect of recycling on mechanical behaviour of biocompostable flax/poly(l-lactide) composites. *Composites Part A: Applied Science and Manufacturing.* **2008**, *39* (9), 1471-1478.

116. Fornes, T. D.; Yoon, P. J.; Paul, D. R. Polymer matrix degradation and color formation in melt processed nylon 6/clay nanocomposites. *Polymer.* **2003**, *44* (24), 7545-7556.

117. Yoon, P. J.; Hunter, D. L.; Paul, D. R. Polycarbonate nanocomposites: Part 2. Degradation and color formation. *Polymer.* **2003**, *44* (18), 5341-5354.

118. Pitt Falls Injection Molding. Pittfalls in injection Moulding of Plastics: Properties of Plastics. http://www.pitfallsinmolding.com/polyproperties.html (accessed March 3, 2016).

119. Chiang, W; Tzeng, G. Effect of the compatizbilizers on flame-retardant polycarbonate (PC)/ acrylonitrile-butadiene-styrene (ABS) alloy. *J. Appl. Polym. Sci.* **1997**, *65* (4), 795-805.

120. Peydro, M; Juarez, D; Sanchez-Caballero, S; Parres, F. Study of the Thermal Properties of Acrylonitrile Butadiene Styrene – High Impact Polystyrene Blends with Styrene Ethylene Butylene Styrene. *Annals of the Oradea University.* **2013**, (1), 273-276.

121. Blaine, R. Polymer Heats of Fusion. *Thermal Applications Note,* 1-2. (accessed May 11, 2016).

122. Cangelosi, F.; Davis, L.; Samuels, S. New Generation of Long-Term Stabilizers for Polyolefins. *Journal of Vinyl & Additive Technology.* **2001**, *7* (3), 123-133.

123. Gerhardt, L. C.; Jell, G. M. R.; Boccaccini, A. R. Titanium dioxide (TiO2) nanoparticles filled poly(D,L lactid acid) (PDLLA) matrix composites for bone tissue engineering. *J. Mater. Sci.: Mater. Med.* **2007**, *18*, 1287-1298.

124. Mirmohseni, A.; Zavareh, S. Epoxy/acrylonitrile-butadiene-styrene copolymer/clay ternary nanocomposite as impact toughened epoxy. *Journal of Polymer Research.* **2009**, *17*, 191-201.

125. Sung, Y. T.; Kim, Y. S; Lee, Y. K.; Kim, W. N.; Lee, H. S.; Sung, J. Y.; Yoon, H. G. Effects of Clay on the Morphology of Poly(acrylonitrile-butadiene-styrene) and Polypropylene Nanocomposites. *Polym. Eng. Sci.* **2007**, 1672-1677.

126. Magallon-Caco, L.; Perez-Bueno, J. J.; Meas-Vong, Y.; Stremsdoerfer, G.; Espinoza-Beltran, F. J. Surface modification of acrylonitrile-butadiene-styrene (ABS) with heterogeneous photocatalysis (TiO2) for the substitution of the etching stage in the electroless process. *Surf. Coat. Technol.* **2011**, *206*, 1410-1415.

127. Liu, Y.; Bo, S.; Zhu, Y.; Zhang, W. Determination of molecular weight and molecular sizes of polymers by high temperature gel permeation chromatography with a static and dynamic laser light scattering detector. *Polymer.* **2003**, *44*, 7209-7220.

128. Montaudo, G.; Montaudo, M. S.; Puglisi, C.; Samperi, F. Molecular Weight Distribution of Poly(dimethylsiloxane) by Combining Matrix-assisted Laser Desorption/Ionization Time-of-flight Mass Spectrometry with Gel-permeation Chromatography Fractionation. *Rapid Commun. Mass Spectrom.* **1995**, *9*, 1158-1163.

129. Liu, X. M.; Maziarz, E. P.; Heiler, D. J.; Grobe, G. L. Comparative Studies of Poly(Dimethyl Siloxanes) Using Automated GPC-MALDI-TOF MS and On-Line GPC-ESI-TOF MS. *Rapid Commun. Mass Spectrom.* **2003**, *14*, 195-202.

130. Montaudo, G.; Montaudo, M. S.; Puglisi, C.; Samperi, F. Molecular Weight Determination and Structural Analysis in Polydisperse Polymers by Hyphenated Gel Permeation Chromatography/Matrix-Assisted Laser Desorption Ionization-Time of Flight Mass Spectrometry. *International Journal of Polymer Analysis and Characterization.* **1997**, *3*, 177-192.

131. Razack, N. A. *Solvent Selection Guide*; Scribd: San Francisco, 2015; 1-100.

132. Kuo, A. C. M. *Poly(dimethylsiloxane)*; Oxford University Press, Inc: Oxford, 1999; 1-100.

133. Litvinov, V. M.; Barthel, H.; Weis, J. Structure of a PDMS Layer Grafted onto a Silica Surface Studied by Means of DSC and Solid-State NMR. *Macromolecules.* **2002**, *35*, (11), 4356-4364.

134. Yang, H.; Nguyen, Q. T.; Ding, Y.; Long, Y.; Ping, Z. Investigation of poly(dimethyl siloxane) (PDMS)–solvent interactions by DSC. *J. Membr. Sci.* **2000**, *164*, 37-43.

135. Cazacu, M.; Vlad, A.; Alexandru, M.; Budrugeac, P.; Racles, C.; Iacomi, F. Polydimethyldiphenylsiloxanes/silica interconnected networks: preparation and properties evaluation. *Polym. Bull.* **2010**, *264*, 412-434.

136. Jovanovic, J. D.; Govrdarica, M. N.; Dvornic, P. R.; Popovic, I.G. The thermogravimetric analysis of some polysiloxanes. *Polym. Degrad. Stab.* **1998**, *61*, 87-93.

137. Ahmad, S.; Gupta, A. P.; Sharmin, E.; Alam, M.; Pandey, S. K. Synthesis, characterization and development of high performance siloxane-modified epoxy paints. *Prog. Org. Coat.* **2005**, *54*, 248-255.

138. Camino, G.; Lomakin, S. M.; Lageard, M. Ballistreri, A.; Garozzo, D.; Montaudo, G. Thermal polydimethylsiloxane degradation. Part 2. The degradation mechanisms. *Polymer*. **2002**, 2011-2015.

139. Ramirez, I.; Jayaram, S.; Cherney, E. A.; Gauthier, M.; Simon, L. Erosion Resistance and Mechanical Properties of Silicone Nanocomposite Insulation. *IEEE Transactions on Dielectrics and Electrical Insulation.* **2009**, *16*, (1), 52-59.

140. Lauter, U.; Kantor, S. W.; Schmidt-Rohr, K.; MacKnight, W. J. Vinyl-Substituted Silphenylene Siloxane Copolymers: Novel High-Temperature Elastomers. *Macromolecules.* **1999**, *32*, 3426-3431.

141. Chenoweth, K.; Cheung, S.; van Duin, A. C.; Goddard III, W. A.; Kober, E. M. Simulations on the Thermal Decomposition of a Poly(dimethylsiloxane) Polymer Using the ReaxFF Reactive Force Field. *J. Am. Chem. Soc.* **2005**, *127* (19), 7192-7202.

142. Ballistreri, A.; Garozzo, D.; Montaudo, G. Mass Spectral Characterization and Thermal Decomposition Mechanism of Poly(dimethylsiloxane). *Macromolecules.* **1984**, *17* (7), 1312-1315.

143. Sunan, T.; Damrongsakkul, S.; Hemvichian, K. Rimdusit, S. Thermal degradation behaviors of polybenzoxazine and silicon-containing polyimide blends. *Polym. Degrad. Stab.* **2007**, *92*, 1265-1278.

144. Schiavon, M. A.; Redondo, S. U. A.; Pina, S. R. O. Yoshida, I. V. P. Investigation on kinetics of thermal decomposition in polysiloxane networks used as precursors of silicon oxycarbide glasses. *J. Non-Crystal. Solids.* **2002**, *304*, 92-100.

145. Lewicki, J. P.; Liggat, J. J.; Patel, M. The thermal degradation behaviour of polydimethylsiloxane/montmorillonite nanocomposites. *Polym. Degrad. Stab.* **2009**, *94*, 1548-1557.

146. Mazhar, M.; Zulfiqar, M.; Piracha, A.; Ali, S.; Ahmed, A. Comparative Thermal Stability of Homopolysiloxanes and Copolysiloxanes of Dimethyl/Diphenyl Silanes. *J. Chem. Soc. of Pak.* **1990**, *12* (3), 225-229.

147. Deshpande, G.; Rezac, M. E. Kinetic aspects of the thermal degradation of poly(dimethylsiloxane) and poly(dimethyl diphenyl siloxane). *Polym. Degrad. Stab.* **2001**, *76*, 17-24.

148. Pola, J.; Galikova, A.; Galik, A.; Blechta, V.; Bastl, Z.; Subrt, J.; Ouchi, A. UV Laser Photolysis of Disiloxanes for Chemical Vapor Deposition of Nano-Textured Silicones. *Chem. Mater.* **2002**, *14* (1), 144-153.

149. Mahadik, D. B.; Rao, A. V.; Wagh, P. B.; Gupta, S. C. Synthesis of Transparent and Hydrophobic TMOS Based Silica Aerogels. *American Institute of Physics,* **2013**, *1536*, 553-554.

150. Giri, R.; Naskar, K.; Nando, G. B. In-Situ Compatibilization of Linear Low-Density Polyethylene and Polydimethyl Siloxane Rubber Through Reactive Blending. *Mater. Express.* **2012**, *2* (1), 37-50.

151. Zhu, H. D.; Kantor, S. W.; MacKnight, W. J. Thermally Stable Silphenylene Vinyl Siloxane Elastomers and Their Blends. *Macromolecules.* **1997**, 31, 850-856.

152. Ardhyananta, H.; Kawauchi, T.; Takeichi, T. Preparation and Properties of Polybenzoxazine-poly(dimethylsiloxane-co-diphenylsiloxane) Hybrids as High Performance Polymers. *High Performance Polymers.* **2009**, *00*, 1-24.

153. Tjandrawinata, R.; Irie, M.; Yoshida, Y.; Suzuki, K. Effect of Adding Spherical Silica Filler on Physico-mechanical Properties of Resin Modified Glass-ionomer Cement. *Dental Materials Journal.* **2004**, *23*, (2) 148-154.

154. Tobler, D. J.; Shaw, S.; Benning, L. G. Quantification of initial steps of nucleation and growth of silica nanoparticles: An in-situ SAXS and DLS study. *Geochim. Cosmochim. Acta.* **2009**, *73*, 577-5393.

155. Mueller, R.; Kammler, H. K.; Wegner, K.; Pratsinis, S. E. OH Surface Density of SiO2 and TiO2 by Thermogravimetric Analysis. *Langmuir*. **2003**, *19* (1), 160-165.

156. Ji, X.; Hampsey, J. E.; Hu, Q.; He, J.; Yang, Z.; Lu, Y. Mesoporous Silica-Reinforced Polymer Nanocomposites. *Chem. Mater.* **2003**, *15* (19), 3656-3662.

157. Choi, S-S.; Lee, S. G.; Im, S. S.; Kim, S. H.; Joo, Y. L. Silica nanofibers from electrospinning/sol-gel process. *J. Mater. Sci. Lett.* **2003**, *22*, 891-893.

158. Lewicki, J. P.; Liggat, J. J.; Pethrick, R. A.; Patel, M.; Rhoney, I. Investigating the ageing behavior of polysiloxane nanocomposites by degradative thermal analysis. *Polym. Degrad. Stab.* **2008**, *93*, 185-168.

159. Lim, L.; Auras, R.; Rubino, M. Processing technologies for poly(lactic acid). *Progress in Polymer Science.* **2008**, *33*, 820-852.

160. Klapiszewski, L.; Bula, K.; Sobczak, M.; Jesionowski, T. Influence of Processing Conditions on the Thermal Stability and Mechanical Properties of PP/Silica-Lignin Composites. *International Journal of Polymer Science.* **2016**, *2016*, 1-9.

161. Wacker Chemie AG. Solid and Liquid Silicone Rubber Material and Processing Guidelines. https://www.wacker.com/cms/media/publications/downloads/6709_EN.pdf (accessed February 23, 2017).

162. Cha, J. Y.; Chung, D. S.; Seib, P. A.; Flores, R. A.; Hanna, M. A. Physical properties of starch-based foams as affected by extrusion temperature and moisture content. *Industrial Crops and Products.* **2001,** *14*, 23-30.

163. Baudouin, A.; Auhl, D.; Tao, F.; Devaux, J.; Bailly, C. Polymer blend emulsion stabilization using carbon nanotubes interfacial confinement. *Polymer.* **2011,** *52*, 149-156.

164. Borggreve, R. J. M.; Gaymans, R. J. Impact behaviour of nylon-rubber blends: 4. Effect of the coupling agent, maleic anhydride *Polymer.* **1989,** *30*, 63-70.

165. Ma, P.; Siddiqui, N. A.; Marom, G.; Kim, J. Dispersion and functionalization of carbon nanotubes for polymer-based nanocomposites: A review. *Composites: Part A: Applied Science and Manufacturing.* **2010,** *41*, 1345-1367.

166. Villmow, T.; Kretzschmar, B.; Potschke, P. Influence of screw configuration, residence time, and specific mechanical energy in twin-screw extrusion of polycaprolactone/multi-walled carbon nanotube composites. *Compos. Sci. Technol.* **2010**, *70*, (14) 1-26.

167. Pickering, K. L.; Khimi, S. R.; Ilanko, S. THE EFFECT OF SILANE COUPLING AGENT ON IRON SAND FOR USE IN MAGNETORHEOLOGICAL ELASTOMERS PART 1: SURFACE CHEMICAL MODIFICATION AND CHARACTERIZATION. *Composites Part A: Applied Science and Manufacturing.* **2015**, *68*, 377-386.

168. Hong, J.; Lee, J.; Hong, C. K.; Shim, S. E. Improvement of thermal conductivity of poly(dimethyl siloxane) using silica-coated multi-walled carbon nanotube. *J. Therm. Anal. Calorim.* **2010**, *101*, 297-302.

169. Dey, T. K.; Tripathi, M. Thermal properties of silicon powder filled high-density polyethylene composites. *Thermochim. Acta.* **2010**, *502*, 35-42.

170. Laachachi, A.; Coches, M.; Ferriol, M.; Lopez-Cuesta, J. M.; Leroy, E. Influence of TiO2 and Fe2O3 fillers on the thermal properties of poly(methyl methacrylate) (PMMA). *Mater. Lett.* **2005**, *59*, 36-39.

171. Chien, A.; Maxwell, R. S.; DeTeresa, S.; Thompson, L.; Cohenour, R.; Balazs, B. The Effect of Filler-Polymer Interactions on Cold-Crystallization Kinetics in Crosslinked, Silica Filled PDMS/PDPS Copolymer Melts. *J. Polym. Sci., Part B: Polym. Phys.* **2006**, *44*, 1898-1906.

172. Reynaud, E.; Jouen, T.; Gauthier, C.; Vigier, G.; Varlet, J. Nanofillers in polymeric matrix: a study on silica reinforced PA6. *Polymer.* **2001,** *42*, 8759-8768.

173. Pedrazzoli, D.; Dorigato, A.; Pegoretti, A. Monitoring the Mechanical Behaviour of Electrically Conductive Polymer Nanocomposites Under Ramp and Creep Conditions. *Journal of Nanoscience and Nanotechnology.* **2012**, *12*, (5), 4093-4102.

174. Raghavan, S. R.; Khan, S. A. Shear-Thickening Response of Fumed Silica Suspensions under Steady and Oscillatory Shear. *J. Colloid Interface Sci.* **1997**, *185*, 57-67.

175. Robertson, C. G.; Wang, X. Isoenergetic Jamming Transition in Particle-Filled Systems. *Phys. Rev. Lett.* **2005**, *95*, 1-4.

176. Duoss, E. B.; Weisgraber, T. H.; Hearon, K.; Zhu, C.; Small IV, W.; Metz, T. R.; Vericella, J. J.; Barth, H. D.; Kuntz, J. D., Maxwell, R. S.; Spadaccini, C. M.; Wilson, T. S. Three-Dimensional Printing of Elastomeric, Cellular Architectures with Negative Stiffness. *Advanced Functional Materials.* **2014**, 1-9.

177. Aral, B. K.; Kalyon, D. M. Viscoelastic material functions of noncolloidal suspensions with spherical particles. *J. Rheol.* **1998**, *41*, 599-620.

178. Kopesky, E. T.; Haddad, T. S.; Cohen, R. E.; McKinley, G. H. Thermomechanical Properties of Poly(methyl methacrylates) containing Tethered and Untethered Polyhedral Oligomeric Silsesquioxanes (POSS). *Macromolecules.* **2004**, *37*, (24), 8992-9004.

179. Zhang, Q.; Lippits, D. R.; Rastogi, S. Dispersion and Rheological Aspects of SWNTs in Ultrahigh Molecular Weight Polyethylene. *Macromolecules.* **2006**, *39*, (2), 658-666.

180. Kim, K. J.; White, J. L. Rheological Investigations of Suspensions of Talc, Calcium Carbonate, and Their Mixtures in a Polystyrene Melt. *Polym. Eng. Sci.* **1999**, *39*, 2189-2198.

181. Tanoue, S.; Utracki, L. A.; Garcia-Rejon, A.; Sammut, P.; Ton-That, M.; Pesneau, I.; Kamal, M. R.; Lyngaae-Jorgensen, J. Melt Compounding of Different Grades of Polystyrene With Organoclay. Part 2: Rheological Properties. *Polym. Eng. Sci.* **2004**, *44*, (6), 8816-8824.

182. Du, F.; Scogna, R. C.; Zhou, W.; Brand, S.; Fischer, J. E.; Winey, K. I. Nanotube Networks in Polymer Nanocomposites: Rheology and Electrical Conductivity. *Macromolecules.* **2004**, *37*, (24), 9048-9055.

183. Adeyeye, M. C.; Jain, A. C.; Ghorab, M. K.; Reilly, W. J. Viscoelastic Evaluation of Topical Creams Containing Microcrystalline Cellulose/Sodium Carboxymethyl Cellulose as Stabilizer. AAPS *PharmSciTech.* **2003**, *3*, (2), 1-10.

184. Koleske, J. V. *Paint and Coating Testing Manual*: Fourteenth Edition of the Gardner-Sward Handbook (Astm Manual Series); ASTM International: New York, 1995; 1-100.

185. Paul, M.; Alexandre, M.; Degee, P.; Henrist, C.; Rulmont, A.; Dubois, P. New nanocomposite materials based on plasticized poly(L-lactide) and organo-modified montmorillonites: thermal and morphological study. *Polymer.* **2003**, *44*, 443-450.

186. Tunc, S.; Angellier, H.; Cahyana, Y.; Chalier, P.; Gontard, N.; Gastaldi, E. Functional properties of wheat gluten/montmorillonite nanocomposite films processed by casting. *J. Membr. Sci.* **2007**, *289*, 159-168.

187. Pignon, F.; Magnin, A.; Piau, J.; Cabane, B.; Lindner, P.; Diat, O. Yield stress thixotropic clay suspension: Investigations of structure by light, neutron, and x-ray scattering. *American Physical Society* **1996**, *56*, (3), 3281-3289.